INTERNATIONAL JOURNAL OF QUANTUM CHEMISTRY, VOL. XX, 955–1065 (1981)

Unrestricted Hartree–Fock Theory and Its Applications to Molecules and Chemical Reactions

HIDEO FUKUTOME

Department of Physics, Faculty of Science, Kyoto University, Kyoto 606, Japan

Contents

1. Introduction

The Hartree–Fock (HF) theory is the most basic approximation for fermion many-body systems that is based on the independent particle picture for motion of fermions. At an early stage of its development, it was considered indispensable to impose a symmetry restriction on its orbitals and total wave function, a Slater determinant, in order to make the theory consistent to the symmetry principle of quantum mechanics; namely, only the orbitals and the Slater determinants which are irreducible representations of the symmetry group were considered physically allowable. The HF theory with this symmetry restriction is called the restricted HF (RHF) theory. The HF theory which does not impose the symmetry restriction and allows broken symmetry orbitals and Slater determinants is called the unrestricted HF (UHF) theory. We use the term UHF when a broken symmetry is involved and the term HF in the wide sense including both the RHF and UHF cases.

The HF equation is a nonlinear equation owing to its self-consistent field (SCF) character and its solution may not be unique. It has been rather slowly recognized that the HF equation without the symmetry restriction may have

 CCC0020-7608/81/110955-109$10.90

solutions with energies lower than the RHF ground state and the broken symmetry wave functions of such solutions are able to well describe physical properties which arise from correlation effects beyond the RHF approximation. Existence and importance of such broken symmetry solutions were firstly suggested by Mott (1949) and Slater (1951). Mott pointed out for a linear array of hydrogen atoms that the state of electrons moving in delocalized Bloch orbitals is of the lowest energy and the system is a conductor when the interatomic distances are small, while the state with each electron bound to an atom is lower in energy and the system becomes an insulator when the interatomic distances become large. Based on this argument he predicted the existence of conductor–insulator phase transitions due to changes of interatomic distances. Slater pointed out that for the hydrogen molecule when the interatomic distance is large, the state in which the two electrons of different spins are localized toward different atoms is lower in energy than the RHF state with the two electrons occupying the same symmetric orbital because such localization of electrons decreases the Coulombic repulsion between them. He suggested that such spin polarized localization of electrons due to their Coulombic repulsion may be the origin of antiferromagnetism. Slater's idea was substantiated by the Matsubara–Yokota (1954) split band model for antiferromagnets.

The fact that a large part of correlation effects in molecules can be described by a single determinantal wave function with broken symmetry orbitals and projection to an eigenstate of total spin was pointed out first by Coulson and Fisher (1949) and Kotani (1951) in the semilocalized molecular orbital theory for hydrogen molecule. Their idea was generalized as the alternant orbital theory by Löwdin (1954, 1955), Yoshizumi and Itoh (1955), and Itoh and Yoshizumi (1955). The alternant orbitals in alternant hydrocarbons are of the same character as the split band orbitals in antiferromagnets. Löwdin (1963) called the puzzling situation in the HF theory, in which introduction of broken symmetry orbitals may bring about lowering of the variational energy, the symmetry dilemma. His proposal for the projection of broken symmetry UHF wave functions, Löwdin (1955), opened later developments of the extended HF theory (for a review see Pauncz, 1967).

Concerning the problem whether the broken symmetry components of a UHF wave function are a mere mathematical artifact to be eliminated or have a physical significance, Peierls and Yoccoz (1957) proposed an ingenious idea. The ground state of deformed nuclei can be described by a UHF wave function breaking the rotational symmetry. They pointed out that making the symmetry operation of rotation on the UHF wave function is equivalent to rotating all nucleons retaining their relative positions unchanged, namely, making rigid rotation of a deformed nucleus. They showed that the projection of the UHF wave function to eigenstates of angular momentum is just equivalent to selecting out eigenstates of rigid rotation. Based on these facts they concluded that the components with different angular momenta in the UHF wave function represent a series of rotational excited states of a deformed nucleus. The microscopic foundation of the Peierls–Yoccoz theory has not been established for long, but

we shall show that it has a universal foundation on the group theoretical structure of fermion many-body systems that arises from the canonical anticommutation relation.

A demonstration for the ability of broken symmetry wave functions in describing important physical phenomena was also provided by the BCS theory of superconductivity (Bardeen et al., 1957). The breaking of electron number conservation in the BCS wave function was shown to arise from the essence of superconductivity, the coherence in the phases of superconducting electrons. The formalism by Bogoliubov (1958) indicated that the BCS wave function has the character of an extension of the HF approximation. Bogoliubov's formalism is now called the Hartree–Bogoliubov theory. The Hartree–Bogoliubov theory was also applied successfully to the description of superconducting nuclei (Belyaev, 1959).

The finding of Overhauser (1960) that the HF equation of one dimensional electron gas always has solutions with helical spin arrangements, the helical spin density waves (SDW), which are lower in energy than the RHF ground state, stimulated many studies on the nature and origin of antiferromagnetism from the itinerant picture of electrons. In the same year, Thouless (1960) gave the mathematical condition for instability of a HF state which is nothing but the condition for the appearance of a new solution of the HF equation. His condition was applied to studies on antiferromagnetic states including the helical SDW in three dimensional electron gases (for a review, see Herring, 1966). HF instabilities and UHF solutions in solids, in particular the charge density wave (CDW) solutions which have modulations of the electron charge density, were also studied in connection with Mott's conductor–insulator phase transition and Wigner's crystalized electron gas (for a review, see Halperin and Rice, 1968).

Early applications of the UHF theory to molecules were made for open shell systems without consideration for HF instabilities. Studies of molecules with strong enough electronic correlation to yield instabilities of the HF ground state were first undertaken by Misurkin and Ovchinnikov (1967), Čižek–Paldus (1967), and Fukutome (1968) for long polyenes. Misurkin and Ovchinnikov showed that the HF ground state of infinite nonbond alternated polyene is a SDW with alternating modulation of the spin density. Čižek and Paldus showed that the RHF ground state of long polyenes is unstable but the instabilities considered by them were not the ones leading to the UHF ground state. The author showed that the instability leading to the SDW ground state occurs first with an increase in the chain length. The SDW ground state leads to a finite energy gap in electronic excitations even in the absence of bond alternation which is of the same nature as the band gap in antiferromagnets. It was pointed out that the energy gap of the electronic origin may contribute to the finite energy gap observed in absorption spectra of long polyenes as well as the gap due to bond alternation proposed by Longuet-Higgins and Salem (1959). After these works, many UHF theoretical studies were made about conjugated molecules by Paldus–Čižek (1969, 1970a, 1970b, 1970c, 1971), Čižek and Paldus (1970, 1971), Harris and Falicov (1969), Tric (1970), Cazes et al. (1970),

Andre and Leroy (1971), Laidlaw (1973), Laforgue et al. (1973), Paldus and Veillard (1978), Bénard and Paldus (1980), and the Russian group (for reviews of the works of the Russian group and related works, see Ovchinnikov et al. (1973) and Misurkin and Ovchinnikov (1977)).

Application of the UHF theory to chemical reactions was first made by Salotto and Burnelle (1970) in the calculation of the ground state potentials of the diatomic molecules H_2, HF, and LiH. Significance of HF instabilities and the UHF ground state of SDW types in chemical reactions were first recognized by the author (Fukutome, 1972, 1973a, 1973b). The author pointed out that the UHF wave functions of SDW type well represent states of the diradical nature in chemical reactions and the instability of the RHF ground state leading to the SDW ground state can be used as a theoretical criterion for the diradical character of chemical reactions. The author also developed a theory for complete classification and characterization of HF wave functions and their instabilities (Fukutome, 1974a, 1974b). Using this theory, the author and his collaborators showed that surprisingly plentiful instabilities occur in the HF ground state of chemical reactions and the resultant UHF ground state represents states of a multiradical nature with beautiful spin structures of many varieties including alternating, helical, and three dimensionally modulated ones. The UHF theory opened a new viewpoint about previously unknown aspects of chemical reactions with strong correlation of electrons.

In this paper, we review works of the author and his collaborators and intimately related works about the UHF theory and its applications to molecules and chemical reactions. The review consists of three additional sections. In Section 2 we review mathematical aspects of the UHF theory. The HF approximation has a deep group theoretical foundation that is intimately connected with the group theoretical structure of fermion many-body systems that arises from the canonical anticommutation relation of annihilation–creation operators of fermions and the spin, time reversal, and spatial symmetries. Emphasis is on clarifying the group theoretical foundation of the UHF theory. Construction of HF wave functions and their orbitals is made on the $U(N)$ (N dimensional unitary) group generated by particle–hole type pair operators of fermions. Classification and characterization of HF wave functions and their instabilities are made on the subgroup structure of the symmetry group consisting of spin rotation, time reversal and a spatial point symmetry group. We also discuss the bifurcation structures of HF adiabatic potential surfaces in the vicinity of instability thresholds and on a direct optimization algorism for a HF calculation that has secured and efficient convergence in the SCF procedure. Finally, we discuss the relation of HF wave functions to exact ones and the physical significance of broken symmetry components in UHF wave functions.

In Section 3 we review applications of the UHF theory to molecules and chemical reactions. Emphasis is on demonstrating chemical significance of HF instabilities and UHF wave functions and discussing the new concepts about electronic structures of molecules and electronic mechanisms of chemical reactions with strong electronic correlation revealed by the UHF theory using concrete

examples. We also compare results of UHF calculations with those of configuration interaction (CI) calculations to demonstrate the ability of the UHF theory in incorporating important correlation effects.

In Section 4 we discuss some basic problems related to the UHF theory. The topics discussed are the relation of UHF spin and charge structures to exact correlation structures, the problem of how to describe excited states in systems with the HF ground state of UHF type, and the presence of systems whose ground state cannot be approximated by a UHF wave function.

2. Mathematical Theory

A. $U(N)$ Group Formulation of the HF Theory

There are various ways to formulate the HF theory. Usually it is formulated by the variational method to minimize the energy expectation value by a Slater determinant (the HF energy functional) and to obtain the variational equation for the orbitals in the Slater determinant (the HF equation). We consider here the $U(N)$ group formulation of the HF theory in order to clarify the group theoretical foundation of the HF theory. The $U(N)$ group governs not only the structure of HF wave functions, but also the structure of exact wave functions as we shall discuss in Section 2.E, so that the $U(N)$ group formulation is the most suitable in elucidating the relation of the HF approximation to the exact theory.

i. Preliminaries. In this paper we use the second quantization formalism for electrons. Let $a(i) \equiv a(x_i, s_i)$ and $a^\dagger(i) \equiv a^\dagger(x_i, s_i)$ be the annihilation and creation operators of electron in the coordinate representation. The variable i denotes the coordinate x_i and the spin s_i of electron and the dagger (†) represents the Hermitian conjugate. They satisfy the canonical anticommutation relation

$$\{a(1), a^\dagger(2)\} = \delta(1, 2), \{a(1), a(2)\} = \{a^\dagger(1), a^\dagger(2)\} = 0, \tag{1}$$

where the curly brackets represent the anticommutator and $\delta(1,2) = \delta(x_1 - x_2)\delta_{s_1,s_2}$. We consider a molecular system with the nonrelativistic spin independent Hamiltonian

$$H = V + \int a^\dagger(1)h(1)a(1)d(1) + \tfrac{1}{2}\int\int a^\dagger(1)a^\dagger(2)\frac{e^2}{r_{12}}a(2)a(1)d(1)d(2), \tag{2}$$

where $h(1)$ is the single particle Hamiltonian of the electron, V is the Coulombic potential between nuclei, and the integration for the variable i includes both the integration for x_i and the summation for s_i.

We introduce a finite and given basis set $\psi_\zeta(1), \zeta = 1, 2, \ldots, N$ for spin orbitals satisfying the orthonormal condition

$$\langle \psi_\zeta | \psi_\eta \rangle = \int \psi_\zeta^*(1)\psi_\eta(1)d(1) = \delta_{\zeta\eta}, \tag{3}$$

where the asterisk represents a complex conjugate. We do not specify ψ_ζ's here. We restrict the Hilbert space of spin orbitals to the N dimensional space spanned by ψ_ζ's. The number N must be an even number $2M$ for the subspaces of up and down spins to be of the same dimension M. The annihilation and creation operators of the electron in the ψ_ζ basis are given by

$$a_\zeta = \int a(1)\psi_\zeta^*(1)d(1), \qquad a_\zeta^\dagger = \int a^\dagger(1)\psi_\zeta(1)d(1). \tag{4}$$

They satisfy the anticommutation relation

$$\{a_\zeta, a_\eta^\dagger\} = \delta_{\zeta\eta}, \qquad \{a_\zeta, a_\eta\} = \{a_\zeta^\dagger, a_\eta^\dagger\} = 0. \tag{5}$$

The Hamiltonian in the ψ_ζ basis is

$$H = V + h_{\zeta\eta}a_\zeta^\dagger a_\eta + \tfrac{1}{4}[\zeta\eta|\iota\kappa]a_\zeta^\dagger a_\iota^\dagger a_\kappa a_\eta, \tag{6}$$

where $h_{\zeta\eta}$ is the matrix element of the single particle Hamiltonian and $[\zeta\eta|\iota\kappa]$ is the antisymmetrized Coulomb repulsion integral

$$\begin{aligned} h_{\zeta\eta} &= \langle\psi_\zeta|h|\psi_\eta\rangle, \\ [\zeta\eta|\iota\kappa] &= \langle\zeta\eta|\iota\kappa\rangle - \langle\zeta\kappa|\iota\eta\rangle, \\ \langle\zeta\kappa|\iota\kappa\rangle &= \int\int \frac{e^2}{r_{12}}\psi_\zeta^*(1)\psi_\eta(1)\psi_\iota^*(2)\psi_\kappa(2)d(1)d(2). \end{aligned} \tag{7}$$

We use in the following formulas the dummy index convention to sum up repeated indices.

We introduce a reference Slater determinant with n electrons occupying the spin orbitals ψ_α, $\alpha = 1, 2, \ldots, n$,

$$|\Psi\rangle = a_1^\dagger \cdots a_n^\dagger|0\rangle = \det[\psi_\alpha(i)], \tag{8}$$

where $|0\rangle$ is the vacuum satisfying

$$a_\zeta|0\rangle = 0, \tag{9}$$

and det represents determinant. We denote the occupied spin orbitals in the reference Slater determinant by the indices $\alpha, \beta, \gamma, \ldots$ and the unoccupied ones by the indices $\mu, \nu, \xi, \ldots$. We use the indices $\zeta, \eta, \iota, \kappa, \ldots$ to denote spin orbitals without specification of occupancy. The Slater determinants with single, double and multiple excitations of electrons are given by

$$|\Psi_{\mu\alpha}\rangle = a_\mu^\dagger a_\alpha|\Psi\rangle, \; |\Psi_{\mu\nu\alpha\beta}\rangle = a_\mu^\dagger a_\alpha a_\nu^\dagger a_\beta|\Psi\rangle, \cdots. \tag{10}$$

The Slater determinants $|\Psi_{\mu\nu\cdots\alpha\beta\cdots}\rangle$, $\alpha < \beta < \cdots$, and $\mu < \nu < \cdots$ constitute an orthonormal complete set of the space with n electrons.

Let ϕ_ζ, $\zeta = 1, 2, \ldots, N$ be another set of orthonormal spin orbitals

$$\langle\phi_\zeta|\phi_\eta\rangle = \delta_{\zeta\eta}. \tag{11}$$

ϕ_ζ's can be expanded by ψ_ζ's as

$$\phi_\zeta = \psi_\eta u_{\eta\zeta}, \qquad u_{\eta\zeta} = \langle\psi_\eta|\phi_\zeta\rangle. \tag{12}$$

The N dimensional matrix $u = (u_{\zeta\eta})$ is unitary and belongs to the $U(N)$ group

$$u^{\dagger}u = uu^{\dagger} = 1. \tag{13}$$

The creation operator of the electron in the spin orbital ϕ_ζ is given by

$$\int a^{\dagger}(1)\phi_\zeta(1)d(1) = a^{\dagger}_{\eta}u_{\eta\zeta} = (a^{\dagger}u)_\zeta, \tag{14}$$

where $a^{\dagger}$ is the row vector $(a^{\dagger}_{\zeta})$. The Slater determinant with n electrons occupying the spin orbitals ϕ_α, $\alpha = 1, 2, \ldots, n$ is therefore given by

$$|\Phi\rangle = (a^{\dagger}u)_1 \cdots (a^{\dagger}u)_n|0\rangle \equiv \det[\phi_\alpha(i)]. \tag{15}$$

ii. $U(N)$ Lie Algebra and $U(N)$ Canonical Transformation. We define the pair operators of particle–hole type by

$$E^{\zeta}_{\eta} = a^{\dagger}_{\zeta}a_{\eta}. \tag{16}$$

They satisfy the relations

$$E^{\zeta\,\dagger}_{\eta} = E^{\eta}_{\zeta}, \tag{17}$$

$$[E^{\zeta}_{\eta}, E^{\iota}_{\kappa}] = \delta_{\eta\iota}E^{\zeta}_{\kappa} - \delta_{\zeta\kappa}E^{\iota}_{\eta}, \tag{18}$$

where the term in square brackets represents the commutator. Equation (18) is an important consequence of the canonical anticommutation relation (5) and shows that the set of the pair operators E^{ζ}_{η} is closed under the Lie multiplication forming a basis of a Lie algebra. The Lie algebra spanned by E^{ζ}_{η}'s is the Lie algebra of the $U(N)$ group. This fact was utilized in many-body theories of nuclei (for review see Moshinsky, 1968) and molecules (for review see Paldus, 1976).

The $U(N)$ Lie algebra of the pair operators generates a set of canonical transformations which forms a representation of the $U(N)$ group. We call it the $U(N)$ canonical transformation. It was introduced firstly by Thouless (1960) and sometimes is called the Thouless transformation. Let Γ be an anti-Hermitian operator in the $U(N)$ Lie algebra

$$\Gamma = \gamma_{\zeta\eta}a^{\dagger}_{\zeta}a_{\eta}, \qquad \gamma^{*}_{\zeta\eta} = -\gamma_{\eta\zeta}. \tag{19}$$

Using the relations

$$[\Gamma, a^{\dagger}_{\zeta}] = a^{\dagger}_{\eta}\gamma_{\eta\zeta}, \qquad [\Gamma, a_\zeta] = a_\eta\gamma^{*}_{\eta\zeta} \tag{20}$$

and the operator identity

$$e^{X}Ae^{-X} = A + [X, A] + (1/2!)[X, [X, A]] + \cdots, \tag{21}$$

we obtain

$$e^{\Gamma}a^{\dagger}_{\zeta}e^{-\Gamma} = a^{\dagger}_{\eta}u_{\eta\zeta}, \qquad e^{\Gamma}a_\zeta e^{-\Gamma} = a_\eta u^{*}_{\eta\zeta}, \tag{22}$$

where $u = (u_{\zeta\eta})$ is the $U(N)$ matrix given by

$$u = e^{\gamma}, \qquad \gamma = (\gamma_{\zeta\eta}), \qquad u^{\dagger}u = uu^{\dagger} = 1. \tag{23}$$

Thus, the $U(N)$ canonical transformation e^{Γ} induces a linear transformation of the creation operators by a $U(N)$ matrix u. Hence, we denote it by u as

$$U(u) \equiv e^{\Gamma}. \tag{24}$$

The $U(u)$ satisfies the group property

$$U(u)U(u') = U(uu'), \tag{25}$$

and is a representation of the $U(N)$ group. Operating $U(u)$ on the Slater determinant $|\Psi\rangle$, we obtain

$$U(u)|\Psi\rangle = (a^{\dagger}u)_1 \cdots (a^{\dagger}u)_n|0\rangle = |\Phi\rangle. \tag{26}$$

Thus, the $U(N)$ canonical transformation transforms a Slater determinant to another Slater determinant and any Slater determinant is obtained by a $U(N)$ canonical transformation of a given Slater determinant. This was proved first by Thouless (1960) and is known as the Thouless theorem. It is the group theoretical basis to construct the HF theory. A $U(N)$ group formulation of the HF theory was given by Matsen and Nelin (1979). In the following, we shall derive a particle–hole formalism of the HF theory using the Thouless theorem, which is equivalent to the density matrix formalism given by the author (Fukutome, 1971).

iii. Particle–Hole Formalism. The pair operators E^{μ}_{α} annihilate an electron in an occupied orbital and create an electron in an unoccupied orbital, namely, they are the creation operators of a particle–hole pair. Their Hermitian conjugates E^{α}_{μ} annihilate a particle–hole pair. On the other hand, the operators E^{α}_{β} and E^{μ}_{ν} transform an electron within occupied orbitals and within unoccupied ones, respectively. Hence, they do not change the number of particle–hole pairs. The operators E^{α}_{β} and E^{μ}_{ν}, respectively, are closed under the Lie multiplication and form $U(n)$ and $U(N-n)$ subalgebras of the $U(N)$ Lie algebra.

We decompose the generator of the $U(N)$ canonical transformation into the components unchanging and changing the number of particle–hole pairs

$$\begin{aligned} &\Xi = \xi_{\alpha\beta}a^{\dagger}_{\alpha}a_{\beta} + \bar{\xi}_{\mu\nu}a^{\dagger}_{\mu}a_{\nu}, \qquad \xi^{*}_{\alpha\beta} = -\xi_{\beta\alpha}, \qquad \bar{\xi}^{*}_{\mu\nu} = -\bar{\xi}_{\nu\mu}, \\ &\Lambda = \lambda_{\mu\alpha}a^{\dagger}_{\mu}a_{\alpha} - \lambda^{*}_{\mu\alpha}a^{\dagger}_{\alpha}a_{\mu}. \end{aligned} \tag{27}$$

By the same way as the derivation of Eq. (22), we obtain

$$e^{\Xi}a^{\dagger}_{\alpha}e^{-\Xi} = a^{\dagger}_{\beta}w_{\beta\alpha}, \qquad e^{\Xi}a^{\dagger}_{\mu}e^{-\Xi} = a^{\dagger}_{\nu}\bar{w}_{\nu\mu}, \tag{28}$$

where $w = (w_{\alpha\beta})$ and $\bar{w} = (\bar{w}_{\mu\nu})$ are the $U(n)$ and $U(N-n)$ matrices given by

$$w = e^{\xi}, \qquad \xi = (\xi_{\alpha\beta}), \qquad \bar{w} = e^{\bar{\xi}}, \qquad \bar{\xi} = (\bar{\xi}_{\mu\nu}). \tag{29}$$

As seen from Eq. (14), the transformation (28) is equivalent to the following transformation of the orbitals ψ_{ζ} which does not mix the occupied and unoccupied ones:

$$\psi'_{\alpha} = \psi_{\beta}w_{\beta\alpha}, \qquad \psi'_{\mu} = \psi_{\nu}\bar{w}_{\nu\mu}. \tag{30}$$

Using the relations

$$[\Lambda, a_\alpha^\dagger] = a_\mu^\dagger \lambda_{\mu\alpha}, \qquad [\Lambda, a_\mu^\dagger] = -a_\alpha^\dagger \lambda_{\mu\alpha}^*, \tag{31}$$

and Eq. (21), we obtain

$$\begin{aligned} e^\Lambda a_\alpha^\dagger e^{-\Lambda} &= a_\beta^\dagger [C(\lambda)]_{\beta\alpha} + a_\mu^\dagger [S(\lambda)]_{\mu\alpha}, \\ e^\Lambda a_\mu^\dagger e^{-\Lambda} &= a_\nu^\dagger [\tilde{C}(\lambda)]_{\nu\mu} - a_\alpha^\dagger [S^\dagger(\lambda)]_{\alpha\mu}. \end{aligned} \tag{32}$$

The transformation (32) is equivalent to the following transformation of the orbitals ψ_ζ to mix the occupied and unoccupied ones:

$$\begin{aligned} \phi_\alpha &= \psi_\beta [C(\lambda)]_{\beta\alpha} + \psi_\mu [S(\lambda)]_{\mu\alpha}, \\ \phi_\mu &= \psi_\nu [\tilde{C}(\lambda)]_{\nu\mu} - \psi_\alpha [S^\dagger(\lambda)]_{\alpha\mu}. \end{aligned} \tag{33}$$

The $S(\lambda)$, $C(\lambda)$, and $\tilde{C}(\lambda)$ are the $(N-n)\times n$, $n\times n$, and $(N-n)\times(N-n)$ matrices defined from the $(N-n)\times n$ matrix $\lambda = (\lambda_{\mu\alpha})$ by

$$\begin{aligned} S(\lambda) &= \sum_{k=0}^{\infty} \frac{(-1)^k}{(2k+1)!} \lambda (\lambda^\dagger \lambda)^k, \\ C(\lambda) &= 1_n + \sum_{k=1}^{\infty} \frac{(-1)^k}{(2k)!} (\lambda^\dagger \lambda)^k, \\ \tilde{C}(\lambda) &= 1_{N-n} + \sum_{k=1}^{\infty} \frac{(-1)^k}{(2k)!} (\lambda \lambda^\dagger)^k, \end{aligned} \tag{34}$$

where 1_n is the unit matrix of n dimension. They are matrix functions having properties similar to the triangular functions. $\lambda^\dagger\lambda$ and $\lambda\lambda^\dagger$ are positive definite Hermitian matrices and there are $U(n)$ and $U(N-n)$ matrices $v = (v_{\alpha A})$ and $\tilde{v} = (\tilde{V}_{\mu A})$ to diagonalize them

$$\begin{aligned} (\lambda^\dagger \lambda)_{\alpha\beta} &= \sum_{A=1}^{k} v_{\alpha A} \lambda_A^2 v_{\beta A}^*, \\ (\lambda \lambda^\dagger)_{\mu\nu} &= \sum_{A=1}^{k} \tilde{v}_{\mu A} \lambda_A^2 \tilde{v}_{\nu A}^*, \end{aligned} \tag{35}$$

where λ_A's are real and $K = \min(n, N-n)$. Since the maximal rank of λ is K, we can put $\lambda_A = 0$ for $A > K$. From Eq. (35), we have the following diagonalization of λ:

$$\lambda_{\mu\alpha} = \sum_{A=1}^{k} \tilde{v}_{\mu A} \lambda_A v_{\alpha A}^*. \tag{36}$$

Substituting Eq. (36) into Eq. (34), we have

$$[S(\lambda)]_{\mu\alpha} = \sum_{A=1}^{k} \tilde{v}_{\mu A} \sin \lambda_A v^*_{\alpha A},$$

$$[C(\lambda)]_{\alpha\beta} = \sum_{A=1}^{n} v_{\alpha A} \cos \lambda_A v^*_{\beta A}, \tag{37}$$

$$[\tilde{C}(\lambda)]_{\mu\nu} = \sum_{A=1}^{N-n} \tilde{v}_{\mu A} \cos \lambda_A \tilde{v}^*_{\nu A}.$$

From Eq. (37), the following relations are satisfied:

$$C^2(\lambda) + S^\dagger(\lambda) S(\lambda) = 1_n, \tag{38a}$$

$$\tilde{C}^2(\lambda) + S(\lambda) S^\dagger(\lambda) = 1_{N-n}, \tag{38b}$$

$$S(\lambda) C(\lambda) = \tilde{C}(\lambda) S(\lambda). \tag{38c}$$

We define the $U(N)$ matrices u_λ and u_ξ by

$$u_\lambda = \begin{bmatrix} C(\lambda), & -S^\dagger(\lambda) \\ S(\lambda), & \tilde{C}(\lambda) \end{bmatrix}, \qquad u_\xi = \begin{bmatrix} w, & 0 \\ 0, & \bar{w} \end{bmatrix}. \tag{39}$$

The $U(N)$ character of u_λ follows from Eq. (38). The above arguments show that a $U(N)$ matrix u and a $U(N)$ canonical transformation $U(u)$ can be decomposed as

$$u = u_\lambda u_\xi, \qquad U(u) = U(u_\lambda) U(u_\xi) \equiv e^{\Lambda} e^{\Xi}. \tag{40}$$

We next determine the structure of the $U(N)$ transformed Slater determinant $U(u)|\Psi\rangle$. Since the transformation $U(u_\xi)$ induces a unitary transformation of the orbitals ψ_ξ restricted within the space of occupied orbitals, it leaves the Slater determinant $|\Psi\rangle$ unchanged, while $U(u_\lambda)$ which mixes the occupied and unoccupied orbitals produces a nontrivial change:

$$U(u_\xi)|\Psi\rangle = (a^\dagger w)_1 \cdots (a^\dagger w)_n |0\rangle = \det(w)|\Psi\rangle, \tag{41a}$$

$$U(u_\lambda)|\Psi\rangle = \prod_{\alpha=1}^{n} \{a^\dagger_\beta [C(\lambda)]_{\beta\alpha} + a^\dagger_\mu [S(\lambda)]_{\mu\alpha}\}|0\rangle = |\Phi\rangle. \tag{41b}$$

The Slater determinant $|\Phi\rangle$ has the occupied orbitals ϕ_α given by Eq. (33). It can be expressed as

$$|\Phi\rangle = \langle\Psi|U(u_\lambda)|\Psi\rangle \prod_{\alpha=1}^{n} (a^\dagger_\alpha + a^\dagger_\mu p_{\mu\alpha})|0\rangle, \tag{42a}$$

$$p_{\mu\alpha} = [S(\lambda) C^{-1}(\lambda)]_{\mu\alpha} = \sum_{A=1}^{k} \tilde{v}_{\mu A} \tan \lambda_A v^*_{\alpha A}, \tag{42b}$$

$$\langle\Psi|U(u_\lambda)|\Psi\rangle = \det[C(\lambda)]. \tag{42c}$$

We can express $\langle\Psi|U(u_\lambda)|\Psi\rangle$ also in terms of the matrix $p=(p_{\mu\alpha})$. Multiplying $C^{-1}(\lambda)$ to Eq. (38a) from both the left- and right-hand sides, we obtain

$$\begin{aligned} 1_n + p^\dagger p &= C^{-2}(\lambda), \\ \langle\Psi|U(u_\lambda)|\Psi\rangle &= [\det(1+p^\dagger p)]^{-1/2}. \end{aligned} \tag{43}$$

Expanding the product in Eq. (42a), we can rewrite $|\Phi\rangle$ as

$$\begin{aligned} |\Phi\rangle = {} & \langle\Psi|U(u_\lambda)|\Psi\rangle \\ & \times\Big(|\Psi\rangle + p_{\mu\alpha}|\Psi_{\mu\alpha}\rangle + \sum_{\substack{\alpha<\beta \\ \mu<\nu}} \mathscr{A}(p_{\mu\alpha}p_{\mu\beta})|\Psi_{\mu\nu\alpha\beta}\rangle + \cdots\Big), \end{aligned} \tag{44}$$

where $\mathscr{A}$ is the antisymmetrizer for the indices $\mu, \nu, \ldots$, which brings about simultaneous antisymmetrization for the indices $\alpha, \beta, \ldots$. By using the relation

$$\sum_{\substack{\alpha<\beta<\cdots \\ \mu<\nu<\cdots}} \mathscr{A}(p_{\mu\alpha}p_{\nu\beta}\cdots)a^\dagger_\mu a_\alpha a^\dagger_\nu a_\beta \cdots = \frac{1}{m!}(p_{\mu\alpha}a^\dagger_\mu a_\alpha)^m, \tag{45}$$

Equation (44) can be rewritten

$$|\Phi\rangle = \langle\Psi|U(u_\lambda)|\Psi\rangle\, e^{p_{\mu\alpha}a^\dagger_\mu a_\alpha}|\Psi\rangle. \tag{46}$$

This expression of a Slater determinant was obtained by Thouless (1960).

The Thouless theorem indicates that the Slater determinant of a UHF solution can be obtained by a $U(N)$ canonical transformation of the Slater determinant of the RHF solution. Let us identify $|\Phi\rangle$ and $|\Psi\rangle$ with the Slater determinants of a UHF and the RHF soutions, respectively. Then, Eq. (46) shows that when the Slater determinant of a UHF solution is expanded by the RHF orbitals it contains RHF configurations with from one to n particle–hole pairs. All the particle–hole pairs, however, are in the same pair state specified by $p/|p|$, where $p=(p_{\mu\alpha})$ and $|p|^2 = p^*_{\mu\alpha}p_{\mu\alpha}$. Therefore, a UHF wave function represents a Bose condensation of RHF particle–hole pairs into a pair state. The Bose condensation of RHF particle–hole pairs in a UHF wave function endows a collective character of the electronic correlation incorporated into a UHF wave function and produces an ordered spin and charge structure as we shall show later.

iv. HF Density Matrix and Energy Functional. The density matrix of an HF solution with occupied orbitals ϕ_α is given in the ψ_ζ orbital basis by

$$\begin{aligned} Q_{\zeta\eta} &= \langle\psi_\zeta|\phi_\alpha\rangle\langle\phi_\alpha|\psi_\eta\rangle = u_{\lambda,\zeta\alpha}u^*_{\lambda,\eta\alpha}, \\ u_{\lambda,\zeta\alpha} &= \langle\psi_\zeta|u_\lambda|\psi_\alpha\rangle. \end{aligned} \tag{47}$$

Let $\bar{u}_\lambda$ be the $N\times n$ matrix

$$\bar{u}_\lambda = (u_{\lambda,\zeta\alpha}) = \begin{bmatrix} C(\lambda) \\ S(\lambda) \end{bmatrix}. \tag{48}$$

The density matrix $Q = (Q_{\zeta\eta})$ can be expressed

$$Q = \bar{u}_\lambda \bar{u}_\lambda^\dagger = \begin{bmatrix} C^2(\lambda), C(\lambda)S^\dagger(\lambda) \\ S(\lambda)C(\lambda), S(\lambda)S^\dagger(\lambda) \end{bmatrix}. \tag{49}$$

Using the following formulas analogous to twice-angle formulas of triangular functions

$$\begin{aligned} 2C^2(\lambda) - 1_n &= C(2\lambda), \\ 2S(\lambda)C(\lambda) &= S(2\lambda), \\ 1_{N-n} - 2S(\lambda)S^\dagger(\lambda) &= \tilde{C}(2\lambda), \end{aligned} \tag{50}$$

we obtain

$$Q = \frac{1}{2}\begin{bmatrix} 1_n + C(2\lambda), S^\dagger(2\lambda) \\ S(2\lambda), 1_{N-n} - \tilde{C}(2\lambda) \end{bmatrix}. \tag{51}$$

The HF energy functional is given in terms of Q by

$$E_H(\Phi) = \langle \Phi | H | \Phi \rangle = V + h_{\zeta\eta} Q_{\eta\zeta} + \tfrac{1}{2}[\zeta\eta|\iota\kappa] Q_{\eta\zeta} Q_{\kappa\iota}. \tag{52}$$

Equation (52) can be rewritten

$$\begin{aligned} E_H(\Phi) &= E_H(\Psi) + F_{\zeta\eta}(Q-P)_{\eta\zeta} + \tfrac{1}{2}[\zeta\eta|\iota\kappa](Q-P)_{\eta\zeta}(Q-P)_{\kappa\iota}, \\ F_{\zeta\eta} &= h_{\zeta\eta} + [\xi\eta|\alpha\alpha], \qquad E_H(\Psi) = V + h_{\alpha\alpha} + \tfrac{1}{2}[\alpha\alpha|\beta\beta], \end{aligned} \tag{53}$$

where $P = 1_n$ is the density matrix composed of the occupied reference orbitals ψ_α, and $F_{\zeta\eta}$ and $E_H(\Psi)$ are the Fock operator and the HF energy functional for the reference Slater determinant $|\Psi\rangle$. The HF energy functional changes its value only for transformations of orbitals to mix occupied and unoccupied ones. Hence, the parameters $\lambda_{\mu\alpha}$ are the independent parameters to affect the value of the HF energy functional and the variational space of the HF energy functional can be identified with the space of $\lambda_{\mu\alpha}$'s. Formula (53) with (51) is very useful in analysis of the energy functional since it gives a clear cut dependence of the energy functional on the independent variational parameters.

We can introduce the representation of orbitals to diagonalize the matrix λ. We define

$$\begin{aligned} \phi_A &= \phi_\alpha v_{\alpha A}, \qquad \tilde{\phi}_A = \phi_\mu \tilde{v}_{\mu A}, \\ \psi_A &= \psi_\alpha v_{\alpha A}, \qquad \tilde{\psi}_A = \psi_\mu \tilde{v}_{\mu A}. \end{aligned} \tag{54}$$

The orbitals defined in Eq. (54) satisfy

$$\begin{aligned} \langle \psi_A | \psi_B \rangle &= \langle \tilde{\psi}_A | \tilde{\psi}_B \rangle = \delta_{AB}, \qquad \langle \psi_A | \tilde{\psi}_B \rangle = 0, \\ \langle \phi_A | \phi_B \rangle &= \langle \tilde{\phi}_A | \tilde{\phi}_B \rangle = \delta_{AB}, \qquad \langle \phi_A | \tilde{\phi}_B \rangle = 0. \end{aligned} \tag{55}$$

We obtain, from Eqs. (33) and (55),

$$\begin{aligned} \phi_A &= \psi_A \cos\lambda_A + \tilde{\psi}_A \sin\lambda_A, \\ \tilde{\phi}_A &= \tilde{\psi}_A \cos\lambda_A - \psi_A \sin\lambda_A, \end{aligned} \qquad A = 1, \ldots, k$$
$$\phi_A = \psi_A \quad \text{for } n > M \quad \text{and} \quad n \geq A > N = n,$$
$$\tilde{\phi}_A = \tilde{\psi}_A \quad \text{for } n < M \quad \text{and} \quad N - n \geq A > n. \tag{56}$$

The density matrix (51) in this representation becomes

$$(Q-P)_{\zeta\eta} = \sum_{A=1}^{k} \frac{1}{2} \begin{bmatrix} v, 0 \\ 0, \tilde{v} \end{bmatrix}_{\zeta A} \begin{bmatrix} \cos 2\lambda_A - 1, \sin 2\lambda_A \\ \sin 2\lambda_A, 1 - \cos 2\lambda_A \end{bmatrix} \begin{bmatrix} v^\dagger, 0 \\ 0, \tilde{v}^\dagger \end{bmatrix}_{A\eta}. \tag{57}$$

Substitution of Eq. (57) into Eq. (53) yields

$$\begin{aligned} E_H(\Phi) = E_H(\Psi) &+ \tfrac{1}{2} \sum_{A=1}^{k} \{k_A(1-\cos 2\lambda_A) + 1_A \sin 2\lambda_A\} \\ &+ \tfrac{1}{8} \sum_{A,B=1}^{k} \{[\tilde{A}\tilde{A} - AA | \tilde{B}\tilde{B} - AA](1-\cos 2\lambda_A)(1-\cos 2\lambda_B) \\ &+ [A\tilde{A} + \tilde{A}A | B\tilde{B} + \tilde{B}B] \sin 2\lambda_A \sin 2\lambda_B \\ &+ 2[A\tilde{A} + \tilde{A}A | \tilde{B}\tilde{B} - BB] \sin 2\lambda_A (1-\cos 2\lambda_B)\}, \\ k_A = F_{\tilde{A}\tilde{A}} - F_{AA}, &\qquad 1_A = F_{\tilde{A}A} + F_{A\tilde{A}}, \end{aligned} \tag{58}$$

where the indices A and $\tilde{A}$ represent the orbitals ψ_A and $\tilde{\psi}_A$, respectively. Expressions (58) are useful in direct optimization of the energy functional as we shall show later.

B. Group Theoretical Classification and Characterization of HF Wave Functions

The HF equation may have many solutions owing to its nonlinear character. In fact, many solutions of the UHF type with different characters in the manner breaking the symmetry have been found as mentioned in Section 1. However, there is a rather simple group theoretical rule to determine possible types of broken symmetry in HF wave functions. We consider here the group theoretical classification and characterization of HF wave functions according to Fukutome (1974a) and Ozaki and Fukutome (1978).

i. Subgroups of the Symmetry Group Consisting of Spin Rotation and Time Reversal. Hamiltonian (2) or (6) of molecules is always invariant to the symmetry group consisting of spin rotation and time reversal. We consider here the structure of the symmetry group. The case of systems with a spatial point symmetry will be considered in Section 2.B.iv. Spin orbitals ϕ_ζ are in general two component spinors and can be represented in terms of the up and down spin eigenfunctions

η_1 and η_2 as

$$\phi_\zeta(x, s) = \chi_{1\zeta}(x)\eta_1(s) + \chi_{2\zeta}(x)\eta_2(s) = \begin{bmatrix} \chi_{1\zeta} \\ \chi_{2\zeta} \end{bmatrix},$$
$$\eta_1 = \begin{bmatrix} 1 \\ 0 \end{bmatrix}, \qquad \eta_2 = \begin{bmatrix} 0 \\ 1 \end{bmatrix}. \tag{59}$$

Spin rotation and time reversal are defined on the space of two component spinor orbitals as follows.

(a). *Spin rotation*: Let σ_i, $i = 1, 2, 3$ be the Pauli spin matrices

$$\sigma_1 = \begin{bmatrix} 0 & 1 \\ 1 & 0 \end{bmatrix}, \qquad \sigma_2 = \begin{bmatrix} 0 & -i \\ i & 0 \end{bmatrix}, \qquad \sigma_3 = \begin{bmatrix} 1 & 0 \\ 0 & -1 \end{bmatrix}. \tag{60}$$

They satisfy

$$\{\sigma_i, \sigma_j\} = 2\delta_{ij}, \qquad \sigma_i\sigma_j = i\sigma_k \quad \text{for cyclic } i, j, k. \tag{61}$$

The spin vector on the space of two component spinors is given by

$$\mathbf{S} = \tfrac{1}{2}\hbar\boldsymbol{\sigma}, \tag{62}$$

where $\boldsymbol{\sigma} = (\sigma_1, \sigma_2, \sigma_3)$. The spin rotation around an axis $\mathbf{e}$ by an angle θ is defined by the following 2×2 matrix operating on two component spinors

$$s(\mathbf{e}, \theta) = \exp[i(\theta/2)(\mathbf{e} \cdot \boldsymbol{\sigma})] = \cos(\theta/2) + i \sin(\theta/2)(\mathbf{e} \cdot \boldsymbol{\sigma}), \tag{63}$$

where $\mathbf{e} = (e_1, e_2, e_3)$ is a unit vector, $\mathbf{e}^2 = 1$. The matrix $s(\mathbf{e}, \theta)$ induces a rotation of the spin vector:

$$\begin{aligned} &s(\mathbf{e}, \theta)(\mathbf{e} \cdot \boldsymbol{\sigma})s^{-1}(\mathbf{e}, \theta) = (\mathbf{e} \cdot \boldsymbol{\sigma}), \\ &s(\mathbf{e}, \theta)(\mathbf{e}' \cdot \boldsymbol{\sigma})s^{-1}(\mathbf{e}, \theta) = \cos\theta(\mathbf{e}' \cdot \boldsymbol{\sigma}) + \sin\theta(\mathbf{e}'' \cdot \boldsymbol{\sigma}), \\ &s(\mathbf{e}, \theta)(\mathbf{e}'' \cdot \boldsymbol{\sigma})s^{-1}(\mathbf{e}, \theta) = \cos\theta(\mathbf{e}'' \cdot \boldsymbol{\sigma}) - \sin\theta(\mathbf{e}' \cdot \boldsymbol{\sigma}), \end{aligned} \tag{64}$$

where $\mathbf{e}$, $\mathbf{e}'$, and $\mathbf{e}''$ are orthogonal unit vectors forming a right-hand coordinate system and we have used Eq. (61) and

$$s^{-1}(\mathbf{e}, \theta) = s(\mathbf{e}, -\theta). \tag{65}$$

We denote the three dimensional rotation (64) of the spin vector as

$$s(\mathbf{e}, \theta)\boldsymbol{\sigma}s^{-1}(\mathbf{e}, \theta) = R(\mathbf{e}, \theta)\boldsymbol{\sigma}. \tag{66}$$

All the spin rotations (63) form a group S that is identical with the SU(2) (two dimensional special unitary) group. The range of the angle θ must be taken to be $0 \leq \theta \leq 4\pi$ because $s(\mathbf{e}, \theta)$ and $-s(\mathbf{e}, \theta) = s(\mathbf{e}, \theta + 2\pi)$ induce the same rotation of the spin vector that is the well known double value correspondence of the SO(3) (three dimensional special orthogonal) group to the SU(2) group. We denote the operation of spin rotation on spin orbitals as

$$\phi_\zeta^s = s\phi_\zeta. \tag{67}$$

(b). *Time reversal*: The operation of time reversal t on spin orbitals is defined by

$$\phi_\zeta^t = \rho\phi_\zeta^* = \begin{bmatrix} -\chi_{2\zeta}^* \\ \chi_{1\zeta}^* \end{bmatrix}, \qquad \rho = -i\sigma_2 = \begin{bmatrix} 0 & -1 \\ 1 & 0 \end{bmatrix}. \tag{68}$$

The twice operation of t leads to inversion of the phase of spin orbitals

$$(\phi_\zeta^t)^t = -\phi_\zeta, \qquad t^2 = -1. \tag{69}$$

The group T generated by time reversal t therefore consists of four elements, $T = \{1, -1, t, -t\}$.

The operation of t on the spin vector is given by

$$\boldsymbol{\sigma}^t = \rho\boldsymbol{\sigma}^*\rho^{-1} = \sigma_2(\sigma_1, -\sigma_2, \sigma_3)\sigma_2 = -\boldsymbol{\sigma}, \tag{70}$$

namely, time reversal inverts the direction of the spin vector. Time reversal does not affect spin rotation

$$s^t(\mathbf{e}, \theta) = \rho s^*(\mathbf{e}, \theta)\rho^{-1} = s(\mathbf{e}, \theta), \tag{71}$$

and the group T is commutable with the group S. Therefore, we can write the symmetry group consisting of spin rotation and time reversal in the direct product form $S \times T$.

(c). *Subgroups of the symmetry group* $S \times T$: The set $A(\mathbf{e}) = \{s(\mathbf{e}, \theta), 0 \leq \theta < 4\pi\}$ of all the spin rotations around a fixed axis $\mathbf{e}$ forms a continuous subgroup of S. No other continuous subgroup of S exists except the subgroups of this type.

The presence of a discrete element t yields the following subgroups in $S \times T$. The product of t and a spin rotation $s(\mathbf{e}', \pi)$ by the angle π is a twofold element

$$[ts(\mathbf{e}', \pi)]^2 = 1, \tag{72}$$

because $t^2 = -1$ and $s^2(\mathbf{e}', \pi) = s(\mathbf{e}', 2\pi) = -1$. So that the set $M(\mathbf{e}') = \{1, ts(\mathbf{e}', \pi)\}$ consisting of two elements is a subgroup of $S \times T$.

In connection with this subgroup, we define a symmetry operation $m_\mathbf{e}$ called the magnetic operation by

$$\begin{aligned} &m_\mathbf{e} = ts(\mathbf{e}, \pi) = i(\mathbf{e} \cdot \boldsymbol{\sigma})t, \qquad m_\mathbf{e}^2 = 1, \\ &\phi_\zeta^{m_\mathbf{e}} = i(\mathbf{e} \cdot \boldsymbol{\sigma})\rho\phi_\zeta^*. \end{aligned} \tag{73}$$

The operation of $m_\mathbf{e}$ on the spin vector does not affect its component parallel to $\mathbf{e}$ but inverts its component orthogonal to $\mathbf{e}$,

$$\begin{aligned} &\boldsymbol{\sigma}^{m_\mathbf{e}} = (\mathbf{e} \cdot \boldsymbol{\sigma})\rho\boldsymbol{\sigma}^*\rho^{-1}(\mathbf{e} \cdot \boldsymbol{\sigma}), \\ &(\mathbf{e} \cdot \boldsymbol{\sigma}^{m_\mathbf{e}}) = (\mathbf{e} \cdot \boldsymbol{\sigma}), \qquad (\mathbf{e}' \cdot \boldsymbol{\sigma}^{m_\mathbf{e}}) = -(\mathbf{e}' \cdot \boldsymbol{\sigma}). \end{aligned} \tag{74}$$

We note that when $\mathbf{e} = y = (0, 1, 0)$ the magnetic operation m_y is identical with complex conjugation

$$\phi_\zeta^{m_y} = \phi_\zeta^*. \tag{75}$$

The product $A(\mathbf{e})M(\mathbf{e}') = \{s(\mathbf{e}, \theta),\ ts(\mathbf{e}',\ \pi)s(\mathbf{e}, \theta);\ 0 \leq \theta < 4\pi\}$ of the two subgroups $A(\mathbf{e})$ and $M(\mathbf{e}')$ with orthogonal $\mathbf{e}$ and $\mathbf{e}'$ is also a subgroup of $S \times T$ owing to the relation

$$s(\mathbf{e}', \pi)s(\mathbf{e}, \theta) = s(\mathbf{e}, -\theta)s(\mathbf{e}', \pi), \qquad \mathbf{e} \cdot \mathbf{e}' = 0. \tag{76}$$

It is evident that S, T, $A(\mathbf{e}) \times T$, and $E = \{1, -1\}$ are subgroups of $S \times T$. The groups listed above exhaust all the subgroups of $S \times T$. We show in Figure 1 the structure of the symmetry group $S \times T$, namely, its subgroups and their inclusion relations. The group structure of $S \times T$ determines group theoretically distinguishable classes of HF wave functions and their interconnection relation via instabilities as we shall show in the Section 2.B.ii and in Section 2.C.

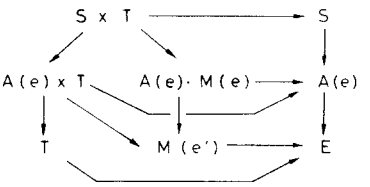

Figure 1. Subgroups of $S \times T$. Arrows indicate the inclusion relation of the subgroups.

ii. Classification of HF Wave Functions by Their Invariance Groups. Let g be an element of the symmetry group $S \times T$ to leave a Slater determinant $|\Phi\rangle$ invariant except for a change in the phase of $|\Phi\rangle$,

$$|\Phi^g\rangle = e^{i\delta}|\Phi\rangle. \tag{77}$$

It is easy to see that all the g's used to satisfy condition (77) form a subgroup G of $S \times T$. We call group G the invariance group of $|\Phi\rangle$. This fact provides the basis for group theoretical classification of HF wave functions. Since the groups of eight kinds given in Figure 1 exhaust all the subgroups of $S \times T$, the invariance group G of an HF wave function must be either one of them. Therefore, HF wave functions are classified into eight classes with distinct responses to spin rotation and time reversal according to the type of their invariance groups. We show in Table I the names of the eight classes of HF wave functions, which have the invariance groups at the corresponding positions of Figure 1, proposed by the author (Fukutome, 1974a).

The eight classes of HF wave functions listed in Table I exhaust all the group theoretically possible ways to break spin and time reversal symmetries forming a hierarchy of broken symmetry. The classes invariant to all spin rotations are called S invariant. The classes invariant only to the spin rotations in the subgroup $A(\mathbf{e})$ are called $S_{\mathbf{e}}$ axial. The classes not invariant to any spin rotation are called S torsional. These namings are due to the spin structures of the classes as we shall discuss below. The S invariant, S axial, and S torsional classes have wave functions of closed shell type, of different orbitals for different spins (DODS) type, and with general spin orbitals (GSO), respectively, as we shall show in

TABLE I. Classification of HF wave functions.

	T invariant	M invariant	TM noninvariant
S invariant (closed shell)	Time reversal invariant closed shell (TICS)		Charge current wave (CCW)
S axial (DODS)	Axial spin current wave (ASCW)	Axial spin density wave (ASDW)	Axial spin wave (ASW)
S torsional (GSO)	Torsional spin current wave (TSCW)	Torsional spin density wave (TSDW)	Torsional spin wave (TSW)

Section 2.B.iii. The classes invariant to time reversal are called T invariant. The classes invariant to the magnetic operation m_e are called M_e invariant. The classes invariant neither to t nor m_e are called TM noninvariant. The names of the eight classes also are due to their spin and charge structures.

The first concrete example of ASDW wave function was Slater's (1951) "antiferromagnetic" solution in the hydrogen molecule. The Matsubara–Yokota (1954) split band model for antiferromagnets and the Löwdin (1954) and Itoh–Yoshizumi (1955) alternant orbitals also belong to this class. Overhauser's (1960, 1962) helical SDW was the first example of TSDW. UHF solutions belonging to CCW and ASCW classes were obtained first by Čižek and Paldus (1967) in polyenes and also by Halperin and Rice (1968) in solid. CCW and ASCW solutions in two electron system were obtained by Pople (1971), Ostlund (1972), Fukutome (1973b), and Jordan and Silbey (1973). First examples of the HF ground state of TSW and ASW types in molecular systems were obtained by Fukutome et al. (1975) and Takahashi and Fukutome (1978). The five classes TICS, ASDW, TSDW, ASW, and TSW have been known to appear as the HF ground state in molecules and chemical reactions. Examples of those UHF ground states will be discussed in Section 3.

The physical properties characterizing the eight classes of HF wave functions can be obtained from the structure of the density matrix. Here, we use the spin orbital basis ψ_ζ separable to spatial orbitals ψ_i and spin eigenfunctions η_r,

$$\psi_\zeta = \psi_i \eta_r, \qquad i = 1, 2, \ldots, M, \qquad r = 1, 2. \tag{78}$$

Then, the density matrix $Q = (Q_{\zeta\eta}) = (Q_{ir,js})$ can be decomposed into the number density matrix $N = (N_{ij})$ and the spin density matrix $\mathbf{S} = (\mathbf{S}_{ij})$ as

$$\begin{aligned} Q &= \begin{bmatrix} Q_{11} & Q_{12} \\ Q_{21} & Q_{22} \end{bmatrix} = N + \mathbf{S} \cdot \boldsymbol{\sigma}, \\ N &= \tfrac{1}{2}(Q_{11} + Q_{22}), \qquad S_1 = \tfrac{1}{2}(Q_{21} + Q_{12}), \\ S_2 &= (1/2i)(Q_{21} - Q_{12}), \qquad S_3 = \tfrac{1}{2}(Q_{11} - Q_{22}), \end{aligned} \tag{79}$$

where Q_{rs} is the $M \times M$ matrix $(Q_{ir,js})$. We may use real spatial orbital basis ψ_i without loss of generality. The electron density $N(x)$, the spin densitity $\mathbf{S}(x)$, the electron current density $\mathbf{j}(x)$ and the spin current density $\mathbf{J}_k(x)$, $k = 1, 2, 3$ in an HF state $|\Phi\rangle$ are given by

$$\begin{aligned} N(x) &= \psi_i(x)\psi_j(x)N_{ij}, \\ \mathbf{S}(x) &= \psi_i(x)\psi_j(x)\mathbf{S}_{ij}, \\ \mathbf{j}(x) &= (\hbar/im)(\nabla\psi_i(x)\cdot\psi_j(x) - \psi_i(x)\nabla\psi_j(x))N_{ij}, \\ \mathbf{J}_k(x) &= (\hbar/im)(\nabla\psi_i(x)\cdot\psi_j(x) - \psi_i(x)\nabla\psi_j(x))S_{k,ij}. \end{aligned} \tag{80}$$

Hence, the symmetric parts of N and $\mathbf{S}$ contribute to the electron and spin densities, respectively, but their antisymmetric parts to the electron and spin current densities. Since N and $\mathbf{S}$ are hermitian their symmetric parts are real and the antisymmetric ones are imaginary.

The density matrix is transformed by spin rotation, time reversal and magnetic operation as follows:

spin rotation:

$$\begin{gathered} Q^s = sQs^{-1} = N + \mathbf{S}\cdot s\boldsymbol{\sigma}s^{-1} = N + \mathbf{S}\cdot R\boldsymbol{\sigma} = N + R^{-1}\mathbf{S}\cdot\boldsymbol{\sigma}, \\ N^s = N, \qquad \mathbf{S}^s = R^{-1}\cdot\mathbf{S}. \end{gathered} \tag{81}$$

time reversal:

$$\begin{gathered} Q^t = \rho Q^*\rho^{-1} = N^* + \mathbf{S}^*\cdot\boldsymbol{\sigma}^t = N^* - \mathbf{S}^*\cdot\boldsymbol{\sigma}, \\ N^t = N^*, \qquad \mathbf{S}^t = -\mathbf{S}^*. \end{gathered} \tag{82}$$

magnetic operation:

$$\begin{aligned} Q^{m_e} &= (\mathbf{e}\cdot\boldsymbol{\sigma})Q^t(\mathbf{e}\cdot\boldsymbol{\sigma}) = N^* - \mathbf{S}^*\cdot(\mathbf{e}\cdot\boldsymbol{\sigma})\boldsymbol{\sigma}(\mathbf{e}\cdot\boldsymbol{\sigma}), \\ &= N^* - \mathbf{S}^*\cdot\mathbf{e}(\mathbf{e}\cdot\boldsymbol{\sigma}) + \mathbf{S}^*\cdot(\boldsymbol{\sigma} - \mathbf{e}(\mathbf{e}\cdot\boldsymbol{\sigma})), \\ S_{\parallel}^{m_e} &= -S_{\parallel}^*, \qquad \mathbf{S}_{\perp}^{m_e} = \mathbf{S}_{\perp}^*, \end{aligned} \tag{83}$$

where $\mathbf{S}_{\parallel}$ and $\mathbf{S}_{\perp}$ are the components of the vector $\mathbf{S}$ parallel and transverse to $\mathbf{e}$, respectively. From Eqs. (81) and (83), we see that invariance requirements impose the following restrictions on N and $\mathbf{S}$:

$$\begin{aligned} \text{invariance to } S\text{:} \quad & \mathbf{S} = 0; \\ \text{invariance to } A(\mathbf{e})\text{:} \quad & \mathbf{S}_{\perp} = 0; \\ \text{invariance to } t\text{:} \quad & N^* = N,\ \mathbf{S}^* = -\mathbf{S}; \\ \text{invariance to } m_{\mathbf{e}}\text{:} \quad & N^* = N,\ \mathbf{S}_{\perp}^* = \mathbf{S}_{\perp},\ \mathbf{S}_{\parallel}^* = -\mathbf{S}_{\parallel}. \end{aligned} \tag{84}$$

Combining the conditions in Eqs. (84), we have the structures of the density matrix in the eight classes as summarized in Table II. We use in Table II the following notation for real and imaginary parts of N and $\mathbf{S}$,

$$N = n + i\tilde{n}, \qquad \mathbf{S} = \mathbf{s} + i\tilde{\mathbf{s}}. \tag{85}$$

TABLE II. Density matrix in the eight classes of HF wave functions.[a]

	T invariant	$M_{e'}$ invariant	TM noninvariant
S invariant		n	N
S_e axial	$n+i\tilde{s}(\mathbf{e}\cdot\boldsymbol{\sigma})$	$n+s(\mathbf{e}\cdot\boldsymbol{\sigma})$	$N+S(\mathbf{e}\cdot\boldsymbol{\sigma})$
S torsional	$n+i\tilde{\mathbf{s}}\cdot\boldsymbol{\sigma}$	$n+i\tilde{s}(\mathbf{e}'\cdot\boldsymbol{\sigma})+\mathbf{s}_\perp\cdot\boldsymbol{\sigma}$	$N+\mathbf{S}\cdot\boldsymbol{\sigma}$

[a] n, s, $\mathbf{s}_\perp$: real symmetric; $\mathbf{s}_\perp$: orthogonal to $\mathbf{e}'$, $\mathbf{e}'\cdot\mathbf{s}_\perp=0$; $\tilde{s}$, $\tilde{\mathbf{s}}$: real antisymmetric; N, S, $\mathbf{S}$: complex Hermitian; $\mathbf{e}\cdot\mathbf{e}'=0$.

The real parts n and $\mathbf{s}$ contribute to the electron and spin densities, while the imaginary parts $\tilde{n}$ and $\tilde{\mathbf{s}}$ to the electron and spin current densities. Only the TM noninvariant classes have an electron current density. The S invariant classes have neither spin nor spin current densities. The T invariant classes, ASCW and TSCW, have a spin current density but have no spin density. The ASDW class has a spin density but has no spin current density. The three classes, ASW, TSDW, and TSW, have both spin and spin current densities.

We show in Figure 2 schematically the ways of spin modulation in the S axial and S torsional classes. The S axial classes have one dimensional modulation of spin vector in the direction of the vector $\mathbf{e}$. The TSCW class has three dimensional modulation of spin current density vector. The TSW class has three dimensional modulations of spin density and spin current density vectors. In TSDW class, the spin density vector is modulated two dimensionally in the directions orthogonal to the vector $\mathbf{e}'$, while the spin current density vector is modulated one dimensionally in the direction of the vector $\mathbf{e}'$. We summarize in Table III the properties of the eight classes.

iii. Structure of the Orbitals. The condition (77) for invariance of a Slater determinant $|\Phi\rangle$ means that $|\Phi\rangle$ spans a one dimensional irreducible representation of the invariance group G. This condition implies that the occupied spin orbitals φ_α span a, in general reducible, representation of G, namely, there is a unitary matrix $W(g)$ within the space of occupied orbitals for every g in G such

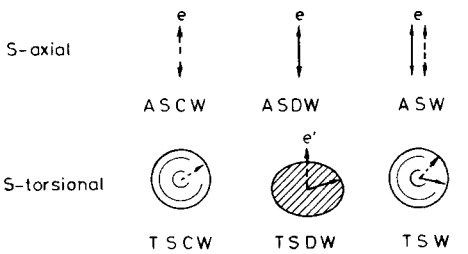

Figure 2. Modes of spin modulation in the six UHF classes. Arrow and dashed arrow represent spin density and spin current density vectors, respectively. Circle and sphere represent two and three dimensional modulations, respectively.

TABLE III. Spin and charge properties of the eight classes of HF wave functions.[a]

	Charge current	Spin density	Spin current
TICS	x	x	x
CCW	o	x	x
ASCW	x	x	o
ASDW	x	o	x
ASW	o	o	o
TSCW	x	x	o
TSDW	x	o	o
TSW	o	o	o

[a] o and x represent the presence and absence of the relevant property, respectively.

that

$$\varphi_\alpha^g = \varphi_\beta W_{\beta\alpha}(g), \qquad |\Phi^g\rangle = \det[W(g)]|\Phi\rangle. \tag{86}$$

Therefore, the set of occupied orbitals, after a suitable unitary transformation, consists of irreducible representations of G. This fact enable us to determine the structure of orbitals in the eight classes of HF wave functions.

Determination of irreducible representations for the four groups S, T, $A(z)$ and $M(y)$ is sufficient for determining the structure of orbitals in all the eight classes.

S: It is well known that η_1 and η_2 are the bases of the irreducible two dimensional spinor representation of S. Hence, a pair of spin orbitals

$$\varphi_{i1} = \phi_i \eta_1, \qquad \varphi_{i2} = \phi_i \eta_2, \tag{87}$$

with a common spatial orbital ϕ_i forms an irreducible two dimensional representation of S. No other kind of irreducible representation of S can be constructed in the space of spin orbitals with $\frac{1}{2}$ spin. Therefore, Slater determinants of S invariant classes have to be of closed shell type. The spatial orbitals ϕ_i are in general complex.

$A(z)$ is an Abelian group, all its irreducible representations are one dimensional. η_1 and η_2, respectively, are the bases of one dimensional irreducible representations of $A(z)$. The representations on η_1 and η_2 are inequivalent. Hence, each spin orbital with up (+) and down (−) spin

$$\varphi_{i1} = \phi_i^+ \eta_1, \qquad \varphi_{i2} = \phi_i^- \eta_2, \tag{88}$$

belongs to a one dimensional irreducible representation of $A(z)$. Because of the inequivalence of the representations on η_1 and η_2, the spatial orbitals ϕ_i^+ and ϕ_i^- for up and down spins can be chosen independently and the numbers of up and down spin orbitals in a Slater determinant may be different. Therefore,

Slater determinants of the S axial classes are of DODS type. The spatial orbitals ϕ_i^+ are in general complex.

T: We note that there is no spin orbital belonging to one dimensional irreducible representation of T because if such a φ exists then it must satisfy $\varphi^t = e^{i\delta}\varphi$ but $-\varphi = (\varphi^t)^t = (e^{i\delta}\varphi)^t = e^{i\delta}\varphi^t = \varphi$ so that $\varphi = 0$. The spin eigenfunctions η_1 and η_2 are transformed by t as

$$\eta_1^t = \eta_2, \qquad \eta_2^t = -\eta_1, \tag{89}$$

so that they span a two dimensional irreducible representation of T. Consequently, a pair of spin orbitals in the form

$$\varphi_{i1} = \chi_i\eta_1 + \chi_i'^*\eta_2, \qquad \varphi_{i2} = \chi_i^*\eta_2 - \chi_i'\eta_1, \tag{90}$$

span a two dimensional irreducible representation of T because φ_{i1} and φ_{i2} are transformed by t in the same manner as η_1 and η_2

$$\varphi_{i1}^t = \varphi_{i2}, \qquad \varphi_{i2}^t = -\varphi_{i1}. \tag{91}$$

The orthonormal conditions

$$\begin{aligned}
&\langle\varphi_{i1}|\varphi_{j1}\rangle = \langle\chi_i|\chi_j\rangle + \langle\chi_j'|\chi_i'\rangle = \delta_{ij},\\
&\langle\varphi_{i2}|\varphi_{j2}\rangle = \langle\chi_j|\chi_i\rangle + \langle\chi_i'|\chi_j'\rangle = \delta_{ij},\\
&\langle\varphi_{i1}|\varphi_{j2}\rangle = -\langle\chi_i|\chi_j'\rangle + \langle\chi_j|\chi_i'\rangle = 0,
\end{aligned} \tag{92}$$

must be satisfied by the spatial functions χ_i and χ_i'. Slater determinants of the T-invariant classes therefore consist of pairs of spin orbitals in the form (90) and the number of electrons n must be even.

$M(y)$: Since the magnetic operation My is identical with complex conjugation, Eq. (75), a real spin orbital spans a one dimensional irreducible representation of $M(y)$. No irreducible representation of other type exists as can be easily verified. Hence, Slater determinants of the My-invariant classes consist of real spin orbitals.

Irreducible representations of $A(\mathbf{e})$ and $M(\mathbf{e}')$ are obtained from those of $A(z)$ and $M(y)$ by making a spin rotation to bring z and y axes to $\mathbf{e}$ and $\mathbf{e}'$ axes.

Combining the above results, we obtain the characterization for the structure of orbitals in the eight classes as shown in Table IV. We note that ASCW is the complex DODS whose up and down spin spatial orbitals are complex conjugate of each other.

We next derive standard forms of orbitals which are useful in later applications.

GSO: The spatial functions of GSO's have to satisfy the normalization condition

$$\begin{aligned}
&\varphi_\zeta = \chi_{1\zeta}\eta_1 + \zeta_{2\zeta}\eta_2,\\
&\langle\varphi_\zeta|\varphi_\eta\rangle = \langle\chi_{1\zeta}|\chi_{1\eta}\rangle + \langle\chi_{2\zeta}|\chi_{2\eta}\rangle = \delta_{\zeta\eta}.
\end{aligned} \tag{93}$$

TABLE IV. Structure of orbitals in the eight classes of HF wave functions.[a]

Closed shell	TICS	real	n = even	
	CCW	complex	n = even	
DODS	ASCW	complex	n = even	$\phi_i^- = \phi_i^{+*}$
	ASDW	real	n = even, odd	
	ASW	complex	n = even, odd	
GSO	TSCW	complex	n = even	Eq. (98)
	TSDW	real	n = even, odd	
	TSW	complex	n = even, odd	

[a] n is the electron number. Real and complex mean that the orbitals can be and cannot be brought into real ones by a unitary transformation within occupied orbitals, respectively. The last column shows the constraint for ASCW and TSCW orbitals.

The matrix $(\langle\chi_{1\alpha}|\chi_{1\beta}\rangle)$ composed of the occupied orbitals is hermitian and positive definite, so that there is a $U(n)$ matrix $V=(V_{\alpha\beta})$ such that

$$\begin{aligned} V_{\gamma\alpha}^{*}\langle\chi_{1\gamma}|\chi_{1\delta}\rangle V_{\delta\beta} &= \delta_{\alpha\beta}\cos^2\kappa_\alpha, \\ V_{\gamma\alpha}^{*}\langle\chi_{2\gamma}|\chi_{2\delta}\rangle V_{\delta\beta} &= \delta_{\alpha\beta}\sin^2\kappa_\alpha. \end{aligned} \tag{94}$$

Then we obtain the spatial orbitals $\phi_\alpha^\pm$, which are orthonormal within + and − families, respectively,

$$\begin{aligned} \chi_{1\beta}V_{\beta\alpha} &= \phi_\alpha^+\cos\kappa_\alpha, \\ \chi_{2\beta}V_{\beta\alpha} &= \phi_\alpha^-\sin\kappa_\alpha. \\ \langle\phi_\alpha^\pm|\phi_\beta^\pm\rangle &= \delta_{\alpha\beta}. \end{aligned} \tag{95}$$

Making the unitary transformation by V, we obtain the standard form of GSO's

$$\varphi_\alpha = \phi_\alpha^+\cos\kappa_\alpha\eta_1 + \phi_\alpha^-\sin\kappa_\alpha\eta_2. \tag{96}$$

In the TSW and TSDW classes, $\phi_\alpha^\pm$ are complex and real, respectively.

In the TSCW class, orbitals are in the form of (90) and the orbital indices α's are in pairs of $a1$ and $a2$, $a=1,\cdots,n/2$. Substitution of Eq. (96) into Eq. (90) and use of Eq. (92) shows

$$\phi_{ar}^- = \phi_{ar}^{+*}, \qquad \kappa_{a2} = \kappa_{a1} + \tfrac{1}{2}\pi. \tag{97}$$

We then obtain the standard form of TSCW orbitals

$$\begin{aligned} \varphi_{a1} &= \phi_{a1}\cos\kappa_a\eta_1 + \phi_{a2}^{*}\sin\kappa_a\eta_2, \\ \varphi_{a2} &= \phi_{a1}^{*}\cos\kappa_a\eta_2 - \phi_{a2}\sin\kappa_a\eta_1, \end{aligned} \tag{98}$$

where $\kappa_a = \kappa_{a1}$ and $\phi_{ar} = \phi_{ar}^+$.

DODS: In DODS cases, the numbers n_1 and n_2 of occupied up and down spin orbitals may be different and we denote the occupied up and down spin spatial

orbitals by the indices $a1 = 1, \ldots, n_1$ and $a2 = 1, \ldots, n_2$. The $n_2 \times n_1$ matrix $(\langle \phi^-_{a2} | \phi^+_{a1} \rangle)$ can be diagonalized in the same manner as Eq. (36),

$$\langle \phi^-_{a2} | \phi^+_{a1} \rangle = \sum_{A=1}^{k} \tilde{W}_{a2,A} \cos 2\kappa_A W^*_{a1,A}, \tag{99}$$

where $k = \min(n_1, n_2)$. We define

$$\phi^+_A = \phi^+_{a1} W_{a1,A}, \qquad \phi^-_A = \phi^-_{a2} \tilde{W}_{a2,A}. \tag{100}$$

These orbitals satisfy

$$\langle \phi^\pm_A | \phi^\pm_B \rangle = \delta_{AB}, \qquad \langle \phi^+_A | \phi^-_B \rangle = \delta_{AB} \cos 2\kappa_A. \tag{101}$$

Equation (101) shows that the following orbitals are orthonormal:

$$\begin{aligned} \phi_A &= (\phi^+_A + \phi^-_A)/2 \cos \kappa_A, \\ \bar{\phi}_A &= (\phi^+_A - \phi^-_A)/2 \sin \kappa_A, \\ \langle \phi_A | \phi_B \rangle &= \langle \bar{\phi}_A | \bar{\phi}_B \rangle = \delta_{AB}, \qquad \langle \phi_A | \bar{\phi}_B \rangle = 0. \end{aligned} \tag{102}$$

Then we get the standard form for DODS spatial orbitals

$$\begin{aligned} &\phi^\pm_A = \phi_A \cos \kappa_A \pm \bar{\phi}_A \sin \kappa_A, \qquad A = 1, \ldots, k, \\ &\phi^+_A = \phi_A \quad \text{for } n_1 > n_2 \quad \text{and} \quad n_1 > A > n_2, \\ &\phi^-_A = \bar{\phi}_A \quad \text{for } n_1 < n_2 \quad \text{and} \quad n_2 > A > n_1. \end{aligned} \tag{103}$$

This representation for DODS orbitals was obtained by Amos and Hall (1961). The orbital pair $\phi^\pm_A$ is called the corresponding orbitals and the orthonormal orbitals ϕ_A and $\bar{\phi}_A$ the DODS natural orbitals (NO). In the ASW and ASDW classes, DODS NO's are complex and real, respectively. In the ASCW class, $n_1 = n_2$ and ϕ^+_A and ϕ^-_A are complex conjugate to each other, so that ϕ_A's are real but $\bar{\phi}_A$'s are imaginary.

We note that a closed shell RHF wave function belongs to either of TICS or CCW class and an open shell one to ASDW or ASW.

iv. Classification of HF Wave Functions in a System with a Spatial Point Symmetry. Here we consider classification of HF wave functions in a system with a spatial point symmetry group P. The symmetry group of such a system is $S \times T \times P$. According to the principle mentioned in Section 2.B.ii, classification of all possible types of HF wave functions with distinct broken symmetries can be achieved by listing up all subgroups of the symmetry group $S \times T \times P$. The problem was solved by Ozaki and Fukutome (1978). To list up all subgroups of $S \times T \times P$ is not so simple as the case of $S \times T$ and we give here only an outline.

Ozaki and Fukutome's listing up procedure bases on the fact that the $O(3)$ (three dimensional orthogonal) group is isomorphic in a double valued manner to the group $S \times T$ because a proper rotation R in $O(3)$ can be corresponded to spin rotations s and $-s$ and inversion in $O(3)$ to time reversal t which inverts the spin vector. Since P is a discrete subgroup of $O(3)$, it can be homomorphically

embedded into $S \times T$. Let $h_\pm$ be a double valued homomorphism of P into $S \times T$ and $g(h_\pm(p))$ be the element in $S \times T$ which is the image of an element p in P by the homomorphism $h_\pm$. Note that $g(h_-(p)) = -g(h_+(p))$. The set

$$_{II}P_h = \{pg(h_\pm(p)); p \in P\}, \tag{104}$$

obviously forms a subgroup of $S \times T \times P$. In the group $_{II}P_h$, the spin vector is rotated jointly with spatial rotations P in a manner homomorphic to P. Let P' be a subgroup of P. The set

$$_{II}P'_h = \{p'q(h_\pm(p')); p' \in P'\} \tag{105}$$

constructed from P' with the same manner as $_{II}P_h$ is also a subgroup of $S \times T \times P$. The subgroups in the forms of (104) and (105) exhaust all the subgroups of $S \times T \times P$ which do not contain elements consisting only of spin rotation and time reversal. We call these subgroup the subgroups of TSW type because the HF wave functions having the invariance groups of this type belong to the TSW class. The subgroups of TSW type include as special cases the double groups and magnetic groups constructed from P or P' (for double groups and magnetic groups see, Bradley and Cracknell, 1972) and may be called generalized magnetic double groups. The left-hand side index II denotes the double group nature of the groups.

The well known homomorphism theorem shows that the set N of p's,

$$N = \{p; h_\pm(p) = \pm 1\}, \tag{106}$$

whose homomorphic image in $S \times T$ is the subgroup $E = \{1, -1\}$ with no rotation of the spin vector, is a normal subgroup of P and the homomorphism $h_\pm$ for P becomes an isomorphism $I_\pm$ of the factor group $F = P/N$ into $S \times T$. Therefore, the group $_{II}P_h$ can be specified by a normal subgroup N of P, the factor group $F = P/N$ and an isomorphism I of F,

$$_{II}P_h = \{p_N, fg(I_\pm(f)); p_N \in N, f \in F\} \equiv {}_{II}P(N, F, I). \tag{107}$$

Isomorphisms I' and I of F are physically equivalent if there is an element $g' \in S \times T$ such that

$$g(I'_\pm(f)) = g'g(I_\pm(f))g'^{-1}, \tag{108}$$

because an HF wave function with the invariance group $_{II}P(N, F, I')$ can be transformed by the symmetry operation g' to the one with the invariance group $_{II}P(N, F, I)$. Therefore, listing up of all invariance groups in the form of $_{II}P_h$ is achieved by listing up all normal subgroups N of P and all inequivalent isomorphisms of the factor groups $F = P/N$. Inequivalent isomorphisms of a point group F consist of outer automorphisms of F and isomorphic mappings of F to the other point group $\bar{F}$ with isomorphic structure to F, for instance, the point groups C_{2m}, S_{2m}, and C_{mh} have isomorphic structures. The same situation holds also for the group $_{II}P'_h$ and it is specified by a normal subgroup N' of P', the factor

group $F' = P'/N'$ and an isomorphism I' of F',

$$_{II}P'_h = \{p'_N, f'g(I'_{\pm}(f')); p'_N \in N', f' \in F'\} \equiv {}_{II}P'(N', F', I'). \quad (109)$$

It is to be noted that a normal subgroup N' of P' may not be a normal subgroup of P. Complete listing up of normal subgroups and outer automorphisms of all point groups were given by Ozaki and Fukutome (1978).

All subgroups of $S \times T \times P$ are obtained as the intersections of the eight subgroups of $S \times T$ listed in Figure 1 with the groups ${}_{II}P(N, F, I)$ and ${}_{II}P'(N', F', I')$. For an intersection to be a group, an admissibility condition must be satisfied, but we do not enter into the problem here.

An HF wave function with the invariance group ${}_{II}P(N, F, I)$ is invariant to the spatial rotations in the normal subgroup N but not invariant to the ones not included in N. However, it becomes invariant if the spin rotation by $g(I \pm (f))$ is made simultaneously with the spatial rotations in the form of $p_N f$, $p_N \in N$, $f \in F$, and $\neq 1$. This shows that the HF wave function has an ordered spin structure determined by N, F, and I.

The spin structure can be visualized as follows. Put a spin vector **S** on an atomic orbital χ. The AO which is obtained from χ by a spatial rotation $p \in P$ is denoted $p\chi$. Put the same spin vector **S** on the AO's $p_N\chi$, $p_N \in N$, while put the spin vector $\mathbf{S}^g$ rotated by $g = g(I_{\pm}(f))$ on the AO's $p_N f\chi$, $p_N \in N$, $f \in F$, and $\neq 1$. Select another AO χ' which is not contained in the set of AO's $\{p\chi; p \in P\}$, put a spin vector **S'** on χ' and repeat the same procedure as the above. The spin arrangement on the AO's which are transformed by spatial rotations in P to each others is completely determined by the invariance group ${}_{II}P(N, F, I)$, while the magnitudes and relative orientations of the reference spin vectors **S**, **S'**, ... on the AO's which are not connected by spatial rotations in P are not determined by the invariance group. In the classes other than TSW, a restriction is imposed on the possible spin structures and relative orientations of the reference spin vectors **S**, **S'**, ..., but we do not mention about the restriction here. We illustrate in Figures 3 and 4 the possible inequivalent HF spin structures in the systems with C_6 and C_5 symmetries determined by the above rule.

A HF wave function with the invariance group ${}_{II}P'(N', F', I')$ is invariant to the spatial rotations in N' and has an ordered spin structure among the AO's $p'_N f'\chi$, $p'_N \in N'$, $f' \in F'$, and $\neq 1$. The range of the AO's with the ordered spin structure is narrower than the systems with the invariance group ${}_{II}P(N, F, I)$. Furthermore, in this case, the HF wave function is not invariant to the spatial rotations not contained in P' and has no spin order among the AO's $p\chi$, $p \notin P'$, and $\in P$. The charge densities on the AO's $p'\chi$, $p' \in P'$, are the same because the densities of up and down spin electrons on these AO's are transformed to each others by a spatial rotation p' and spin rotation $g(h'_{\pm}(p'))$. On the other hand, no such symmetry operation exists among the set of AO's $\{p\chi; p \notin P'$, and $\in P\}$. Therefore, there is a difference in the charge densities on these AO's and consequently a charge density modulation exists among the AO's $p\chi$, $p \in P$, which are originally equivalent with respect to the spatial symmetry group P. The HF wave functions with the invariance group in the type of ${}_{II}P'(N', F', I')$ are

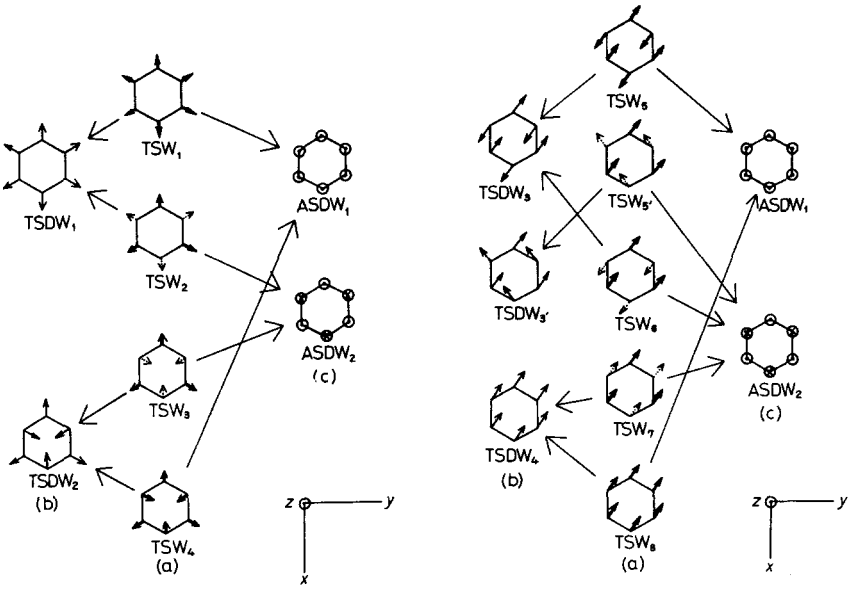

Figure 3. Possible UHF spin structures in a C_6 symmetry system. Spin vectors drawn by heavy and dotted arrows are inclined to up and down directions, respectively, against the paper plane. Those drawn by light arrow are in the paper plane. ⊙ and ⊗ represent vertical spin vectors with up and down directions, respectively.

classified as the charge density wave (CDW) category. If $N' = P'$, then there is no spin modulation and the CDW is called a pure CDW. If $N' \neq P'$, then there is a spin modulation as well as the charge density modulation and the CDW is called a mixed CDW.

Structure of orbitals in a system with the symmetry group $S \times T \times P$ can be determined by the principle mentioned in the preceding section, namely, occupied orbitals must consist of irreducible representations of the invariance group ${}_{II}P(N, F, I)$ or ${}_{II}P'(N', F', I')$. Determination of all double valued irreducible representations of a generalized magnetic double group was carried out by Ozaki (1979). The mathematical procedures involved, however, are rather complicated and readers who have interest in the subject should refer to the original paper.

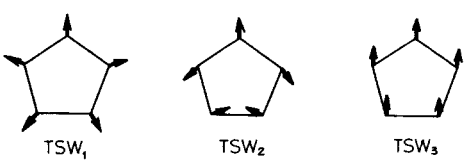

Figure 4. Possible UHF spin structures in a C_5 symmetry system.

C. *Instabilities of HF Wave Functions*

A solution of the HF equation guarantees the condition that it represents an extremum point of the HF energy functional. However, it does not necessarily represent the minimum of the HF energy functional. The condition for a HF solution to be a local minimum was given by Thouless (1960). If this condition is violated, the solution is not a local minimum and unstable and another solution with lower energy exists. There is also a simple group theoretical rule for possible type of HF instabilities and interconnection relation of HF wave functions via instabilities. We consider here the problem according to works of the author (Fukutome, 1974b, 1975).

i. Instability Criterion. We now let the reference spin orbitals ψ_ζ be a solution of the HF equation. Then, from Eqs. (53), (51), and (34) we can calculate the variation of the HF energy functional around the solution Ψ up to any desired order. For small λ, Eq. (34), up to the second order of λ, becomes

$$S(\lambda) \simeq \lambda, \qquad C(\lambda) \simeq l_n - \tfrac{1}{2}\lambda^+\lambda, \qquad \tilde{C}(\lambda) \simeq l_{N-n} - \tfrac{1}{2}\lambda\lambda^+ \tag{110}$$

and the variation of the HF energy functional up to the second order is given by

$$\begin{aligned} E_H(\Phi) - E_H(\Psi) \simeq{}& F_{\mu\alpha}\lambda_{\mu\alpha} + F_{\mu\alpha}\lambda^*_{\mu\alpha} + \lambda^*_{\mu\alpha}\langle\mu\alpha|I|\nu\beta\rangle\lambda_{\nu\beta} + \tfrac{1}{2}\lambda^*_{\mu\alpha}\langle\mu\alpha|I|\beta\nu\rangle\lambda^*_{\mu\beta} \\ &+ \tfrac{1}{2}\lambda_{\mu\alpha}\langle\mu\alpha|I|\beta\nu\rangle^*\lambda_{\nu\beta}, \end{aligned} \tag{111}$$

where

$$\begin{aligned} \langle\mu\alpha|I|\nu\beta\rangle &= F_{\mu\nu}\delta_{\alpha\beta} - F_{\beta\alpha}\delta_{\mu\nu} + [\mu\alpha|\beta\nu], \\ \langle\mu\alpha|I|\beta\nu\rangle &= [\mu\alpha|\nu\beta]. \end{aligned} \tag{112}$$

Since Ψ is a HF solution, the first order variation $\delta E_H(\Psi)$ is zero for any λ,

$$\begin{aligned} \delta E_H(\Psi) &= F_{\mu\alpha}\lambda_{\mu\alpha} + F_{\alpha\mu}\lambda^*_{\mu\alpha} = 0, \\ F_{\mu\alpha} &= F_{\alpha\mu} = 0. \end{aligned} \tag{113}$$

The second order variation can be written in the form

$$\delta^2 E_H(\Psi) = \tfrac{1}{2}\tilde{\lambda}^\dagger\Omega\tilde{\lambda}, \tag{114}$$

where $\tilde{\lambda}$ and Ω are the $2(N-n)n$ dimensional vector and matrix defined by

$$\tilde{\lambda} = \begin{bmatrix} (\lambda_{\mu\alpha}) \\ (\lambda^*_{\mu\alpha}) \end{bmatrix}, \qquad \Omega = \begin{bmatrix} (\langle\mu\alpha|I|\nu\beta\rangle), (\langle\mu\alpha|I|\beta\nu\rangle) \\ (\langle\mu\alpha|I|\beta\nu\rangle^*), (\langle\mu\alpha|I|\nu\beta\rangle^*) \end{bmatrix}. \tag{115}$$

The matrix Ω is called the instability matrix of the HF solution Ψ.

If the instability matrix Ω has no negative eigenvalue, then the second order variation $\delta^2 E_H(\Psi)$ is positive definite. This means that the solution Ψ is a local minimum in the variation space, but not necessarily the absolute minimum, of the HF energy functional and is stable for any small variation. On the other hand, if the instability matrix has negative eigenvalues

$$\Omega\tilde{\lambda}_p = \omega_p\tilde{\lambda}_p, \qquad \omega_p < 0, \tag{116}$$

then the second order variation $\delta^2 E_H(\Psi)$ is negative and consequently the value of the HF energy functional decreases for the variations of λ in the directions

$$\lambda = \sum_p l_p \lambda_p, \tag{117}$$

where λ_p's are the λ's contained in the eigenvectors $\tilde{\lambda}_p$ and l_p's are small parameters. This means that the solution Ψ is a saddle point or a maximum and is unstable and there must be at least a solution with lower energy than Ψ.

A point in the space of adiabatic parameters where an eigenvalue of the instability matrix becomes zero and changes its sign from positive to negative is called an instability threshold. If only an eigenvalue of the instability matrix becomes zero at an instability threshold, then the instability is called nondegenerate. If two or more eigenvalues become zero simultaneously at an instability threshold, then the instability is called degenerate.

If a HF solution Ψ is unstable, then there is at least one other solution Φ. There are three different situations for the relation of the two solutions. An instability is called interconnecting if a new solution Φ which connects continuously with the original solution Φ appears from the instability threshold. Interconnecting instabilities are of a character similar to second order phase transitions and are the ones most frequently met in molecules and chemical reactions as shown in Section 3. There are also instabilities which are not interconnecting but represent a crossing of two HF states, called crossing instabilities. An example of crossing instability will be shown in Section 3. The last type of HF instability is neither interconnecting nor crossing but represents the situation that a lower energy solution Φ separated by a finite energy gap exists below Ψ even at the instability threshold. This case is similar to first order phase transitions but in finite systems like molecules the occurrence of such an instability in the HF ground state appears to be an indication for a breakdown of the HF approximation.

ii. Classification of HF Instabilities and Interconnection Relation of HF Wave Functions via Instabilities. Let us consider a nondegenerate interconnecting instability of a HF solution Ψ. Then, there is another HF solution Φ which connects with Ψ at the instability threshold. Let the invariance group of Ψ be G. The problem we consider here is the kind of invariance group the solution Φ can have. The orbitals φ_ζ of Φ can be expressed in terms of the orbitals ψ_ζ of Ψ in the form of Eq. (33). As we shall show in the next section, in the vicinity of the instability threshold, the matrix λ to connect the orbitals φ_ζ with ψ_ζ is proportional to the matrix λ_1 that is the components of the eigenvector $\tilde{\lambda}_1$ of the instability matrix corresponding to the instability

$$\begin{aligned} &\varphi_\alpha = \psi_\beta [C(\lambda)]_{\beta\alpha} + \psi_\mu [S(\lambda)]_{\mu\alpha}, \\ &\lambda = l\lambda_1, \qquad \Omega\tilde{\lambda}_1 = \omega_1 \tilde{\lambda}_1, \qquad \omega_1 < 0, \end{aligned} \tag{118}$$

where l is a small parameter to become zero at the instability threshold.

An eigenvector of the instability matrix behaves as a second order tensor for the invariance group G of Ψ because it depends on two spin orbital indices μ and α. Owing to the invariance of Ψ to G, the instability matrix can be decomposed into a direct sum of smaller matrices which are irreducible to G and an eigenvector of it belongs to an irreducible representation of G. The same situation holds also for the matrix λ derived from an eigenvector $\tilde{\lambda}_1$ as given in Eq. (118). In the region of the adiabatic parameter space not close to the instability threshold, the matrix λ is in general no more proportional to λ_1. However, the symmetry of λ with respect to G is preserved unless the solution Φ passes another interconnecting instability threshold. The HF equation to determine λ is covariant to G, so that the symmetry of a solution is retained until it meets an interconnecting instability threshold that is a singular point where bifurcation of HF solutions takes place.

We call the symmetry of an eigenvector of the instability matrix of an HF solution Ψ, which has a negative eigenvalue and produces an instability of Ψ, the symmetry of the instability. Eigenvectors of instability matrix depend on occupied and unoccupied orbitals ψ_α and ψ_μ of Ψ, namely on transitions from ψ_α to ψ_μ or equivalently particle–hole pairs $\psi_\mu \psi_\alpha^*$. The symmetry of an instability represents the symmetry of the transitions or particle–hole pairs to cause the instability. The Slater determinant $|\Phi\rangle$ of the new solution Φ appearing from an interconnecting instability of Ψ has the form of Eq. (46). All the particle–hole pairs involved in $|\Phi\rangle$ has the same symmetry as the symmetry of the instability. This coherence in the symmetry of particle–hole pairs in $|\Phi\rangle$ leads to a collective and ordered character of the correlation incorporated into $|\Phi\rangle$.

The group theoretical principle to determine the invariance group G' of the new solution Φ is very simple. If the symmetry of the instability to produce Φ, or equivalently that of the matrix λ, belongs to identity representation of G, then Φ is invariant to G. If the symmetry of λ belongs to a nonidentity representation of G, then Φ is invariant to the subgroup G' of G which leaves λ invariant. Thus, the invariance group G' of Φ must be either G or a subgroup of G. Therefore, we get the interconnection relation for the eight classes of HF wave functions as shown in Figure 5 that shows HF wave functions of what classes may be produced as new solutions appearing via nondegenerate interconnecting instabilities of an HF solution. The interconnection relation shown in Figure 5 is identical with the subgroup structure of the symmetry group $S \times T$ except for the presence of the arrows connecting the same classes. Nondegenerate interconnecting instabilities give rise to new solutions with the invariance groups which are either G or maximal subgroups G' of G as proved below.

Next, we determine instabilities with what symmetry correspond to each interconnecting line in Figure 5. In order to do this, we need to know the generators of each invariance group. The generators of the continuous group S are σ_1, σ_2, and σ_3 as seen in Eq. (63). The generator of the group $A(z)$ is σ_3. The discrete groups T and $M(y)$ are generated by t and m_2 ($\equiv m_y$), respectively. Combining these generators, we get the generators of each invariance group as

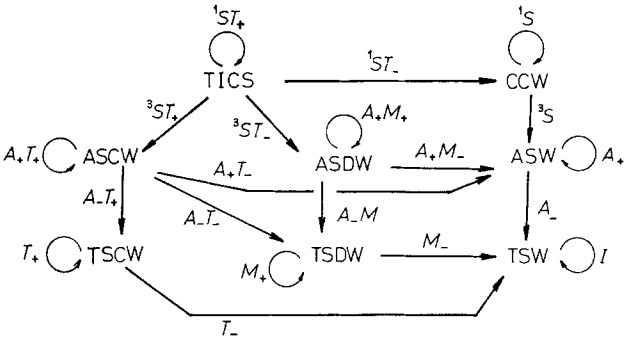

Figure 5. Interconnection relation of the eight HF classes via nondegenerate interconnecting instabilities. Possible interconnections are indicated by arrows. The type of instabilities is indicated beside arrows.

shown in Table V. Twofold elements which are not generators of an invariance group are also listed in Table V.

Spin rotation transforms the matrix λ as

$$s(\mathbf{e},\theta)\lambda s^{-1}(\mathbf{e},\theta)=\cos^2\frac{\theta}{2}\lambda+i\cos\frac{\theta}{2}\sin\frac{\theta}{2}[(\mathbf{e}\cdot\boldsymbol{\sigma}),\lambda]$$

$$+\sin^2\frac{\theta}{2}(\mathbf{e}\cdot\boldsymbol{\sigma})\lambda(\mathbf{e}\cdot\boldsymbol{\sigma}). \tag{119}$$

Equation (119) shows that λ is invariant to the spin rotation $s(\mathbf{e},\theta)$ if, and only if,

$$(\mathbf{e}\cdot\boldsymbol{\sigma})\lambda(\mathbf{e}\cdot\boldsymbol{\sigma})=\lambda, \tag{120}$$

because $[(\mathbf{e}\cdot\boldsymbol{\sigma}),\lambda]=0$ follows from Eq. (120). We define the operation $\lambda^{\sigma i}$ for λ by

$$\lambda^{\sigma i}=\sigma_i\lambda\sigma_i,\qquad(\lambda^{\sigma i})^{\sigma i}=\lambda. \tag{121}$$

TABLE V. Generators and twofold elements in the subgroups of $S\times T$.

Group	Generators	Other twofold elements
$S\times T$	$\sigma_1,\sigma_2,\sigma_3,t$	m_1,m_2,m_3
S	$\sigma_1,\sigma_2,\sigma_3$	
$A(z)\times T$	σ_3,t	m_3
$A(z)\cdot M(y)$	σ_3,m_2	m_1
$A(z)$	σ_3	
$M(y)$	m_2	

The operation $\lambda^{\sigma i}$ is twofold because $\sigma_i^2 = 1$. Time reversal and magnetic operation for λ are given by

$$\begin{aligned} \lambda^t &= \rho\lambda^*\rho^{-1}, \qquad (\lambda^t)^t = 1, \\ \lambda^{mi} &= \sigma_i\lambda^t\sigma_i, \qquad (\lambda^{mi})^{mi} = 1. \end{aligned} \tag{122}$$

The time reversal for the matrix λ becomes a twofold operation because λ is a second order tensor having two spinor indices μ and α. Since these operations are twofold the matrix λ irreducible to the group generated by them must satisfy

$$\lambda^{\sigma i} = \pm\lambda, \qquad \lambda^t = \pm\lambda, \qquad \lambda^{mi} = \pm\lambda. \tag{123}$$

The following relations hold

$$(\lambda^{\sigma i})^{\sigma i} = \lambda^{\sigma k}, \qquad \lambda^{mi} = (\lambda^t)^{\sigma i}, \tag{124}$$

so that the following restrictions are imposed for possible combinations of the sign factors $\varepsilon_{\sigma i}$, ε_t, and ε_{mi} in Eq. (123):

$$\varepsilon_{\sigma i}\varepsilon_{\sigma j} = \varepsilon_{\sigma k}, \qquad \varepsilon_{mi} = \varepsilon_t\varepsilon_{\sigma i}. \tag{125}$$

The above discussion shows that all possible kinds of λ irreducible to an invariance group G can be listed by assigning plus or minus signs to the generators and the twofold elements of G listed in Table V under the restriction of Eq. (125). The symmetry operations which have plus sign leave the matrix λ invariant and form the invariance group G' of the new solution Φ. We show the result in Table VI. We see in Table VI that the invariance group G' of the new solution appearing from a nondegenerate interconnecting instability is either G or a maximal subgroup of G. The notation for the instabilities given in Table VI represents the followings: ^1S and ^3S represent the instabilities caused by spin singlet and triplet excitations, respectively. A_+ and A_- represent conservation and violation of the axial spin invariance of DODS wave functions. A_+ and A_- instabilities are caused by spin unflipping and flipping excitations, respectively. T_+ and T_- (M_+ and M_-) represent conservation and violation of the time reversal invariance (magnetic invariance). In ^3S and A_-M instabilities the different combinations of signs shown in Table VI lead to different UHF wave functions but those wave functions are transformed to each other by a spin rotation and physically equivalent so that further distinction is unnecessary.

The fact that instabilities of a TICS wave function can be subdivided into four different types leading to UHF wave functions of different kinds was pointed out first by Paldus and Čižek (1970a–1970c).

In the case of a doubly degenerate interconnecting instability with two eigenvalues ω_1 and ω_2 of the instability matrix to become negative at the same time over an instability threshold, at least three different solutions with the λ matrices in the forms of

$$\begin{aligned} &\lambda = 1_1\lambda_1, \qquad \lambda' = 1_2\lambda_2, \qquad \lambda'' = 1_1\lambda_1 + 1_2\lambda_2, \\ &\Omega\tilde{\lambda}_1 = \omega_1\tilde{\lambda}_1, \qquad \Omega\tilde{\lambda}_2 = \omega_2\tilde{\lambda}_2, \qquad \omega_1, \omega_2 \leq 0 \end{aligned} \tag{126}$$

TABLE VI. Symmetry of nondegenerate instabilities and the type of UHF solutions appearing from them.

(a) TICS:

	σ_1	σ_2	σ_3	t	m_1	m_2	m_3	
$^1ST_+$	+	+	+	+	+	+	+	TICS
$^1ST_-$	+	+	+	−	−	−	−	CCW
	+	−	−	+	+	−	−	
$^3ST_+$	−	+	−	+	−	+	−	ASCW
	−	−	+	+	−	−	+	
	+	−	−	−	−	+	+	
$^3ST_-$	−	+	−	−	+	−	+	ASDW
	−	−	+	−	+	+	−	

(b) CCW:

	σ_1	σ_2	σ_3	
^1S	+	+	+	CCW
	+	−	−	
^3S	−	+	−	ASW
	−	−	+	

(c) ASCW:

	σ_3	t	m_3	
A_+T_+	+	+	+	ASCW
A_+T_-	+	−	−	ASW
A_-T_+	−	+	−	TSCW
A_-T_-	−	−	+	TSDW

(d) ASDW:

	σ_3	m_2	m_1	
A_+M_+	+	+	+	ASDW
A_+M_-	+	−	−	ASW
A_-M	−	+	−	
	−	−	+	TSDW

(e) ASW:

	σ_3	
A_+	+	ASW
A_-	−	TSW

(f) TSCW:

	t	
T_+	+	TSCW
T_-	−	TSW

(g) TSDW:

	m_2	
M_+	+	TSDW
M_-	−	TSW

appear simultaneously from the instability threshold as we shall show in the next section. In order for a degenerate instability to occur, the symmetries of λ_1 and λ_2 either in spin, time reversal, or spatial point group must be different. The new solutions Φ_1 and Φ_2 with λ and λ', respectively, obey the interconnection rule same as nondegenerate instabilities. On the other hand, the matrix λ'' breaks symmetry more than λ and λ'. It is invariant only for symmetry operations in order to leave both λ and λ' invariant, so that the solution Φ_{12} with λ'' has the invariance group G'_{12} that is the intersection of the invariance groups G'_1 and G'_2 of the solutions Φ_1 and Φ_2,

$$G'_{12} = G'_1 \cap G'_2. \tag{127}$$

Therefore, the solution Φ_{12} obeys an interconnection rule different from the one of nondegenerate cases. We show in Figure 6 the interconnection relation of a HF wave functions realizable via doubly degenerate instabilities.

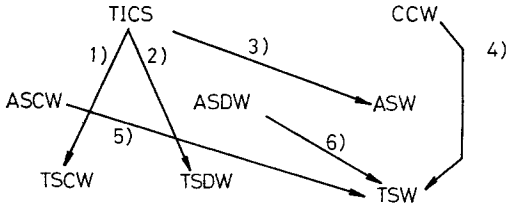

Figure 6. Interconnection relation realizable via doubly degenerate instabilities. The degenerate instabilities leading to the interconnections shown this figure are (1) $({}^3ST_+, {}^3ST_+)$; (2) $({}^3ST_-, {}^3ST_-)$ and $({}^3ST_+, {}^3ST_-)$; (3) $({}^3ST_+, {}^3ST_-)$, $({}^1ST_-, {}^3ST_+)$, and $({}^1ST_-, {}^3ST_-)$; (4) $({}^3S, {}^3S)$; (5) (A_-T_+, A_-T_-), (A_+T_-, A_-T_+), and (A_+T_-, A_-T_-); (6) (A_-M, A_-M) and (A_-M, A_+M_-).

The instability matrix of a HF solution Ψ can be decomposed into submatrices which are irreducible to the invariance group G of Ψ and correspond to the instabilities of different symmetries listed in Table VI and Figure 5. The explicit forms of all the irreducible submatrices were given in Fukutome (1974b). We quote here only the results for TICS and ASDW cases which are the most important in application to molecules.

A TICS solution is a closed shell with real orbitals. We denote its occupied and unoccupied orbitals by the indices $a, b, \ldots$ and $m, n, \ldots$, respectively. An irreducible λ matrix is separable into the spatial and spin parts and is a spin scalar or a spin vector. Its spatial part is either real or pure imaginary. The assignment of irreducible λ matrices to the four kinds of TICS instability is

$$\begin{gathered}
\psi_\zeta = \psi_i \eta_r, \qquad \lambda_{\mu\alpha} = \lambda_{mr,as}, \\
\left.\begin{matrix} {}^1ST_+ \\ {}^1ST_- \end{matrix}\right\} \lambda_{mr,as} = \lambda^{S}_{ma}\delta_{rs}, \qquad \lambda^{S}_{ma} \begin{cases} \text{real}, \\ \text{imaginary}, \end{cases} \\
\left.\begin{matrix} {}^3ST_+ \\ {}^3ST_- \end{matrix}\right\} \lambda_{mr,as} = \lambda^{T}_{ma}(\sigma_i)_{rs}, \qquad \lambda^{T}_{ma} \begin{cases} \text{imaginary}, \\ \text{real}. \end{cases}
\end{gathered} \tag{128}$$

We note that the spin scalar and spin vector λ's arise from singlet and triplet excitations, respectively. The irreducible instability matrices $\bar{\Omega}$ corresponding to the four kinds of TICS instability are

$$\begin{aligned}
\bar{\Omega} &= (\langle ma|\Omega|nb\rangle), \\
{}^1ST_+ &: = (F_{mn}\delta_{ab} - F_{ba}\delta_{mn} + 4\langle_{ma}|nb\rangle - \langle mn|ab\rangle - \langle mb|na\rangle), \\
\left.\begin{matrix} {}^1ST_- \\ {}^3ST_+ \end{matrix}\right\} &: = (F_{mn}\delta_{ab} - F_{ba}\delta_{mn} - \langle mn|ab\rangle + \langle mb|na\rangle), \\
{}^3ST_- &: = (F_{mn}\delta_{ab} - F_{ba}\delta_{mn} - \langle mn|ab\rangle - \langle mb|na\rangle).
\end{aligned} \tag{129}$$

Note that the $^1ST_-$ and $^3ST_+$ instability matrices are identical and these instabilities occur always simultaneously. Furthermore, the CCW and ASCW solutions appear simultaneously and are always degenerate in energy as can be proved from the identity of their energy functional.

An ASDW solution is a DODS with real orbitals. We denote its occupied and unoccupied orbitals by the indices a_r, b_r, ... and m_r, n_r, ..., respectively, which have the spin subscripts r, s, ... because the orbitals for up and down spins are different. The irreducible λ matrices for the A_+ and A_- type instabilities are a scalar and a two dimensional vector for, say, $A(z)$ rotation. The spatial components in the irreducible $A(z)$ scalar λ is either real or pure imaginary while those in the irreducible $A(z)$ vector λ may be complex. The assignment of irreducible λ's to the three kinds of ASDW instability is

$$\psi_\zeta = \phi_{ar}\eta_r, \qquad \lambda_{\mu\alpha} = \lambda_{mr,as},$$

$$\left.\begin{matrix} A_+M_+ \\ A_+M_- \end{matrix}\right\}: \quad \lambda = \begin{bmatrix} \lambda_{11} & 0 \\ 0 & \lambda_{22} \end{bmatrix}, \qquad \lambda_{rr}: \begin{cases} \text{real}, \\ \text{imaginary}, \end{cases} \tag{130}$$

$$A_-M: \quad \lambda = \begin{bmatrix} 0 & \lambda_{12} \\ \lambda_{21} & 0 \end{bmatrix}, \qquad \lambda_{rs}: \text{complex},$$

where $\lambda_{rs} = (\lambda_{mr,as})$. We note that the $A(z)$ scalar and vector λ's arise from spin unflipping and flipping excitations, respectively. The irreducible instability matrices $\bar{\Omega}$ for the three kinds of ASDW instability are

$$A_+M_\pm: \quad \bar{\Omega} = (\langle m_r a_r|I|n_s b_s\rangle \pm \langle m_r a_r|I|b_s n_s\rangle),$$

$$A_-M: \quad \bar{\Omega} = \begin{bmatrix} (\langle m_1 a_2|I|n_1 b_2\rangle) & (\langle m_1 a_2|I|b_1 n_2\rangle) \\ (\langle m_2 a_1|I|b_2 n_1\rangle) & (\langle m_2 a_1|I|n_2 b_1\rangle) \end{bmatrix}, \tag{131}$$

$$\langle m_r a_s|I|n_u b_v\rangle = \delta_{ru}\delta_{sv}(F_{m_r n_r}\delta_{a_s b_s} - F_{b_s a_s}\delta_{m_r n_r} - \langle m_r m_r|b_s a_s\rangle) + \delta_{rs}\delta_{uv}\langle m_r a_r|b_u n_u\rangle,$$

$$\langle m_r a_s|I|b_v n_u\rangle = \delta_{rs}\delta_{uv}\langle m_r a_r|b_u n_u\rangle - \delta_{rv}\delta_{su}\langle m_r b_r|n_s a_s\rangle.$$

iii. Bifurcation Structures of HF Potential Surfaces. At an interconnecting instability threshold, a new solution (or solutions) of the HF equation appears and a bifurcation occurs in the HF potential surface. All the possible bifurcation structures arising from nondegenerate and doubly degenerate instabilities were obtained by Fukutome (1975). We outline here the theory of bifurcations of HF potential surfaces.

The HF equation contains nuclear coordinates as adiabatic parameters. Let $\Psi(R)$ be a HF solution at a nuclear conformation R and Φ be the HF solution(s) at the nuclear conformation $R+\delta R$ with a small displacement δR of nuclear coordinates which connects with $\Psi(R)$ in the limit $\delta R = 0$. Let $\Psi^0(R+\delta R)$ be the Slater determinant which is obtained from $\Psi(R)$ by the continuation of the AO bases from R to $R+\delta R$ but with the LCAO MO coefficients unchanged. $\Psi^0(R+\delta R)$ is not a HF solution at $R+\delta R$ but is an approximation of Φ. Let $\Omega(R)$ be the instability matrix of $\Psi(R)$. We can expand the λ matrix to connect

the orbitals of Φ with those of $\Psi^0(R+\delta R)$ by the eigenvectors of $\Omega(R)$,

$$\lambda = \sum_p \frac{x_p}{2} \lambda_p, \qquad \Omega(R)\tilde{\lambda}_p = \omega_p \tilde{\lambda}_p, \tag{132}$$

with small real parameters x_p. Expanding Eq. (53) with (51) into the power series of λ up to the fourth order and substituting Eq. (132), we obtain the expansion of the HF energy of Φ in terms of the parameters x_p,

$$\Delta E_H = E_H(\Phi) - E_H(\Psi(R)) = \delta E_H^0 + \tfrac{1}{2}\sum \delta F_p x_p + \tfrac{1}{8}\sum (\omega_p \delta_{pq} + \delta\Omega_{pq}) x_p x_q + \tfrac{1}{6}\sum c_{pqr} x_p x_q x_r + \tfrac{1}{8}\sum d_{pqrs} x_p x_q x_r x_s. \tag{133}$$

The quantities

$$\begin{aligned} \delta E_H^0 &= E_H(\Psi^0(R+\delta R)) - E_H(\Psi(R)), \\ \delta F_p &= 2\,\mathrm{Re}\,[\{F^0_{\alpha\mu}(R+\delta R) - F_{\alpha\mu}(R)\}\lambda_{p,\mu\alpha}], \\ \delta\Omega_{pq} &= \tilde{\lambda}_p^{+}\{\Omega^0(R+\delta R) - \Omega(R)\}\tilde{\lambda}_q, \end{aligned} \tag{134}$$

which are constructed from the differences of the HF energy, Fock operator and instability matrix of $\Psi^0(R+\delta R)$ and $\Psi(R)$, are small in the order of δR while the quantities c_{pqr} and d_{pqrs} are of zeroth order in δR and not small. From the variation of Eq. (133), we get the algebraic equation to determine x_p's,

$$\delta F_p + \tfrac{1}{2}\sum_q (\omega_p \delta_{pq} + \delta\Omega_{pq}) x_q + \sum_{qr} c_{pqr} x_q x_r + \sum_{qrs} d_{pqrs} x_q x_r x_s = 0 \tag{135}$$

If R is not an instability threshold, i.e., $\omega_p \neq 0$ for all p, Eq. (135) can be solved perturbationally and has only one solution which is the continuation $\Psi(R+\delta R)$ of $\Psi(R)$ to $R+\delta R$. If R is an instability threshold, i.e., $\omega_p = 0$ for some p's, then Eq. (135) has more than one solution. We quote here only the results for nondegenerate and doubly degenerate instabilities that occur in the HF ground state. Let $\omega_1 = 0$ and $\omega_p \neq 0$ for $p \neq 1$ in the nondegenerate case and $\omega_1, \omega_2 = 0$ and $\omega_p \neq 0$ for $p \neq 1, 2$ in the doubly degenerate case. We denote the p's with $\omega_p = 0$ by the indices $i, j, \ldots$. The x_p's with $\omega_p \neq 0$ can be eliminated from Eq. (133) by using Eq. (135) for the x_p's. By also using symmetry properties that are to be satisfied by ground state instabilities, ΔE_H becomes a function depending only on the x_i's with $\omega_i = 0$,

$$\begin{aligned} \Delta E_H &= -\tfrac{1}{2}\sum_p{}' \frac{(\delta F_p)^2}{\omega_p} + \Delta E', \\ \Delta E' &= \tfrac{1}{4}\left(\sum_i \delta V_i x_i^2 + \tfrac{1}{2}\sum_{ij} a_{ij} x_i^2 x_j^2\right), \\ \delta V_i &= \tfrac{1}{2}\delta\Omega_{ii} - 4\sum_p{}' \frac{c_{iip}\delta F_p}{\omega_p}, \\ a_{ij} &= d_{iijj} - 4\sum_p{}' \frac{c_{iip} c_{jjp}}{\omega_p}, \end{aligned} \tag{136}$$

where $\sum'$ is the summation over the p's with $\omega_p \neq 0$. Then Eq. (135) for x_i's becomes

$$\left(\delta V_i + \sum_j a_{ij} x_j^2\right) x_i = 0. \tag{137}$$

Equation (137) always has the solution $x_i = 0$ that represents the continuation $\Psi(R + \delta R)$ of $\Psi(R)$. In the nondegenerate case $i, j = 1$, and the inequality $a_{11} > 0$ must be satisfied in order for $\Delta E'$ to have a lower bound. Equation (137) has another doubly degenerate solution Φ,

$$x_1 = \pm(-\delta V_{11}/a_{11})^{1/2}, \qquad \Delta E' = -(\delta V_{11})^2/8a_{11}, \tag{138}$$

with lower energy than the solution $\Psi(R + \delta R)$ in the region of δR determined by the inequality

$$-\delta V_{11} > 0. \tag{139}$$

We show in Figure 7(a) the x_1 dependence of $\Delta E'$ which is nothing but the profile of the HF energy functional in a direction of the variation space and in Figure 7(b) the bifurcation behavior of the adiabatic potentials of the solutions Ψ and Φ.

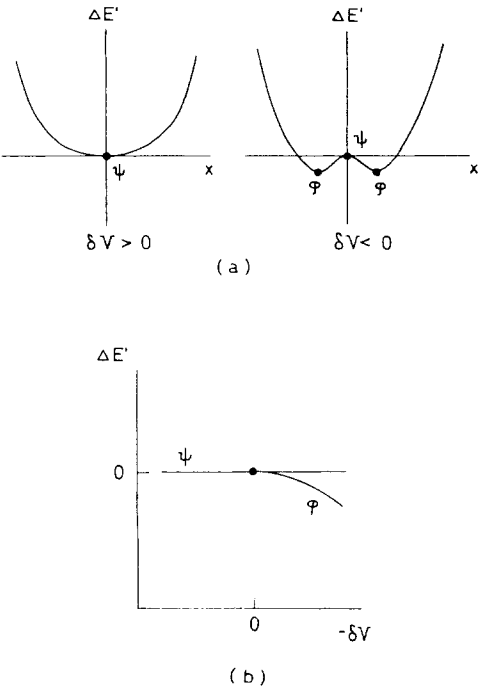

Figure 7. Ground state bifurcation by a nondegenerate instability. (a) and (a') Structures of the HF energy functional before and after instability, respectively. (b) Bifurcation of HF potential.

In the doubly degenerate case, $i, j = 1, 2$ and the inequalities a_{11}, a_{22}, $a_{12} > 0$ and $a_{11}a_{22} - a_{12}^2 > 0$ must be satisfied in order for $\Delta E'$ to have a lower bound. Equation (137) has the following three solutions:

$$\begin{aligned}
\Phi_1: &\quad x_2 = 0, \qquad x_1^2 = -\delta V_{11}/a_{11} = \delta v_1 > 0, \\
\Phi_2: &\quad x_1 = 0, \qquad x_2^2 = -\delta V_{22}/a_{22} = \delta v_2 > 0, \\
\Phi_{12}: &\quad x_1^2 = -(a_{22}\delta V_{11} - a_{12}\delta V_{22})/(a_{11}a_{22} - a_{12}^2) = \delta v_{21} > 0, \\
&\quad x_2^2 = -(a_{11}\delta V_{22} - a_{12}\delta V_{11})/(a_{11}a_{22} - a_{12}^2) = \delta v_{12} > 0,
\end{aligned} \tag{140}$$

with lower energies than $\Psi(R + \delta R)$. Their existence domains are given by the inequalities in Eq. (140). We show in Figure 8(a) their existence domains and in Figure 8(b) the bifurcation behavior of their adiabatic potentials in the vicinity of the degenerate instability threshold. We see in Figure 8 that the degenerate instability threshold R is a crossing point of the boundaries of two nondegenerate instabilities and the solution Φ_{12} that is produced only by a degenerate instability has a wedge-shaped existence domain with the vertex at R. The solution Φ_{12} smoothly interconnects solutions Φ_1 and Φ_2.

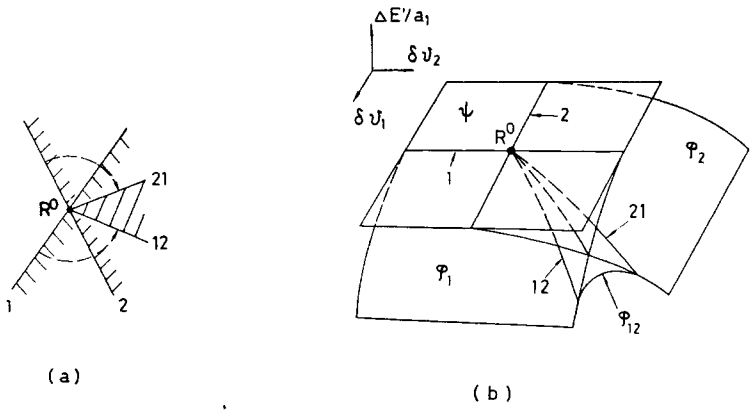

Figure 8. Ground state bifurcation in the vicinity of a doubly degenerate instability threshold. (a) Boundaries of the existence domains of the solutions Φ_1, (1), Φ_2, (2), and Φ_{12}, (12), and (21). (b) Bifurcation of the potentials of Φ_1, Φ_2, and Φ_{12}.

D. Direct Minimization Algorism for HF Calculation

The HF equation in the conventional form is a nonlinear eigenvalue equation. It has been customary to solve the equation iteratively. However, as has been widely experienced, the iterative eigenvalue procedure frequently meets trouble in convergence, the iteration being trapped in an oscillatory cycle. To avoid the trouble of nonconvergence, various direct minimization algorisms were proposed by McWeeny (1956), Hinze and Roothaan (1967), Fletcher (1970), and Bonacić and Koutecký (1972). However, these methods are not entirely satisfactory in convergence or in computational speed. Igawa and Fukutome (1975) developed

a direct minimization method with secured convergence and good computational speed.

The method is based on the formalism given in Sections 2.A.iii and 2.A.iv. The parameters $\lambda_{\mu\alpha}$ are independent variables of the HF energy functional. If we determine $\lambda_{\mu\alpha}$ so as to minimize the quadratic approximation [Eq. (111)] of the HF energy functional, we get the Hinze–Roothaan (1967) method. However, the direct determination of $\lambda_{\mu\alpha}$'s requires a huge computational time because of the large dimension, in general $2(N-n)n$, of the equation for $\lambda_{\mu\alpha}$'s and the use of the quadratic approximation leads to the trouble of nonconvergence. Hence, we used the representation (36) to diagonalize the matrix λ and expression (58) for the HF energy functional. The use of the representation (36) brings about a drastic decrease in the dimension of the equations to be solved to the order of $k=\min(N-n, n)$. Formula (58) involves the Coulomb repulsion integrals depending only on two MO indices, also leading to a huge reduction in the time for the computation of the energy functional. It also yields easy computation of the energy functional up to any desired order of λ, leading to secured covergence of the iteration in the method.

Let Ψ and Φ be the Slater determinants in the iteration cycles i and $i+1$. Their orbitals are related by by a matrix $\lambda^{(i)}=(\lambda^{(i)}_{\mu\alpha})$ in the manner of Eq. (33). We first determine the matrices $v^{(i)}$ and $\tilde{v}^{(i)}$ to diagonalize $\lambda^{(i)}$. Since the off diagonal matrix elements $F_{\mu\alpha}$ of the Fock operator must satisfy $F_{\mu\alpha}=0$ in the SCF limit, we determine $v^{(i)}$ and $\tilde{v}^{(i)}$ so as to diagonalize the Fock operator $F^{(i)}_{\mu\alpha}$ at the iteration cycle i,

$$F^{(i)}_{\mu\alpha}=\sum_{A=1}^{k}\tilde{v}^{(i)}_{\mu A}F^{(i)}_{A}v^{(i)*}_{\alpha A}. \tag{141}$$

Then, in the MO basis of the orbitals defined in Eq. (54),

$$\psi^{(i)}_{A}=\psi^{(i)}_{\alpha}v^{(i)}_{\alpha A}, \qquad \tilde{\psi}^{(i)}_{A}=\psi^{(i)}_{\mu}\tilde{v}^{(i)}_{\mu A}, \tag{142}$$

the number of nonzero matrix elements of the off diagonal Fock operator is minimized. In order to optimize convergence efficiency, we introduce the Fletcher–Reeves (1964) conjugate gradient technique in the determination of $v^{(i)}$ and $\tilde{v}^{(i)}$. Instead of Eq. (141), they are determined to diagonalize the matrix $R^{(i)}=(R^{(i)}_{\mu\alpha})$ defined by

$$\begin{aligned} R^{(i)}_{\mu\alpha}&=F^{(i)}_{\mu\alpha}+\beta^{(i-1)}R^{(i-1)}_{\mu\alpha}, \qquad R^{(1)}_{\mu\alpha}=F^{(1)}_{\mu\alpha},\\ \beta^{(i-1)}&=\sum_{\mu\alpha}|F^{(i)}_{\mu\alpha}|^2/\sum_{\mu\alpha}|F^{(i-1)}_{\mu\alpha}|^2,\\ R^{(i)}_{\mu\alpha}&=\sum_{A=1}^{k}\tilde{v}^{(i)}_{\mu A}R^{(i)}_{A}v^{(i)*}_{\alpha A}. \end{aligned} \tag{143}$$

Next, we determine the λ_A's to minimize the quadratic approximation of Eq. (58) at the iteration cycle i,

$$\delta E^{(i)}_{H}=\sum_{A=1}^{k}(l^{(i)}_{A}\lambda_A+\tfrac{1}{2}k^{(i)}_{A}\lambda^2_A)+\tfrac{1}{2}\sum_{A,B=1}^{k}[A\tilde{A}+\tilde{A}A|B\tilde{B}+\tilde{B}B]^{(i)}\lambda_A\lambda_B \tag{144}$$

and put

$$\lambda_A^{(i)} = 1\lambda_A. \tag{145}$$

By substituting Eq. (145) into Eq. (58), the energy functional becomes a function of l. We determine l so as to minimize the energy functional using the power series expansion in l up to the fourth or sixth order. The use of the fourth order approximation sufficed in most cases to get a good convergence but in some cases the sixth order approximation was necessary.

Summarizing, our direct minimization procedure consists of the following iteration cycle:

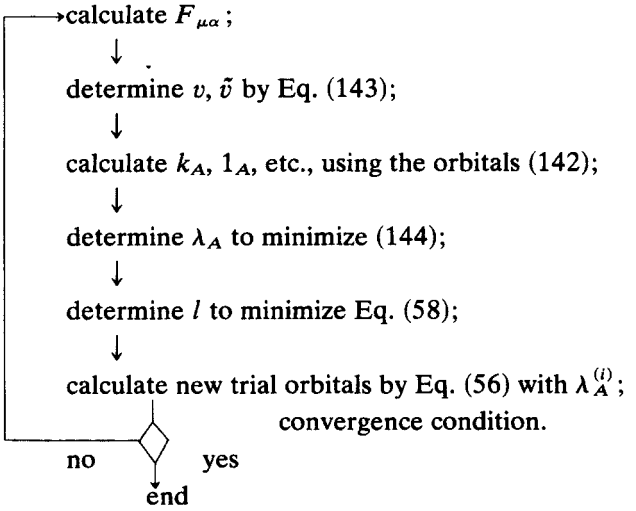

In the case of UHF calculations, search for new solutions is made by calculating irreducible instability matrices and their eigenvalues and eigenvectors. If an eigenvalue ω_1 of an instability matrix is negative, the trial orbitals for the new solution appearing from the instability is put in the form of Eq. (118) using the eigenvector $\tilde{\lambda}_1$ of the instability. The parameter l is determined so as to minimize the energy functional using the fourth order power series approximation in l. Then, the above iteration starts using the trial UHF orbitals.

The computer program based on the algorism and using the CNDO/2, INDO, and MINDO/2 approximations was written by Igawa for the RHF case and by Takahashi for the UHF case. It has secured and fast convergence and is capable of obtaining any desired solution. Its convergence speed is comparable to the iterative eigenvalue method in systems where the latter method exhibits best convergence and remains almost constant even in systems where the latter method fails to converge. Our experience shows that the iterative eigenvalue method frequently fails to converge in regions of nuclear conformation where an instability of the HF ground state is taking place. Therefore, it seems indispensable to use a calculation technique with secured convergence in studies of UHF states in molecules and chemical reactions.

Our method can be used in the study of the structure of the HF energy functional in the variation space. The variation space is the $2(N-n)n$ dimensional space of the parameters $\lambda_{\mu\alpha}$. Our method restricts the variation space to the k dimensional subspace of the parameters λ_A at each iteration. However, by changing the matrices v and $\tilde{v}$ at each iteration the subspace sweeps over the whole variation space. Thus, our method is a kind of relaxation technique but the subspace with an efficient sweeping is chosen. Formula (58) reveals that the HF energy functional is constructed from cosine and sine functions of λ_A's, so that it has always at least two extrema with respect to λ_A and consequently may have a lot of extrema in the whole space of λ_A's. The RHF energy functional of carbon mono-oxide constructed on valence AO bases has only two independent λ_A's, so that its λ_A dependence can be written in a two dimensional map. We illustrate in Figure 9 the λ_A dependence of the RHF energy functional of carbon mono-oxide with varying interatomic distance at the first iteration cycle starting from Hückel type trial orbitals. We see in Figure 9 that even the RHF energy functional has many extrema and its structure changes very much with increase of the interatomic distance accompanying increase of the number of extrema. The complicated structure of the energy functional is the origin of the nonconvergence trouble. The quadratic approximation in λ may fail to correctly approximate even a local structure of the energy functional and in fact the direct minimization using the quadratic approximation frequently meets the nonconvergence trouble.

E. Relation of the HF Approximation to the Exact Theory

The HF approximation has its group theoretical foundation on the $U(N)$ group generated by the particle–hole type pair operators as we have shown in Section 2.A. The $U(N)$ group whose origin is in the canonical anticommutation relation of annihilation–creation operators imposes a universal group theoretical structure on fermion many-body systems. The HF approximation has an intimate connection with this $U(N)$ group structure of Fermion many-body systems and is not a mere technical approximation. We consider here about the relation of HF wave functions to exact ones from the $U(N)$ group point of view.

i. Generator Coordinate Representation of Fermion State Vectors on the $U(N)$ Group. Let $U(u)$ be a canonical transformation on the Hilbert space of a fermion many-body system that depends on an element u of a compact Lie group and forms a representation of the group. If state vectors $|f\rangle$, $|g\rangle$, ... are in a space irreducible to $U(u)$, then by the well known orthogonality theorem for matrix elements of an irreducible representation the following orthogonality relation holds:

$$\int \langle f'|U(u)|g'\rangle\langle g|U^{\dagger}(U)|f\rangle\, du = D^{-1}\langle f'|f\rangle\langle g|g'\rangle, \tag{146}$$

where the integration is the group integration on the Lie group with the total volume normalized to 1 and D is the dimension of the irreducible space. Equation

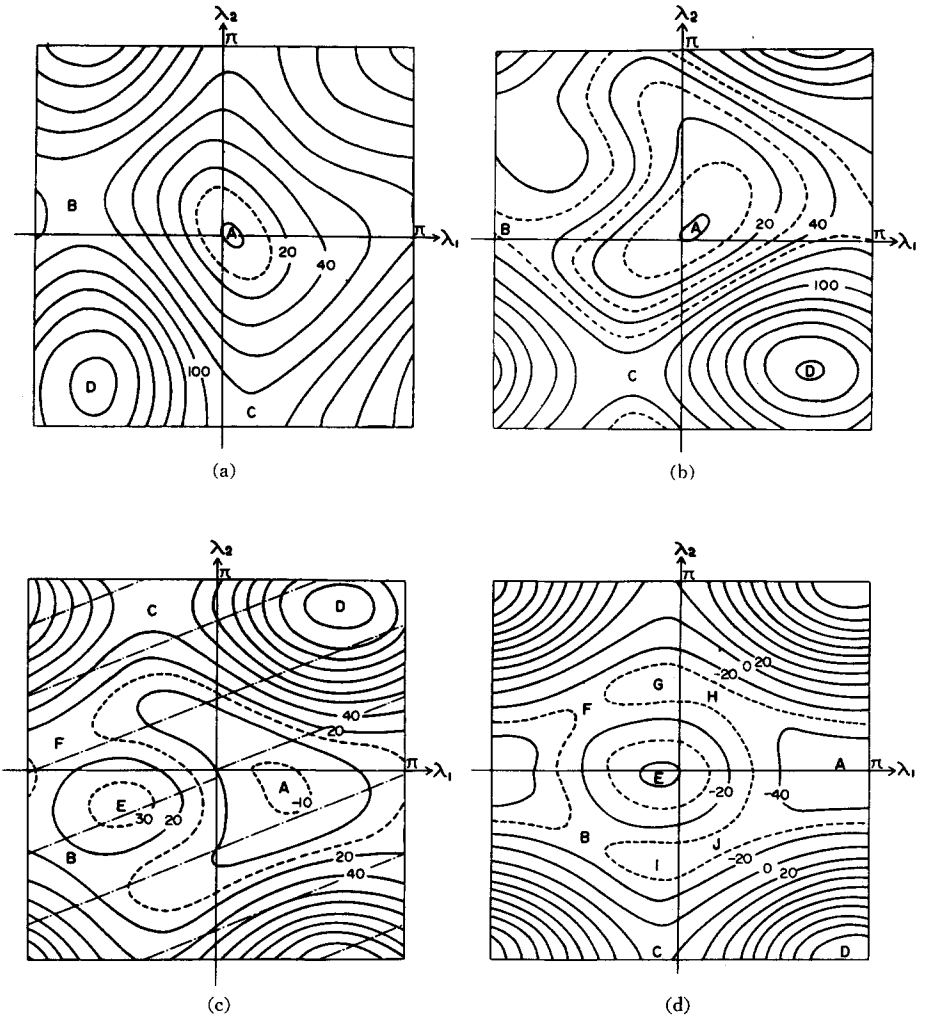

Figure 9. Structure of the RHF energy functional surface of CO at $R = 1.0$ (a), 1.5 (b), 2.0 (c), and 3.0 Å (d). Capital letters $A, B, \ldots$ represent positions of extrema.

(146) shows that any state vector $|f\rangle$ in the irreducible space can be represented in the form

$$|f\rangle = D \int U(u)|g\rangle\langle g|U^{\dagger}(u)|f\rangle \, du, \tag{147}$$

where $|g\rangle$ is an arbitrarily chosen reference state in the irreducible space. The representation of fermion state vectors of this kind was introduced firstly by Hill and Wheeler (1953) in their generator coordinate method without consideration for the group theoretical aspect of the representation. The group theoretical

derivation of the representation on a Lie group was first made by Perlemov (1972, 1977) and the representation was called the generalized coherent state representation because it is a generalization of the coherent state representation for photons introduced by Glauber (1963).

We apply the representation (146) to the $U(N)$ group. A space irreducible to the $U(N)$ canonical transformation $U(u)$ is the space with a definite fermion number n because the number operator n commutes with all the $U(N)$ Lie operators $a_\zeta^\dagger a_\eta$ but there is no other operator except for functions of n commutable with all of $a_\zeta^\dagger a_\eta$. The dimension of the space with n fermions is ${}_NC_n$. Therefore, any state vector $|f\rangle$ in the space with n fermions can be represented as

$$|f\rangle = {}_NC_n \int U(u)|\Psi\rangle\langle\Psi|U^\dagger(u)|f\rangle\, du, \tag{148}$$

where the integration is made over the $U(N)$ group and $|\Psi\rangle$ is an arbitrary Slater determinant with n fermions. We stress that the representation (148) is exact and the generating wave function $U(u)|\Psi\rangle$ is a Slater determinant by the Thouless theorem. The representation (148) provides a key to elucidate the relation of HF wave functions to exact ones. The generator coordinate representation in the form of Eq. (148) was introduced first by Jancovici and Schiff (1964) without recognition of its group theoretical character. The first group theoretical derivation was made by Linderberg and Öhrn (1977). A similar representation on a wider Lie group was introduced by Fukutome et al. (1977).

We next determine the structure of the generator coordinate (GC) wave function $\langle\Psi|U^\dagger(u)|f\rangle$. The GC wave functions corresponding to the Slater determinants $|\Psi_{\mu\nu\cdots\alpha\beta\cdots}\rangle$ are given from Eqs. (44) and Eq. (41a) as

$$\begin{aligned} \langle\Psi|U^\dagger(u)|\Psi_{\mu\nu\cdots\alpha\beta\cdots}\rangle &= \mathscr{A}(p^*_{\mu\alpha}p^*_{\nu\beta}\cdots)\langle\Psi|U^\dagger(u)|\Psi\rangle, \\ \langle\Psi|U^\dagger(u)|\Psi\rangle &= [\det(1+p^\dagger p)]^{-1/2}\det(w^*). \end{aligned} \tag{149}$$

From Eq. (149), we see that the GC wave function $\langle\Psi|U^\dagger(u)|f\rangle$ has the form

$$\langle\Psi|U^\dagger(u)|f\rangle = X_f(p^*)\langle\Psi|U^\dagger(u)|\Psi\rangle, \tag{150}$$

where $X_f(p^*)$ is an antisymmetric polynomial of $p^*_{\mu\alpha}$'s.

The Schrödinger equation $(H-E_f)|f\rangle$ can be converted to an integral equation on the $U(N)$ group. Substituting Eq. (148) into $\delta\langle f|(H-E_f)|f\rangle = 0$ and making variation with respect to the GC wave function, we obtain the Schrödinger equation on the $U(N)$ group

$$\begin{aligned} &\int \{H(u,u') - E_f S(u,u')\}\Psi_f(u')\, du' = 0, \\ &\Psi_f(u') = \langle\Psi|U^\dagger(u')|f\rangle, \\ &H(u,u') = \langle\Psi|U^\dagger(u)HU(u')|\Psi\rangle, \\ &S(u,u') = \langle\Psi|U^\dagger(u)U(u')|\Psi\rangle = \langle\Psi|U^\dagger(u'^\dagger u)|\Psi\rangle. \end{aligned} \tag{151}$$

Note that $H(u, u')$ and $S(u, u')$ are the matrix element of H and the overlap integral between two Slater determinants $|\Phi(u)\rangle = U(u)|\Psi\rangle$ and $|\Phi(u')\rangle$, respectively.

The overlap integral $S(u, u')$ is just identical with the GC wave function of the Slater determinant $|\Phi(u')\rangle$,

$$\langle\Psi|U^{\dagger}(u)|\Phi(u')\rangle = S(u, u'). \tag{152}$$

It has the following special property. Multiplying $\langle\Psi|U^{\dagger}(u)$ to Eq. (148), we obtain

$$\langle\Psi|U^{\dagger}(u)|f\rangle = {}_{N}C_{n}\int S(u, u')\langle\Psi|U^{\dagger}(u')|f\rangle\, du'. \tag{153}$$

By putting $|f\rangle = U(u'')|\Psi\rangle$, Eq. (153) gives

$$S(u, u'') = {}_{N}C_{n}\int S(u, u')S(u', u'')\, du'. \tag{154}$$

Equations (153) and (154) show that ${}_{N}C_{n}S(u, u')$ is the projection operator to the space of all GC wave functions with the fermion number n.

ii. Generator coordinate representation of symmetry adapted state vectors in terms of projected HF wave functions. An eigenstate of the Hamiltonian (6) belongs to an irreducible representation of the group S of spin rotation and is specified by the total spin j, the spin magnetic quantum number m, and the other quantum numbers q. A spin rotation s is an element of the $U(N)$ group and there is a $U(N)$ canonical transformation $U(s)$ corresponding to s. A spin symmetry adapted state vector $|j, m, q\rangle$ is transformed by $U(s)$ as

$$U(s)|j, m, q\rangle = \sum_{m'}|j, m', q\rangle D^{j}_{m'm}(s), \tag{155}$$

where $D^{j}_{m'm}(s)$'s are the so called D functions which are the matrix elements of the representation matrix of the irreducible representation j of the group S (for the D functions see Wigner, 1959). By the orthogonality theorem for irreducible representation matrices, the D functions satisfy the orthogonality relation

$$\int D^{j}_{mk}(s)D^{j'*}_{m'k'}(s)\, ds = \frac{1}{2j+1}\delta_{jj'}\delta_{mm'}\delta_{kk'}, \tag{156}$$

where the integration is made over the group S.

From Eq. (148), we have

$$U(s)|j, k, q\rangle = {}_{N}C_{n}\int U(su)|\Psi\rangle\langle\Psi|U^{\dagger}(u)|j, k, q\rangle\, du. \tag{157}$$

Multiplying Eq. (157) by $D^{j*}_{mk}(s)$, integrating over S, and using Eqs. (155) and (156), we obtain a generator coordinate representation of spin symmetry adapted state vectors

$$|j, m, q\rangle = (2j+1)\,{}_{N}C_{n}\int |\Phi^{j}_{mk}(u)\rangle\langle\Psi|U^{\dagger}(u)|j, k, q\rangle\, du, \tag{158}$$

where

$$|\Phi^j_{mk}(u)\rangle = \int D^{j*}_{mk}(s)U(su)|\Psi\rangle\, ds \tag{159}$$

is the Peierls–Yoccoz (1957) spin projected HF wave function. A generator coordinate representation of symmetry adapted state vectors with a similar form to Eq. (158) was derived by the author (Fukutome, 1977) on a wider Lie group universal for fermion systems.

The projected HF wave functions respond to spin rotation as

$$\begin{aligned} U(s)|\Phi^j_{mk}(u)\rangle &= \int D^{j*}_{mk}(s')U(ss'u)|\Psi\rangle\, ds' \\ &= \int D^{j*}_{mk}(s^{-1}s')U(s'u)|\Psi\rangle\, ds' \\ &= \sum_{m'} D^{j*}_{mm'}(s^{-1}) \int D^{j*}_{m'k}(s')U(s'u)|\Psi\rangle\, ds' \\ &= \sum_{m'} |\Phi^j_{m'k}(u)\rangle D^j_{m'm}(s), \end{aligned} \tag{160}$$

where we have used

$$\begin{aligned} D^j_{mk}(ss') &= \sum_{m'} D^j_{mm'}(s)D^j_{m'k}(s'), \\ D^j_{mm'}(s') &= D^{j*}_{m'm}(s), \end{aligned} \tag{161}$$

which are nothing but the relations to be satisfied by a representation matrix. Equation (160) shows that the projected HF wave function $|\Phi^j_{mk}(u)\rangle$ has the spin symmetry (j, m).

On the other hand, the quantum number k responds to spin rotation of the argument u:

$$\begin{aligned} |\Phi^j_{mk}(su)\rangle &= \int D^{j*}_{mk}(s')U(s'su)|\Psi\rangle\, ds' \\ &= \int D^{j*}_{mk}(s's^{-1})U(s'u)|\Psi\rangle\, ds' \\ &= \sum_{k'} D^{j*}_{k'k}(s^{-1}) \int D^j_{mk'}(s')U(s'u)|\Psi\rangle\, ds' \\ &= \sum_{k'} D^j_{kk'}(s)|\Phi^j_{mk'}(u)\rangle. \end{aligned} \tag{162}$$

The representation (158) has been derived by using only the orthogonality relations of representation matrices of the $U(N)$ and spin rotation groups. The $U(N)$ group is a universal group in fermion many-body systems because it has the origin in the canonical anticommutation relation of annihilation–creation operators. Therefore, the representation in terms of projected HF wave functions

can be obtained in any fermion system with a symmetry group. When the spin rotation $U(s)$ is applied to a Slater determinant $|\Phi(u)\rangle$, all the spin orbitals φ_α in $|\Phi(u)\rangle$ are simultaneously transformed to φ_α^s, namely, spins of all electrons are rotated coherently without changing their relative orientations. It is well known that the eigenstates of a spherical rigid rotator are the D functions of rotation group. Therefore, the Peierls–Yoccoz projection by the D functions is equivalent to selecting out the eigenstates of coherent rotation of spin vectors. The representation (158) gives us a microscopic justification of the Peierls–Yoccoz theory mentioned in Section 1. In the case of nonrelativistic molecular systems now being considered, it can be stated as follows. If the ground state is well approximated by a UHF wave function, then its components with different spin angular momenta represent a series of excited states produced by coherent rotation of spin vectors. The Peierls–Yoccoz theory can be generalized to any fermion system with a symmetry group as noted above. Its microscopic foundation is on the universal $U(N)$ group structure and the symmetry group structure of a fermion many-body system. Thus, the broken symmetry components in a UHF wave function are not mere mathematical artifacts but may have an important physical significance.

We note that the quantum number k in the projected HF wave function (159) has the same significance as the quantum number k in a rigid rotator. The quantum number k represents the component of angular momentum in a direction fixed to the rigid rotator. The quantum number k similarly represents the component of total spin angular momentum in a direction fixed to the assembly of spins which is performing coherent rotation.

Ozaki (1980) proved that the Peierls–Yoccoz projection for a UHF wave function in a aystem with a spatial point symmetry simultaneously recovers spatial symmetry. This fact is due to the structure of the invariance group G that has been discussed in Section 2.B.iv. A UHF wave function with the invariance group in the form of Eq. (104) is invariant to joint operation of a spatial point rotation p and a spin rotation $g(h_\pm(p))$ homomorphic to p. Since the proof for the case of invariance groups involving time reversal, that produces inversion of spin, is somewhat complicated, we restrict discussion in the case of invariance groups

$$_{II}P_h = \{ps(h_\pm(p)), p \in P\}, \tag{163}$$

where $s(h_\pm(p))$ is a proper spin rotation homomorphic to p. A spatial point rotation p belongs to the $U(N)$ group and there is a $U(N)$ canonical transformation $U(p)$ corresponding to p. Let $|\Phi(u)\rangle$ be a Slater determinant with the invariance group (163),

$$U(p)U(s(h_\pm(p)))|\Phi(u)\rangle = e^{i\delta}|\Phi(u)\rangle, \tag{164}$$

we then obtain

$$\begin{aligned} U(p)|\Phi(u)\rangle &= |\Phi(pu)\rangle = U^{-1}(s(h_\pm(p)))|\Phi(u)\rangle\, e^{i\delta} \\ &= |\Phi(s^{-1}(h_\pm(p))u)\rangle\, e^{i\delta}. \end{aligned} \tag{165}$$

From Eqs. (165) and (162), we have

$$U(p)|\Phi^j_{mk}(u)\rangle = |\Phi^j_{mk}(s^{-1}(h_\pm(p))u)\rangle\, e^{i\delta}$$
$$= \sum_{k'} D^j_{kk'}(s^{-1}(h_\pm(p)))|\Phi^j_{mk'}(u)\rangle\, e^{i\delta}. \tag{166}$$

Equation (166) shows that the spin projected UHF wave functions $|\Phi^j_{mk}(u)\rangle$ span an in general reducible representation of P with the representation matrix $[e^{i\delta}D^j_{kk'}(s^{-1}(h_\pm(p)))]$ which operates on the k quantum number of $|\Phi^j_{mk}(u)\rangle$. In the case of a CDW wave function with the invariance group in the form of Eq. (105), the spatial symmetry simultaneously recovered is restricted to the subgroup P'.

iii. Bose Quantized Time Dependent HF theory as an Exact Representation of a Fermion Many-Body System. Dynamics of a fermion system can be expressed in terms of the $U(N)$ Lie operators $E^\zeta_\eta = a^\dagger_\zeta a_\eta$. Hamiltonian (6) can be expressed as

$$H = V + K_{\zeta\eta}E^\zeta_\eta + \tfrac{1}{4}[\zeta\eta|\iota\kappa]E^\zeta_\eta E^\iota_\kappa,$$
$$K_{\zeta\eta} = h_{\zeta\eta} + \tfrac{1}{4}[\zeta\eta|\iota\iota]. \tag{167}$$

We obtain from Eqs. (18) and (167) the Heisenberg equation of motion for the $U(N)$ Lie operators

$$i\hbar\frac{\partial}{\partial t}E^\eta_\zeta = [E^\eta_\zeta, H] = \mathscr{F}_{\zeta\lambda}E^\eta_\lambda - E^\lambda_\zeta\mathscr{F}_{\lambda\eta},$$
$$\mathscr{F}_{\zeta\eta} = h_{\zeta\eta} + \tfrac{1}{2}[\zeta\eta|\iota\kappa]E^\iota_\kappa. \tag{168}$$

The expectation values of the $U(N)$ Lie operators by a Slater determinant $|\Phi(u)\rangle$ are the density matrix Q of $|\Phi(u)\rangle$,

$$\langle\Phi(u)|E^\eta_\zeta|\Phi(u)\rangle = \langle\Psi|U^\dagger(u)a^\dagger_\eta a_\zeta U(u)|\Psi\rangle$$
$$= \langle\Psi|a^\dagger_\iota u^*_{\eta\iota}a_\kappa u_{\zeta\kappa}|\Psi\rangle = u_{\zeta\alpha}u^*_{\eta\alpha} = Q_{\zeta\eta}. \tag{169}$$

We also have

$$\langle\Phi(u)|E^\iota_\kappa E^\eta_\lambda|\Phi(u)\rangle = Q_{\kappa\iota}Q_{\lambda\eta} - Q_{\kappa\eta}Q_{\lambda\iota}. \tag{170}$$

By using Eqs. (169) and (170), the expectation value of the Heisenberg equation of motion (168) by $|\Phi(u)\rangle$ gives us the time dependent HF (TDHF) equation for the density matrix

$$i\hbar\frac{\partial}{\partial t}Q_{\zeta\eta} = F_{\zeta\lambda}(Q)Q_{\lambda\eta} - Q_{\zeta\lambda}F_{\lambda\eta}(Q),$$
$$F_{\zeta\eta}(Q) = h_{\zeta\eta} + [\zeta\eta|\iota\kappa]Q_{\kappa\iota}, \tag{171}$$

where $F_{\zeta\eta}(Q)$ is the Fock operator for $|\Phi(u)\rangle$.

We can construct a boson system with the same dynamics as the $U(N)$ expression of fermion dynamics. We introduce the bosons with the annihilation

and creation operators $b_{\zeta\alpha}$ and $b^{\dagger}_{\zeta\alpha}$ which correspond to the $U(N)$ amplitudes as

$$\sqrt{2}u_{\zeta\alpha} \to b_{\zeta\alpha}, \qquad \sqrt{2}u^{*}_{\zeta\alpha} \to b^{\dagger}_{\zeta\alpha}, \tag{172}$$

and satisfy the commutation relation

$$[b_{\zeta\alpha}, b^{\dagger}_{\eta\beta}] = \delta_{\zeta\eta}\delta_{\alpha\beta}, \qquad [b_{\zeta\alpha}, b_{\eta\beta}] = [b^{\dagger}_{\zeta\alpha}, b^{\dagger}_{\eta\beta}] = 0. \tag{173}$$

The operators defined by

$$\hat{E}^{\zeta}_{\eta} = b^{\dagger}_{\zeta\alpha}b_{\eta\alpha}, \qquad \hat{E}^{\zeta\dagger}_{\eta} = \hat{E}^{\eta}_{\zeta}, \tag{174}$$

satisfy the commutation relation of $U(N)$ Lie operators

$$[\hat{E}^{\zeta}_{\eta}, \hat{E}^{\iota}_{\kappa}] = \delta_{\eta\iota}\hat{E}^{\zeta}_{\kappa} - \delta_{\zeta\kappa}\hat{E}^{\iota}_{\eta}. \tag{175}$$

Hence, we call the bosons $U(N)$. We define the Hamiltonian of the $U(N)$ bosons in the same form as Eq. (167) with the boson $U(N)$ Lie operators

$$\hat{H} = V + K_{\zeta\eta}\hat{E}^{\zeta}_{\eta} + \tfrac{1}{4}[\zeta\eta|\iota\kappa]\hat{E}^{\zeta}_{\eta}\hat{E}^{\iota}_{\kappa}. \tag{176}$$

Then, the Heisenberg equation of motion for $\hat{E}^{\iota}_{\eta}$ becomes of the same form as Eq. (168),

$$\begin{aligned} i\hbar\frac{\partial}{\partial t}\hat{E}^{\eta}_{\zeta} &= \hat{\mathscr{F}}_{\zeta\lambda}\hat{E}^{\eta}_{\lambda} - \hat{E}^{\lambda}_{\zeta}\hat{F}_{\lambda\eta}, \\ \hat{\mathscr{F}}_{\zeta\eta} &= h_{\zeta\eta} + \tfrac{1}{2}[\zeta\eta|\iota\kappa]\hat{E}^{\iota}_{\kappa}. \end{aligned} \tag{177}$$

Thus, the dynamics of the $U(N)$ bosons are identical with the fermion dynamics as long as the $U(N)$ Lie operators are concerned.

The Hilbert space of the $U(N)$ bosons is wider than the Hilbert space of fermions because it contains spaces with any permutation symmetry for permutations of spin orbital indices $\zeta, \eta, \ldots$. However, it contains a subspace which is isomorphic to the Hilbert space of fermions. The totally antisymmetric subspace with n bosons spanned by the state vectors

$$\mathscr{A}(b^{\dagger}_{\zeta 1}b^{\dagger}_{\eta 2}\cdots b^{\dagger}_{\kappa n})|0\rangle_{B}, \tag{178}$$

where $|0\rangle_{B}$ is the boson vacuum satisfying $b_{\zeta\alpha}|0\rangle_{B} = 0$, is isomorphic to the space of n fermions. Hamiltonian (176) has no matrix element to connect this subspace with the outside. Therefore, the $U(N)$ boson gives an exact representation of a fermion system in the totally antisymmetric subspace. In the classical c-number limit of the $U(N)$ bosons

$$b_{\zeta\alpha} \to \sqrt{2}u_{\zeta\alpha}, \qquad b^{\dagger}_{\zeta\alpha} \to \sqrt{2}u^{*}_{\zeta\alpha}, \tag{179}$$

the Lie operator $\hat{E}^{\eta}_{\zeta}$ and the operator $\hat{\mathscr{F}}_{\zeta\eta}$ reduce to the HF density matrix and the Fock operator, respectively,

$$\hat{E}^{\eta}_{\zeta} \to 2Q_{\zeta\eta}, \qquad \hat{\mathscr{F}}_{\zeta\eta} \to F_{\zeta\eta}(Q), \tag{180}$$

so that the equation of motion (177) reduces to the TDHF equation (171) for the density matrix. Thus, the TDHF theory is the classical limit of the $U(N)$

boson system which is an exact boson representation of a fermion system. This result indicates the special and basic position of the HF approximation and explains why it can be a so powerful approximation. We should stress that this result holds for the HF approximation in the wide sense to yield broken symmetries since the $U(N)$ amplitudes $u_{\zeta\eta}$ in general lead to broken symmetry spin orbitals. Similar result was obtained for the Hartree–Bogoliubov theory by Malshalek and Holzwarth (1972) and Yamamura and Nishiyama (1976).

The above results provide a TDHF view for $U(N)$ GC wave functions and the Peierls–Yoccoz theory. A Slater determinant $|\Phi(u)\rangle$ is transformed by a spin rotation s to $U(s)|\Phi(u)\rangle = |\Phi(su)\rangle$. $|\Phi(su)\rangle$ has the same energy as $|\Phi(u)\rangle$, but $|\Phi(su)\rangle \neq |\Phi(u)\rangle$ if s is not included in the invariance group G of $|\Phi(u)\rangle$. Hence, a Slater determinant of broken spin symmetry is always in a family $\{\Phi(su); s \notin G\}$ continuously degenerated in energy. Therefore, if the RHF ground state is unstable and the HF ground state becomes of UHF type with a broken spin symmetry, then the profile of the HF energy functional on the $U(N)$ group must look like Figure 10. The HF energy surface on the $U(N)$ group must have a valley around the point representing the RHF ground state which is cyclic and equienergetic with respect to spin rotation su of u. The cyclic and equienergetic line at the bottom of the valley represents the continuously degenerated family $\{\Phi(su); s \notin G\}$ of the UHF ground state.

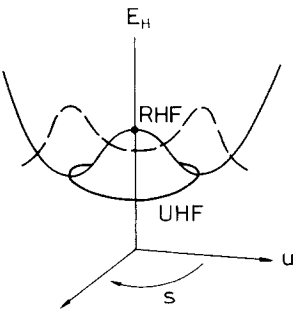

Figure 10. Structure of the HF energy functional surface on the $U(N)$ group around the unstable RHF point. s represents the direction of spin rotation. The dashed line represents the profile of the ground state wave function of quantized TDHF motion.

In the TDHF theory, the representative point u of a Slater determinant $|\Phi(u)\rangle$ moves on the HF energy functional surface according to Eq. (171). The structure of the surface yields two modes of different natures in TDHF motion, the rotational motions on a cyclic and equienergetic trajectory $\{su; s \in S\}$ along the valley and the vibrational motions traversing the valley. The rotational mode corresponds to coherent rotation of spin vectors.

If TDHF motions are quantized, then we get the exact theory for fermion dynamics. GC wave functions on the $U(N)$ group are nothing but the wave

functions for quantized TDHF motions of the representative point u. The ground state probability distribution of quantized TDHF motion must have a profile as depicted in Figure 10. It must have the same value on a line $\{su; s \in S\}$ and the largest probability on the bottom line of the valley which represents the continuously degenerate UHF ground state. The deeper and steeper the valley, the probability distribution becomes the more concentrated on the bottom line of the valley. This is the TDHF criterion for the UHF ground state to be a good approximation for the exact ground state. The Peierls–Yoccoz theory picks up the rotational mode of quantized TDHF motion. Since the rotational TDHF motion occurs on an equienergetic trajectory, the wave functions of quantized rotational TDHF motions are solely determined by the rotational character of the motions and are given by the D functions. Thus the present theory shows that a system with the HF ground state of the UHF type has excitations of two different characters, the excitations due to coherent rotation of spins and the excitations of vibrational character. The former excitations are related to the broken spin symmetry components of the UHF ground state wave function. We shall discuss the nature of excited states further in Section 4. The presence of the two different modes of excitation was pointed out by the author (Fukutome, 1978) on the basis of a generator coordinate representation similar to Eq. (159) on a wider Lie group and a Tamm–Dancoff expansion derived from the representation.

3. Applications of the UHF Theory to Molecules and Chemical Reactions

A. Systems with an ASDW Ground State

We consider here first some simple molecular systems in which the RHF ground state becomes unstable and an ASDW ground state appears with a change in nuclear conformation. The systems are a hydrogen molecule with varying interatomic distance, internal rotation of ethylene, and methylene with a varying bending angle. The essential points of those systems can be well described by a simple two electron–two orbital model. The model provides a clear cut understanding of the mechanism causing a triplet instability of the RHF ground state and the nature of the resultant ASDW ground state to represent a diradical. We next generalize the concepts obtained from the model. We consider about a classification of chemical reaction mechanisms by means of the triplet instability and orbital phase continuity criteria. We also discuss the physical factors contributing to realization or change of reaction mechanisms.

i. Triplet Instability of the RHF Ground State in the Two Electron–Two Orbital Model of a Hydrogen Molecule, Ethylene, and Methylene. We consider here a two electron system with an occupied RHF spatial orbital ϕ_a and an unoccupied one ϕ_m. The two electron–two orbital system can be used as a model for a hydrogen molecule, ethylene in a π-electron approximation, and methylene in an approximation that considers only two nonbonding electrons. In the hydrogen molecule and twisted ethylene, the two RHF orbitals are the bonding

and antibonding orbitals

$$\phi_a \equiv \phi_1 = (1/\sqrt{2})(\chi_1 + \chi_2), \qquad \phi_m \equiv \phi_2 = (1/\sqrt{2})(\chi_1 - \chi_2), \tag{181}$$

where χ_1 and χ_2 are the orthogonalized $1s$ AO's in H_2 and the orthogonalized π AO's on the two CH_2 moieties in C_2H_4 whose $2p$ lobes are mutually twisted by the twisting angle θ. In methylene, they are the σ and π type nonbonding orbitals

$$\phi_a \equiv \phi_1 = s \sin\alpha + p_x \cos\alpha, \qquad \phi_m \equiv \phi_2 = p_z, \tag{182}$$

where s, p_x, and p_z are the $2s$, σ type $2p$, and π type $2p$ AO's, respectively, and α is the parameter of the hybridization in the σ type nonbonding orbital which is a function of the bending angle θ and becomes $\alpha = 0$ at $\theta = \pi$.

The two electron–two orbital model is easy to handle but retains the essential points of those systems. We consider here the mechanism to cause a triplet instability of the RHF ground state using the model according to Fukutome (1972, 1973b) and Takabe et al. (1976). All the irreducible instability matrices of the RHF ground state $(\phi_a)^2$ in the two electron–two orbital model are one dimensional and have only one eigenvalue. From Eq. (130), they are given by

$$\begin{aligned} {}^1ST_+ &: \quad \varepsilon_m - \varepsilon_a + 3\langle ma|ma\rangle - \langle mm|aa\rangle, \\ {}^1ST_-, {}^3ST_+ &; \quad \varepsilon_m - \varepsilon_a - \langle mm|aa\rangle + \langle ma|ma\rangle, \\ {}^3ST_- &: \quad \varepsilon_m - \varepsilon_a - \langle mm|aa\rangle - \langle ma|ma\rangle, \end{aligned} \tag{183}$$

where $\varepsilon_m = F_{mm}$ and $\varepsilon_a = F_{aa}$ are the orbital energies of ϕ_m and ϕ_a. Equation (183) shows that the ordering of the eigenvalues of these instability matrices is

$${}^1ST_+ > {}^1ST_-, {}^3ST_+ > {}^3ST_-; \tag{184}$$

namely, ${}^3ST_-$ instability occurs the easiest. The same situation holds in general for the lowest eigenvalues of these instability matrices. Hereafter, we call the ${}^3ST_-$ instability the triplet instability since it has been customary to do so. The condition for a triplet instability to occur in the model is

$$\varepsilon_m - \varepsilon_a - \langle mm|aa\rangle - \langle ma|ma\rangle \leqq 0. \tag{185}$$

The triplet instability condition (185) is determined by three physical factors. As shown in Figure 11, the spin flipping triplet excitation of an electron in the RHF ground state $(\phi_a)^2$ to the unoccupied orbital ϕ_m leads to an energy loss by the orbital energy gap $\varepsilon_m - \varepsilon_a$ but at the same time it produces energy gains by

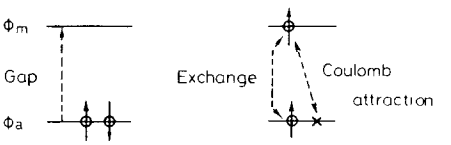

Figure 11. Factors contributing to a triplet instability.

the Coulomb attraction energy $-\langle mm|aa\rangle$ between the excited electron and the hole produced by the excitation and by the exchange interaction energy $-\langle ma|ma\rangle$ between the excited electron and the electron remained on the orbital ϕ_a. If the energy gain due to the particle–hole Coulomb attraction and the exchange interaction exceeds the energy loss due to the orbital energy gap, the system aquires a net energy gain by the triplet excitation, namely, the system is unstable for the triplet excitation. The triplet instability condition (185) just represents this physical situation. We note that Eq. (185) is not the condition for the triplet excited state to be lower in energy than the RHF ground state but is the condition for the RHF ground state to be unstable for production of virtual triplet particle–hole pairs.

The above consideration shows that a triplet instability is realized when the orbital energy gap becomes small. Because of the SCF character of the HF orbitals, the condition for smallness of the HF orbital energy gap is not so obvious. However, a clear cut condition can be obtained for the Hückel type orbital energy gap. The HF orbital energies in the model are given by

$$\varepsilon_a = h_{aa} + \langle aa|aa\rangle, \qquad \varepsilon_m = h_{mm} + 2\langle mm|aa\rangle - \langle ma|ma\rangle. \tag{186}$$

Then, Eq. (185) becomes

$$h_{mm} - h_{aa} + \langle ma|aa\rangle - \langle aa|aa\rangle - 2\langle ma|ma\rangle \leq 0. \tag{187}$$

Because of the inequalities

$$\langle mm|aa\rangle - \langle aa|aa\rangle \leq 0, \qquad \langle ma|ma\rangle \geq 0, \tag{188}$$

the condition (187) is certainly fulfilled if the Hückel type orbital energy gap $h_{mm} - h_{aa}$ becomes zero. This condition is satisfied in all three systems we are now considering. As shown in the orbital correlation diagrams of Figure 12, the Hückel orbital energy gap becomes zero at the infinite interatomic distance $R = \infty$ in H_2, at the linear conformation with the bending angle $\theta = \pi$ in CH_2, and at the orthogonal conformation with the twisting angle $\theta = \frac{1}{2}\pi$ in the internal rotation of C_2H_4. Therefore, the RHF ground state of these systems becomes triplet unstable in a domain surrounding the nuclear conformation with zero Hückel orbital energy gap.

ii. HF Ground States in the Homopolar Two Electron–Two Orbital Model. When the RHF ground state becomes triplet ($^3ST_-$) unstable, an ASDW

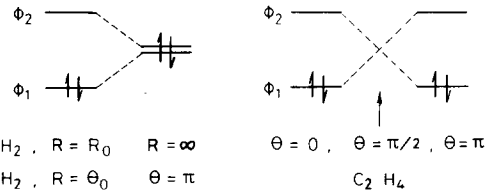

Figure 12. Orbital correlation diagrams for H_2, CH_2, and C_2H_4.

ground state appears from the instability threshold as we have shown in Section 2.C.ii. The three systems considered in the preceding section are homopolar and the orbitals $\phi_a = \phi_1$ and $\phi_m = \phi_2$ have different symmetries. The solutions of the HF equation in such a homopolar two electron–two orbital model were studied by Falicov and Harris (1969), Pople (1971), Fukutome (1972, 1973b), Ostlund (1972), and Jordan and Silbey (1973). We discuss here the properties of the HF ground states in the model according to these works.

The HF equation in the model has two closed shell RHF solutions $(\phi_1)^2$ and $(\phi_2)^2$. It also has triplet RHF solutions $(\phi_1\phi_2)$ and $(\bar{\phi}_1\bar{\phi}_2)$. We use the notation where RHF orbitals in an open shell without and with bars represent those with up and down spins, respectively. An ASDW solution exists below $(\phi_1)^2$ and $(\phi_2)^2$ with the occupied spin orbitals

$$\begin{aligned} \phi_\pm &= [\cos(\tfrac{1}{2}\lambda)\phi_1 + (\mathbf{e}\cdot\boldsymbol{\sigma})\sin(\tfrac{1}{2}\lambda)\phi_2]\eta_\pm, \\ \cos\lambda &= -a/(b+c), \end{aligned} \tag{189}$$

where the unit vector $\mathbf{e}$ is arbitrary so that the ASDW solution is continuously degenerated and

$$\begin{aligned} a &= \tfrac{1}{2}(h_{22}-h_{11}) + \tfrac{1}{4}(\langle 22|22\rangle - \langle 11|11\rangle), \\ b &= \tfrac{1}{4}\langle 11-22|11-22\rangle, \\ c &= \langle 12|12\rangle. \end{aligned} \tag{190}$$

The energies of these solutions are

$$\begin{aligned} (\phi_1)^2: &\quad E_H = \varepsilon + 2a + b, \\ (\phi_2)^2: &\quad E_H = \varepsilon - 2a + b, \\ (\phi_1\phi_2), (\bar{\phi}_1\bar{\phi}_2): &\quad E_H = \varepsilon - c - b, \\ \text{ASDW}: &\quad E_H = \varepsilon - c - a^2/(b+c), \\ \varepsilon &= h_{11} + h_{22} + \tfrac{1}{4}\langle 11+22|11+22\rangle. \end{aligned} \tag{191}$$

We note that the normalized energy

$$e = (E_H - \varepsilon + c)/2c \tag{192}$$

depends only on the two parameters $q = -a/c$ and $r = b/c$ and Eq. (191) may be written

$$\begin{aligned} (\phi_1)^2: &\quad e = \tfrac{1}{2}(1+r) - q, \\ (\phi_2)^2: &\quad e = \tfrac{1}{2}(1+r) + q, \\ (\phi_1\phi_2), (\bar{\phi}_1\bar{\phi}_2): &\quad e = -\tfrac{1}{2}r, \\ \text{ASDW}: &\quad e = -q^2/2(1+r). \end{aligned} \tag{193}$$

We show in Figure 13(a) the q dependences of the normalized energies of these solutions.

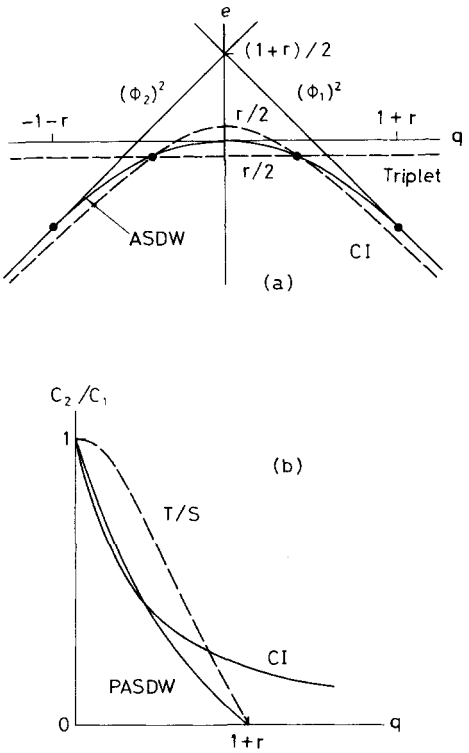

Figure 13. q Dependences of the normalized energies of the RHF, ASDW, and exact singlet and triplet ground states in the two electron model (a) and those of the ratio of the CI coefficients C_2/C_1 in the exact and PASDW ground states. The triplet to singlet ratio of the components of the ASDW state is also shown in (b) (---). $r = 0.2$ in these graphs.

As seen in Figure 13(a), $(\phi_1)^2$ and $(\phi_2)^2$ cross at $q = 0$. They are the singlet RHF ground states in the regions $q > 0$ and $q < 0$, respectively. The existence condition for the ASDW solution (189) is

$$-1 \leq -a/(b+c) \leq 1. \tag{194}$$

The right-hand inequality of Eq. (194) is identical with the triplet instability condition (185) for $(\phi_1)^2$ and the left-hand one with the triplet instability condition for $(\phi_2)^2$. The ASDW solution connects with $(\phi_1)^2$ at $q = 1+r$ and with $(\phi_2)^2$ at $q = -(1+r)$. It gives a potential connecting smoothly the potentials of the two RHF solutions. The series $(\phi_1)^2$–ASDW–$(\phi_2)^2$ is the singlet HF ground state of the system.

When the condition

$$a^2 - b^2 - bc \leq 0 \tag{195}$$

is satisfied, the triplet RHF solution becomes lower in energy than the ASDW solution as seen from Eq. (191). As shown in Fukutome (1973b), condition (195) is nothing but the A_-M instability condition for the ASDW solution. The two solutions, however, do not interconnect but cross at the A_-M instability threshold $q=\pm(r^2+r)^{1/2}$. Therefore, the A_-M instability is a crossing instability representing the crossing of the triplet RHF solution with the ASDW solution. Condition (195) is also the A_-M stability condition for the triplet RHF solution. If it is not satisfied, the triplet RHF solution is A_-M unstable but if it is satisfied, then the triplet solution becomes A_-M stable. There is no other triplet type solution and the triplet RHF solution is the triplet HF ground state of the system.

The exact singlet ground state of the model is given by

$$\begin{aligned} |\Psi_0\rangle &= C_1\|\phi_1\bar{\phi}_1\| - C_2\|\phi_2\bar{\phi}_2\|, \\ C_2/C_1 &= [(4a^2+c^2)^{1/2}+2a]/c = (1+4q^2)^{1/2}-q, \\ E_0 &= \varepsilon + b - (4a^2+c^2)^{1/2}, \qquad e_0 = \tfrac{1}{2}(1+r) - (\tfrac{1}{4}+q^2)^{1/2}. \end{aligned} \tag{196}$$

The exact triplet ground state with spin magnetic quantum number ± 1 coincides with the triplet RHF solution. The Slater determinant of the ASDW solution with $\mathbf{e}=z$ is expanded into RHF configuration as

$$\begin{aligned} |\Phi^{\mathrm{ASDW}}\rangle = {} & \tfrac{1}{2}(1+\cos\lambda)\|\phi_1\bar{\phi}_1\| - \tfrac{1}{2}(1-\cos\lambda)\|\phi_2\bar{\phi}_2\| \\ & + \tfrac{1}{2}\sin\lambda\,(\|\phi_2\bar{\phi}_1\| - \|\phi_1\bar{\phi}_2\|). \end{aligned} \tag{197}$$

The first row of Eq. (197) is singlet but the second row is triplet. We show in Figure 13(b) the q dependences of the ratios C_2/C_1 in the exact singlet ground state and $(1-\cos\lambda)/(1+\cos\lambda)$ in the singlet projected ASDW solution, ^{1}PASDW. We see in Figure 13(b) that the ^{1}PASDW wave function is a good approximation to the exact one in the region of small q. It coincides with the exact wave functions at $q=0$ and $q=\pm(r^2+r)^{1/2}$. The ^{1}PASDW wave function connects with the RHF wave function with a discontinuity in the first order derivative as seen in Figure 13(b). This discontinuity at the instability threshold reflects the second order phase transition like character of interconnecting HF instabilities.

We also show in Figure 13(b) the q dependence of the relative weight of the triplet component in the ASDW wave function. It becomes large at small q and is equal to 1 at $q=0$. The error of the ASDW energy due to the contamination of the triplet state becomes maximal at $q=0$. The error $E_H^{\mathrm{ASDW}}-E_0=-b$ at $q=0$ is solely due to the contamination of the triplet component since the singlet component at $q=0$ is identical with $|\Psi_0\rangle$. Therefore, the error in the ASDW energy may become appreciable if b is not small. Such a situation is met in CH_2 as we shall see in the next section. However, the error of this kind can be eliminated by the projection to the singlet state. We note that the ASDW and triplet solutions have the correct ordering in energy irrespective of the value of r because they cross at the same point as the crossing point of the exact singlet and triplet ground states.

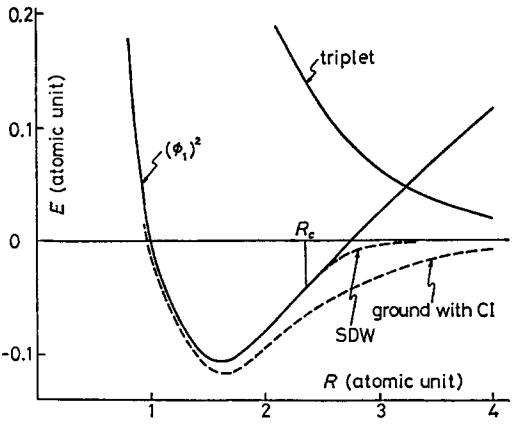

Figure 14. HF and CI potentials in the dissociation of H_2.

iii. HF Ground State of Hydrogen Molecule, Ethylene, and Carbenes. We apply the result of the preceding section to H_2, C_2H_4, and CH_2.

(*a*). *Hydrogen molecule*: In H_2, the RHF orbitals ϕ_1 and ϕ_2 are given by Eq. (181). Hence, the parameters (190) are

$$\begin{aligned} a &= \langle \chi_1 | h | \chi_2 \rangle + \langle \chi_1 \chi_2 | \chi_1 \chi_1 \rangle, \\ b &= \langle \chi_1 \chi_2 | \chi_1 \chi_2 \rangle, \\ c &= \tfrac{1}{2}(\langle \chi_1 \chi_1 | \chi_1 \chi_1 \rangle - \langle \chi_1 \chi_1 | \chi_2 \chi_2 \rangle). \end{aligned} \tag{198}$$

Since $a \leq 0$, only region $q \geq 0$ is realized. We show in Figure 14 the adiabatic potentials against the interatomic distance R of the RHF ground state $(\phi_1)^2$, the ASDW ground state, and the full CI singlet and triplet ground states. The RHF ground state potential does not converge to the two dissociated hydrogen atoms in the limit of $R = \infty$. This well known discrepancy of the RHF potential in the dissociation behavior is rescued by the ASDW solution appearing from the triplet instability of the RHF ground state. The ASDW potential converges to the correct dissociation limit of two hydrogen atoms. Since $a \to 0$ and $b \to 0$ in the limit $R \to \infty$, the ASDW energy is exact at $R = \infty$. Thus, the HF ground state $(\phi_1)^2$–ASDW gives a potential with correct dissociation behavior.

For $\mathbf{e} = z$, the ASDW orbitals (189) are of the DODS type and their spatial orbitals are in the corresponding orbital form

$$\phi_1^{\pm} = \cos(\tfrac{1}{2}\lambda)\phi_1 \pm \sin(\tfrac{1}{2}\lambda)\phi_2. \tag{199}$$

The ASDW orbitals (199) have the structure as depicted in Figure 15. In the ASDW state, the up spin electron localizes toward an atom and the down spin one toward another atom. The localization of two electrons becomes complete in the dissociation limit because $\lambda \to \frac{1}{2}\pi$ or $-\frac{1}{2}\pi$ at $R \to \infty$ (there are two

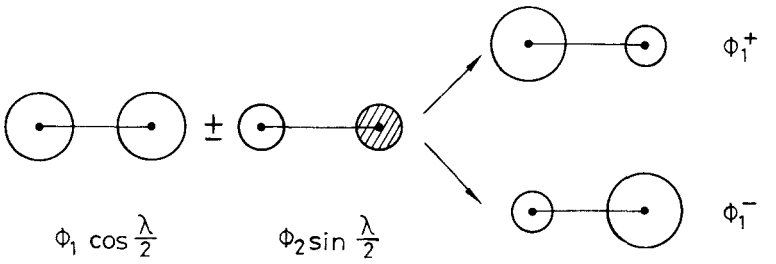

21012
21013

Figure 15. ASDW orbitals in H_2.

possibilities in the sign of $\sin(\frac{1}{2}\lambda)$ for a given $\cos\lambda$ so that the ASDW solution is doubly degenerated for a given **e**), so that

$$\begin{aligned} \phi_1^+ &\to \chi_1 \quad \text{or } \chi_2, \\ \phi_1^- &\to \chi_2 \quad \text{or } \chi_1, \\ |\Phi^{\text{ASDW}}\rangle &\to \|\chi_1\bar{\chi}_2\| \quad \text{or } \|\chi_2\bar{\chi}_1\|. \end{aligned} \tag{200}$$

Thus, the ASDW wave function in the dissociation limit consists of the correct localized atomic states though it involves the component of incorrect total spin. It represents the diradical state H·+H·.

(*b*). *Internal rotation of ethylene*: In the case of twisted C_2H_4 too, the RHF orbitals and the parameters *a*, *b*, and *c* are given in the forms of Eqs. (181) and (198), respectively. The parameter *a*, however, can take both positive and negative values, $a>0$ for $0\le\theta<\frac{1}{2}\pi$ and $a<0$ for $\frac{1}{2}\pi<\theta\le\pi$. At $\theta=\frac{1}{2}\pi$, $a=0$ but $b\neq 0$. We show in Figure 16 the adiabatic potentials against θ of HF solutions and exact eigenstates of two electron–two orbital model. The potentials of all the HF solutions and exact eigenstates not described in the preceding section are drawn also in Figure 16. We see in Figure 16 that the potential of the HF ground

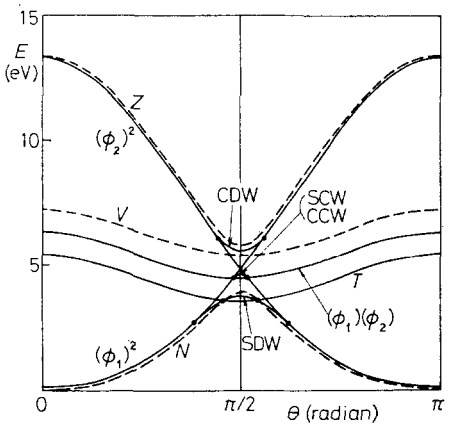

Figure 16. HF (—) and CI (---) potentials in the internal rotation of C_2H_4.

state $(\phi_1)^2$–ASDW–$(\phi_2)^2$ is a good approximation to the potential of the exact singlet ground state. The parameter b is the interatomic exchange integral between the two $2p$ lobes χ_1 and χ_2 and its value is small in the whole range of θ, so that the error in the ASDW energy due to the contamination of the triplet component is small. The ASDW orbitals have the form of Eq. (199) and an electron localizes toward a carbon atom and another one toward another carbon atom in the manner similar to the ASDW state in H_2. The localization of the two electrons becomes complete at $\theta = \frac{1}{2}\pi$ and the ASDW orbitals and wave functions become of the form of Eq. (200). The ASDW state therefore represents the diradical state $\succ\dot{C}—\dot{C}\prec$.

The model has a CCW and an ASCW solutions which are degenerate in energy and connect smoothly the potentials of $(\phi_1)^2$ and $(\phi_2)^2$ as shown in Figure 16. However, their energy is higher than the energy of the ASDW solution and the potential of the series $(\phi_1)^2$–CCW, ASCW–$(\phi_2)^2$ does not cross with the triplet state at the correct position. Hence, they are considered to be unphysical solutions. There is also a CDW solution

$$\begin{aligned} \varphi_{\pm} &= [\cos(\tfrac{1}{2}\lambda)\phi_1 + \sin(\tfrac{1}{2}\lambda)\phi_2]\eta_{\pm}, \\ \cos\lambda &= a/(c-b), \\ E_H &= \varepsilon + c + a^2/(c-b). \end{aligned} \tag{201}$$

It is a closed shell solution breaking the spatial symmetry. It connects smoothly $(\phi_2)^2$ and $(\phi_1)^2$ from the upper side as seen in Figure 16. The potential of the series $(\phi_2)^2$–CDW–$(\phi_1)^2$ is a good approximation to the potential of the singlet excited state Z. The CDW orbitals are also localized toward a carbon atom. The localization of the CDW orbitals becomes complete at $\theta = \frac{1}{2}\pi$; $\varphi_{\pm} = \chi_1\eta_{\pm}$ or $\chi_2\eta_{\pm}$ (the CDW solution is doubly degenerated with $\sin(\frac{1}{2}\lambda)$'s of different signs). Hence, the CDW solution at $\theta = \frac{1}{2}\pi$ represents the zwitter ionic state $\succ C^-—C^+\prec$ or $\succ C^+—C^-\prec$. The singly excited configurations $(\phi_1\bar{\phi}_2)$ and $(\phi_2\bar{\phi}_1)$ also are the HF solutions of the model. They are the equal weighted superpositions of the triplet state T and the singly excited singlet state V. Their potential is just at the middle of the potentials of the T and V states. The error of the potential is constantly large, so that they cannot be regarded as a reasonable approximation to either of the T or V state.

The ASDW potential crosses with the triplet state potential and the lowest energy HF state at the orthogonal conformation is triplet in agreement with the ordering of the exact singlet and triplet ground state. This ordering of the two states in the two electron model, however, is reversed in the full valence electron system. The ASDW state as well as the exact singlet ground state becomes lower than the triplet ground state. The reason for this reversal will be discussed in Section 3.B.i.

(*c*). *Carbenes*: In the case of methylene, the two electron model does not provide potentials that can be compared with the real bending potentials because the relation of the hybridization angle α to the bending angle θ is unknown and

the bonding σ electrons also are contributing to the potentials. However, the essential feature of the state of two nonbonding electrons can be correctly described by the two electron model. The RHF orbitals of nonbonding electrons in the two electron model are given by Eq. (182). The ASDW orbitals [Eq. (199)] have the structure as depicted in Figure 17. As a result of the mixing of the σ

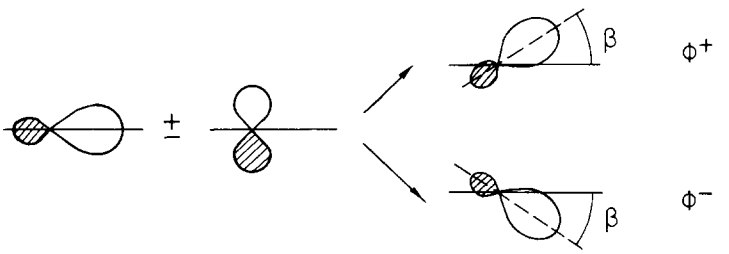

Figure 17. Structure of the nonbonding ASDW orbitals on the carbon atom of CH_2.

and π type RHF orbitals, the ASDW orbitals $\phi_1^{\pm}$ are the hybridized $2p$ lobes whose directions are tilted against the molecular plane by angles $\pm\beta$, $\tan\beta = [\tan(\frac{1}{2}\lambda)]/\cos\alpha$. The two nonbonding electrons enter into the different lobes tilted toward different sides of the molecular plane. The ASDW corresponding orbitals $\phi_1^{\pm}$ become pure $2p$ lobes with the tilting angles $\pm\frac{1}{4}\pi$, i.e., they are orthogonal, at $\theta = \pi$. Hence, the ASDW state in CH_2 represents the one center diradical >C: in contrast to the ASDW states in H_2 and C_2H_4 representing two center diradicals.

The parameters (190) at $\theta = \pi$ become

$$\begin{aligned} a &= 0, \qquad c = \langle p_x p_z \,|\, p_x p_z \rangle, \\ b &= \tfrac{1}{4}\langle (p_x + p_z)(p_x - p_z) \,|\, (p_x + p_z)(p_x - p_z) \rangle = c. \end{aligned} \tag{202}$$

Since b is an intraatomic exchange integral, its value is not small and the projection to the singlet component of the ASDW state is necessary for getting a good potential.

A full valence electron MINDO/2 UHF calculation was carried out by Takabe et al. (1976) for the carbenes CH_2, CHF, and CF_2. We show in Figure 18 the full valence electron UHF bending potentials. The singlet projected ASDW potential is also shown. The RHF ground state of CH_2 and CHF is always triplet unstable for $\theta > 80°$ and the singlet HF ground state at the equilibrium geometry is the ASDW type. On the other hand, the RHF ground state in CF_2 is stable in the region $\theta < 135°$ and the equilibrium geometry belongs to the region of stable RHF ground state. The relative position of the singlet and triplet HF ground state potentials changes sensitively upon substitution by fluorine. The triplet potential of CH_2 lies much below the projected ASDW potential and the ground state of CH_2 is triplet. The projected ASDW and triplet potentials in CHF have the equilibrium geometries with nearly same energies, indicating that CHF may be

present in both singlet and triplet states. The triplet potential of CF_2 is much higher than the singlet potential and the ground state of CF_2 is singlet. These results are in agreement with the results of an ab initio SCF CI calculation by Harrison (1971).

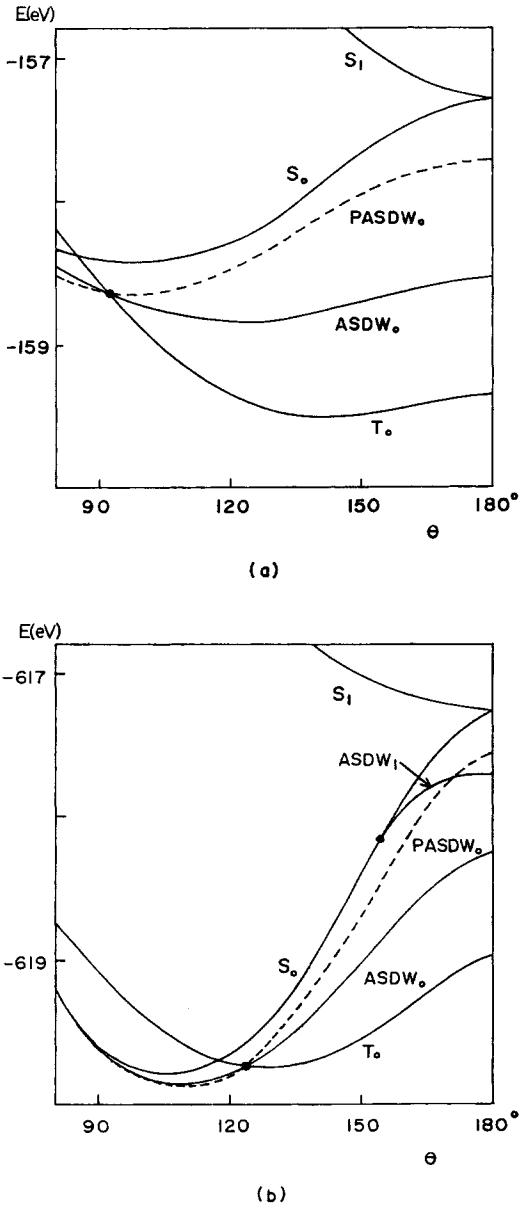

Figure 18. HF bending potentials of CH_2 (a), CHF (b), and CF_2 (c).

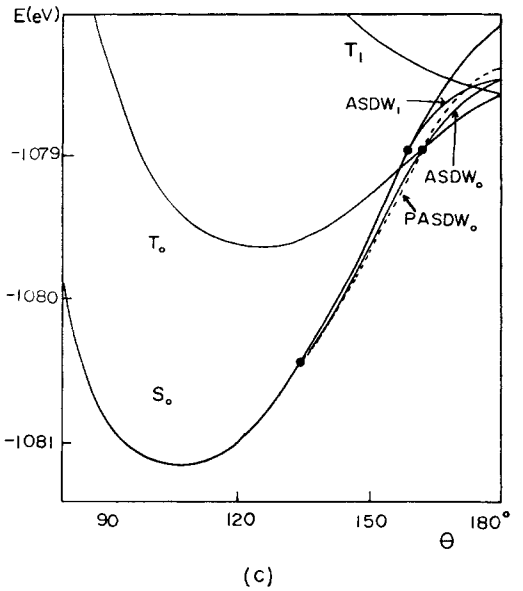

Figure 18. (*Continued from previous page.*)

iv. UHF Theoretical Classification of Singlet Ground State Reaction Mechanisms. The results in the preceding three sections indicate that the ASDW ground state appearing from a triplet instability of the singlet RHF ground state represents a state of diradical character. A singlet diradical, in the intuitive chemical picture, has two electrons of opposite spins localized to different regions of a molecule. An ASDW wave function has different orbitals for electrons with opposite spins. The DODS character of ASDW orbitals provides a natural orbital representation for diradicals.

Hayes and Siu (1971) and Salem and Rowland (1972) characterized a singlet diradical, from the CI point of view, as a molecule having the ground state wave function with a heavy mixing of a pairwise doubly excited RHF configuration. According to their characterization, a two electron system is a singlet diradical if the ratio C_2/C_1 of the CI coefficients in the singlet ground state wave function (196) is large. Our characterization of a singlet diradical as a molecule having the HF ground state of the ASDW type is consistent with theirs. As shown in Figure 13(b), the ratio C_2/C_1 becomes large in the region of the ASDW ground state and the singlet projected ASDW wave function correctly approximates the CI wave function with growing C_2/C_1. In the region of the ASDW ground state, a correlation effect becomes of essential importance. The RHF ground state without the correlation effect leads to qualitatively incorrect results in the region as seen in the incorrect dissociation behavior in H_2 and the failure to give a smooth potential for the internal rotation of ethylene. A triplet instability of the RHF ground state signals the essential importance of a correlation effect. The ASDW ground state appearing from the instability automatically incorporates the

essential correlation as we have seen in the two electron model and shall demonstrate for more complicated systems.

We can use a triplet instability of the RHF ground state as the UHF theoretical criterion for the onset of a diradical character in the singlet ground state. The result in Section 3.A.i can be generalized as a sufficient condition for a triplet instability to occur. A triplet instability of the RHF ground state always takes place in a reaction path with crossing of the Hückel type occupied and unoccupied orbitals, i.e., in a symmetry forbidden reaction path in the sense of Woodward and Hoffmann (1969).

A diradical can be represented by an ASDW wave function. However, ASDW wave functions may also represent tetra, hexa, etc., radicals as we shall show later. Yamaguchi (1975a) proposed a quantitative measure for the radicalness of an ASDW state. ASDW orbitals can be brought into the corresponding orbital representation [Eq. (103)]. Corresponding orbitals $\phi_A^{\pm}$ are in general different from the HF orbitals which are eigenstates of the Fock operator and orbital energies cannot be associated with them. However, the ASDW natural orbitals ϕ_A and $\bar{\phi}_A$ constituting them are not only the natural orbitals of the ASDW wave function, but also coincide with the natural orbitals of the projected ASDW wave function as proved by Harriman (1964). Hence, the number density matrices of the unprojected and projected ASDW wave functions are diagonalized by the ASDW natural orbitals so that they are the orbitals most suitable to see the electron distributions in these wave functions. Each corresponding orbital pair (ϕ_A^+, ϕ_A^-) reduces to a closed shell in the RHF ground state. The parameter d_A defined by

$$\langle \phi_A^+ | \phi_A^- \rangle = \cos 2\kappa_A \equiv 1 - d_A, \tag{203}$$

represents the extent of the splitting of the two corresponding orbitals; $d_A = 0$ for the closed shell $\phi_A^+ = \phi_A^-$ and $d_A = 1$ for the complete diradical with two electrons entering into disjoint orbitals $\phi_A^{\pm}$, $\langle \phi_A^+ | \phi_A^- \rangle = 0$. Therefore, the two electrons in a corresponding orbital pair can be regarded as a diradical if d_A has an appreciable value. If $d_A \approx 0$ except for one, two, or three corresponding orbital pairs, then the ASDW state can be regarded as a diradical, tetraradical, or hexaradical.

In a system with a crossing of occupied and unoccupied orbitals, a triplet instability always occurs. The triplet instability is suppressed by introduction of heteropolarity into the system. Introduction of a heteropolarity in general destroys the orbital crossing and a finite energy gap is produced. The finite energy gap is unfavorable to the triplet instability as discussed in Section 3.A.i and suppresses the occurrence of it. An analysis of the HF solutions in the heteropolar two electron–two center model molecule confirmed the suppressing effect of heteropolarity to the triplet instability of the RHF ground state, Fukutome (1973a). The ASDW ground state disappears when the heteropolarity exceeds a certain limit and the nature of the HF ground state changes at the limit from diradical to zwitter ionic. The effect of fluorine substituent in CH_2 discussed in the preceding section provides an example of the triplet instability suppressing

effect of heteropolarity in real molecules. Single substitution is not sufficient to suppress completely the triplet instability in CHF, but CF_2 with double substitution has the stable RHF ground state at the equilibrium conformation.

Yamaguchi et al. (1973a) proposed a UHF theoretical classification of singlet ground state reaction mechanisms by means of the triplet instability and orbital phase continuity criteria. Radical and nonradical mechanisms can be discriminated by occurrence and nonoccurrence of a triplet instability as discussed above. In concerted reactions of Woodward and Hoffmann (1969), symmetries of occupied RHF orbitals are conserved. Conservation of orbital symmetries implies conservation of signs of MO coefficients of occupied RHF orbitals. The latter criterion, the orbital phase continuity, is wider than the former because it can be applied to systems without symmetry. The orbital phase continuity criterion was utilized by Goddard III (1972) to obtain selection rules for reaction mechanisms from the generalized valence bond (GVB) picture. Yamaguchi et al. (1973a) discriminate symmetry allowed (concerted) and symmetry forbidden (nonconcerted) reactions by conservation and nonconservation of the RHF orbital phases. Thus, singlet ground state reactions are classified into the four mechanisms, the symmetry allowed nonradical (AN), the symmetry forbidden nonradical (FN), the symmetry allowed radical (AR), and the symmetry forbidden radical (FR) mechanisms. We note that the terms allowed and forbidden do not literally represent the allowedness and forbiddenness of the reaction mechanisms except for the AN case which is equivalent to Woodward and Hoffmann's concerted mechanism but represent the orbital correlation and the phase situations to characterize the mechanisms.

We show in Figure 19 the orbital correlation and phase situations for the four mechanisms to be realized. In the AN and FN cases, no crossing of occupied

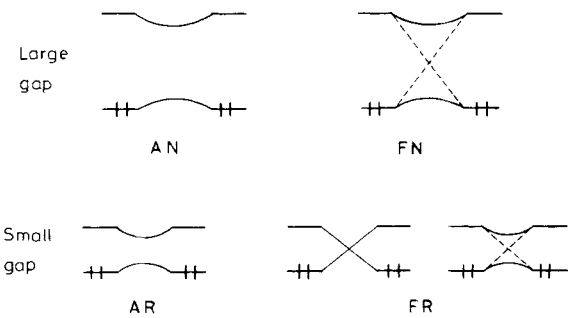

Figure 19. Orbital correlation situations for realization of the four reaction mechanisms. Dashed lines represent that the system is derived from a prototype system with orbital crossing by introduction of a heteropolarity.

and unoccupied orbitals is present and the orbital energy gap is large enough for no triplet instability to occur. The orbital phases are conserved in the AN case but not in the FN case. In FN reactions, there is a point on the reaction path where a MO coefficient of an occupied RHF orbital vanishes and changes sign

beyond it. Such a point is called the transition point. In the vicinity of the transition point, the two electrons in the orbital are repelled from the AO with vanishing MO coefficient so that the system has a zwitter ionic character. An FN reaction usually has a corresponding prototype homopolar system with orbital crossing from which it is derived by introduction of heteroatoms and substituents. If the heteropolarity is strong enough, then a large orbital energy gap is produced but the orbital phases remain nonconserved.

In the AR and FR cases, the orbital energy gap becomes small enough to produce a triplet instability. The orbital phases are conserved in the AR case but not in the FR case. A FR reaction has an orbital crossing or is derived from a prototype system with orbital crossing by introduction of heteropolarity but the orbital energy gap produced by the heteropolarity is not so large as deprives the triplet instability. In order for the FR and AR mechanisms to be realized, the orbital energy gap at the intitial state must be small. As shown in Figure 20, in

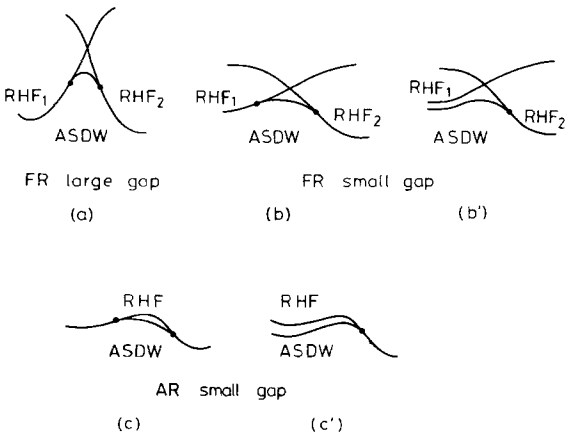

Figure 20. HF state correlation diagrams for an FR path with large initial gap (a), for an FR path with small initial gap, and nonradical (b) or radical (b') initial state and for an AR path with small initial gap and nonradical (c) or radical (c') initial state.

a FR reaction with orbital crossing, the initial and final states have different RHF ground states, RHF_1 and RHF_2. The two RHF states cross in the reaction path. If the orbital energy gap at the initial state is large, the energy gap between the two RHF states is also large and their crossing point usually has much higher energy than the initial state so that the ASDW ground state connecting the two RHF state is also of high energy as depicted in Figure 20(a) and the reaction is forbidden. This argument is the same as for Longuet-Higgins and Abrahamson (1965) for the forbiddenness of symmetry nonconserving reaction paths. However, if the orbital energy gap at the initial state is small, then the energy gap of the two RHF state is small and their crossing point and consequently the ASDW state connecting them are of low energy as depicted in Figure 20(b) so that the

reaction becomes allowed. The initial state of such a realizable FR reaction may be triplet stable [Fig. 20(b)] or unstable [Fig. 20(b')]. In the latter case, the initial state is already a diradical. The above consideration shows that FR reaction paths may be readily realizable in diradicals.

The potential of an AR reaction looks like Figures 20(c) and 20(c'). If the orbital energy gap at the initial state is small, the potential barrier is low and the reaction is allowed. If the initial gap is large, then the potential may be high and the reaction may be forbidden since the triplet instability in the reaction requires a small energy gap in an intermediate stage which requires a shift of the highest occupied orbital (HOMO) to high energy side or of the lowest unoccupied orbital (LUMO) to low energy side. We note that the potentials in FR and AR reactions are lowered by the correlation effect to be incorporated into the ASDW ground state. In a FR reaction, the two diradical electrons attain complete localizations at the point of orbital crossing while their localizations remain always incomplete in an AR reaction without orbital crossing. Therefore, the FR and AR mechanisms can be characterized as the complete and incomplete diradical mechanisms, respectively. An extensive discussion was made by Yamaguchi (1978) for the selection rules of chemical reactions derived from the UHF theory and the other models.

Conversion of reaction mechanism from diradical to zwitter ionic by asymmetric substitutions has been observed in many reaction systems. Yamaguchi et al. (1973b) analyzed the cycloaddition reactions of singlet oxygen to olefins by the UHF criteria:

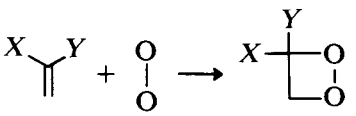

They showed that the reaction has a triplet instability domain for X, $Y = H$ but none for $X = CH_3$ and $Y = NH_2$, so that the latter case is zwitter ionic. Yamaguchi and Fueno (1973) also examined the ring opening reactions of the triangular molecules:

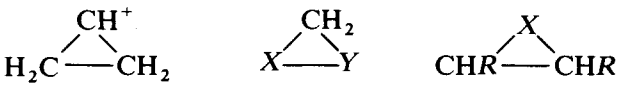

$X, Y = CH_2$, CRR' or O: $X = CH^-$, NR, O, or S.

They showed that a triplet instability occurs in the systems with weak asymmetry and the reactions are diradical but it disappears in the systems with strong asymmetry and the reactions become ionic.

We note that introduction of heteropolarity may convert an unrealizable FR reaction to realizable one. Consider a reactant and a reagent with large orbital energy gaps. If their HOMO's and LUMO's energies are close, then FR reaction between them is impossible. However, when heteroatoms or substituents are

introduced into, say, reagent, the HOMO–LUMO gap between the reactant and reagent may become small sufficient enough to yield an FR reaction between them. A typical example of such reactions is charge transfer reactions. They have both ionic and diradical characters. Yamaguchi (1975b) and Takabe and Yamaguchi (1976) showed that the UHF criteria are a good means to discriminate the ionic and charge transfer (ionic diradical) mechanisms.

We have shown in Section 3.A.i that the Coulombic attraction between excited electron and hole and the exchange interaction of excited electron with electrons remaining in occupied orbitals as well as small orbital energy gap are the factors to control a triplet instability. If the particle–hole attraction and the exchange interaction are small, then triplet instability may not occur even for small but finite orbital energy gap. Such a situation is realized if the differential overlap between the relevant unoccupied and occupied orbitals is small. Takahashi and Fukutome (unpublished) showed that such a mechanism is operating in the reaction to generate benzyne. The RHF HOMO and LUMO of benzyne are symmetric and antisymmetric orbitals composed of the σ AO's without the partner hydrogen atom depicted in Figure 21. Since the lobes of the σ AO's are

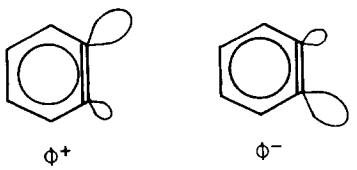

Figure 21. ASDW orbitals of benzyne.

not parallel, their overlap and consequently the HOMO–LUMO gap are small so that the RHF ground state of benzyne is triplet unstable. The HF ground state of benzyne is an ASDW with the structure similar to those of H_2 and C_2H_4. Benzyne is produced most effectively by the ionic abstraction of LiH from Li substituted benzene

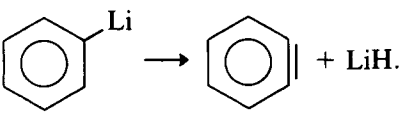

UHF calculation of this system showed that triplet instability does not occur even for the distance of LiH farther than 5 Å indicating that the reaction can proceed ionically. Triplet instability occurs in the abstractions of H_2 and HF as soon as the abstractions begin. The large delay of the triplet instability in the LiH abstraction is due to the fact that the LUMO's of benzyne and LiH have very close energies so that the LUMO of the total system is delocalized over both benzyne and LiH while the HOMO is localized on benzyne. This makes the particle–hole attraction and exchange interaction in the system small and leads to suppression of triplet instability. Thus, the strong LUMO–LUMO interaction

controls the ionic character of the reaction. It should be noted that triplet instability and the correlated ground state of a diradical are controlled not only by occupied RHF orbitals but also by unoccupied ones, so that events in unoccupied orbitals may effect them. We shall discuss in the next section, another example of chemical reactions the nature of whose ground state is controlled by an event in unoccupied RHF orbitals.

B. Systems with ASDW, TSDW, and TSW Ground States

We consider here examples of chemical reaction systems whose HF ground state change the nature between RHF, ASDW, TSDW, and TSW types via instabilities with changes of nuclear conformation. The HF ground state of different natures in a reaction system are called HF phases. The characteristics of the correlation effects in UHF phases can be visualized by "antiferromagnetic" ordered spin structures with different modulations of the spin density vectors for different phases. Instabilities of the HF ground state provide an HF phase map showing the domains where different HF phases arise. The HF phase map and the spin structure representation of UHF phases provide a clear understanding for the electronic processes involved in a complicated correlated wave function undergoing large changes with changes of nuclear conformation.

i. H_4 System. As the first example of a system with plentiful instabilities in the HF ground state, we consider here the system consisting of four hydrogen atoms according to Fukutome et al. (1975).

(a). RHF ground states and their $^3ST_-$ instabilities: We consider the H_4 system in the conformations with D_2 symmetry as depicted in Figure 22(a). The

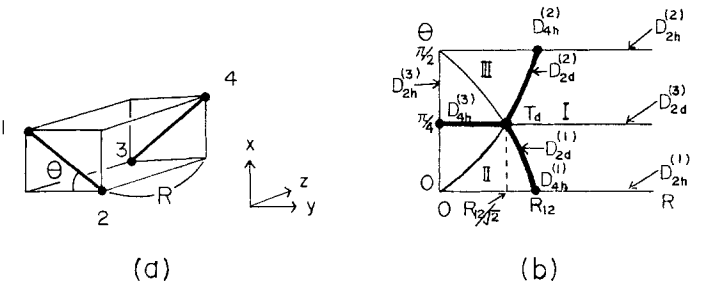

Figure 22. D_2 conformation of the H_4 system (a) and the conformations of higher symmetries contained in the geometry (b). RHF ground states cross on the heavy lines in (b).

intramolecular distances are kept constant and a D_2 conformation is specified by the intermolecular distance R and the twisting angle θ. The conformations contain three D_{2h}, D_{4h}, and D_{2d} conformations and a T_d one as shown in Figure 22(b). The RHF orbitals in the minimal basis approximation are

$$\begin{aligned} \phi_1 &= \tfrac{1}{2}(\chi_1+\chi_2+\chi_3+\chi_4), & \phi_2 &= \tfrac{1}{2}(\chi_1+\chi_2-\chi_3-\chi_4), \\ \phi_3 &= \tfrac{1}{2}(\chi_1-\chi_2+\chi_3-\chi_4), & \phi_4 &= \tfrac{1}{2}(\chi_1-\chi_2-\chi_3-\chi_4). \end{aligned} \tag{204}$$

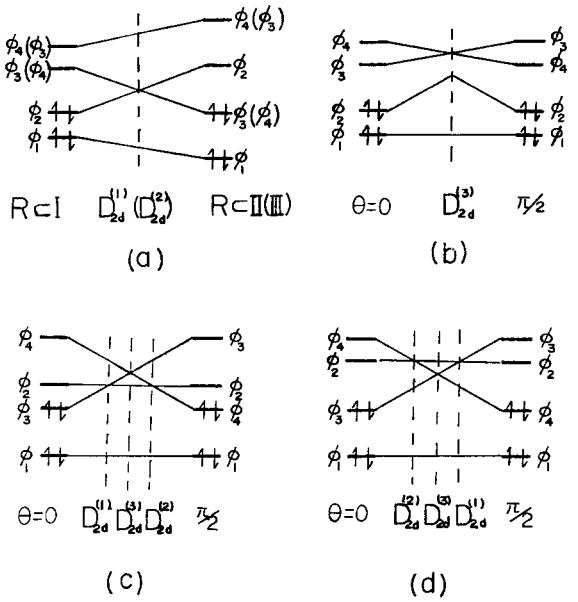

Figure 23. Orbital correlation diagrams in the H_4 system against R on D_{2h} conformations (a) and against θ on a path in the region I (b), traversing regions II, I, and III (c) or regions II and III (d).

We show in Figure 23 the Hückel type correlation diagrams for the RHF orbitals. As seen in Figure 23, the orbitals ϕ_2 and ϕ_3 cross on the $D_{2d}^{(1)}$ and $D_{4h}^{(1)}$ conformations, ϕ_2 and ϕ_4 on $D_{2d}^{(2)}$ and $D_{4h}^{(2)}$, and ϕ_3 and ϕ_4 on $D_{2d}^{(3)}$ and $D_{4h}^{(3)}$. The three orbitals ϕ_2, ϕ_3, and ϕ_4 cross simultaneously on the T_d conformation.

Because of these orbital crossings, there are three different RHF ground states in the system, $\text{RHF}_1 = (\phi_1)^2(\phi_2)^2$, $\text{RHF}_2 = (\phi_1)^2(\phi_3)^2$, and $\text{RHF}_3 = (\phi_1)^2(\phi_4)^2$. They are the RHF ground state in the regions I, II, and III and cross on the D_{2d} and D_{4h} conformations drawn by the heavy lines in Figure 22(b). The RHF ground states become triplet unstable in the regions near the D_{2d} lines because of the orbital crossings in them. The transitions of each RHF ground state are divided into the two groups with different spatial symmetries as shown in Table VII.

TABLE VII. Symmetry of transitions to cause triplet instabilities in the H_4 system.

$(\phi_1)^2(\phi_2)^2$	T_1	$1\to4, 2\to3$	B_3
	T_2	$1\to3, 2\to4$	B_2
$(\phi_2)^2(\phi_3)^2$	T_1'	$1\to4, 3\to2$	B_3
	T_3	$1\to2, 3\to4$	B_1
$(\phi_2)^2(\phi_1)^2$	T_2'	$1\to3, 4\to2$	B_2
	T_3'	$1\to2, 4\to3$	B_1

Because of the presence of the two groups of transitions with different spatial symmetries, the triplet instability matrix of each RHF ground state is decomposed into the two matrices which are irreducible to the D_2 symmetry group. Therefore, each RHF ground state may have two kinds of triplet instability due to transitions with different spatial symmetries. We define in Table VII the names of possible triplet instabilities. The primed ones have the same symmetry as the corresponding unprimed ones.

We show in Figure 24 the triplet instability boundaries of the RHF ground states. RHF_1, RHF_2, and RHF_3 are stable in regions (1), (2), and (3) of Figure 24, respectively, but become triplet unstable in the other regions. We note that both the two kinds of the triplet instability occur in every RHF ground state and their instability boundaries cross on the point A, B, or C as seen in Figure 24; namely, doubly degenerate triplet instabilities occur on the points A, B, and C.

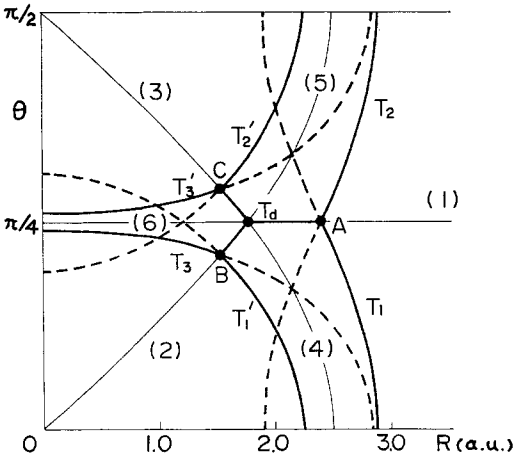

Figure 24. Triplet instability boundaries in the H_4 systems. The type of the triplet instabilities leading to the ASDW ground state is indicated beside the boundaries. The instability leading to high energy ASDW solutions are drawn by dashed lines. Different ASDW ground states cross on the lines connecting the degenerate triplet instability thresholds A, B, and C to T_d. R_{12} is fixed at 2.5 a.u.

(*b*). *ASDW ground states*: From the triplet instability boundaries, ASDW ground states appear. The triplet instabilities with the same symmetry lead to the same ASDW ground state, so that three different ASDW ground states $ASDW_1$, $ASDW_2$, and $ASDW_3$ appear from the T_1 and T_1', T_2 and T_2', and T_3 and T_3' instabilities, respectively. The ASDW ground states have the orbitals

$$\begin{aligned} \text{ASDW}_1: \quad \varphi_1^{\pm} &= [\phi_1 \cos \lambda_1/2 + (\mathbf{e}\cdot\boldsymbol{\sigma})\phi_4 \sin \lambda_1/2]\eta_{\pm}, \\ \varphi_2^{\pm} &= [\phi_2 \cos \lambda_2/2 + (\mathbf{e}\cdot\boldsymbol{\sigma})\phi_3 \sin \lambda_2/2]\eta_{\pm}; \end{aligned} \tag{205}$$

$$\begin{aligned} \text{ASDW}_2: \quad \varphi_{1'}^{\pm} &= [\phi_1 \cos \lambda_1/2 + (\mathbf{e}'\cdot\boldsymbol{\sigma})\phi_3 \sin \lambda_1/2]\eta_{\pm}, \\ \varphi_{2'}^{\pm} &= [\phi_2 \cos \lambda_2/2 + (\mathbf{e}'\cdot\boldsymbol{\sigma})\phi_4 \sin \lambda_2/2]\eta_{\pm}; \end{aligned} \tag{206}$$

$$\text{ASDW}_3: \quad \varphi_{1''}^{\pm} = [\phi_1 \cos \lambda_1/2 + (\mathbf{e}'' \cdot \boldsymbol{\sigma})\phi_2 \sin \lambda_1/2]\eta_{\pm},$$
$$\varphi_{2''}^{\pm} = [\phi_3 \cos \lambda_2/2 + (\mathbf{e}'' \cdot \boldsymbol{\sigma})\phi_4 \sin \lambda_2/2]\eta_{\pm}. \tag{207}$$

ASDW$_1$, ASDW$_2$, and ASDW$_3$ are the ASDW ground states in regions (4), (5), and (6) respectively, of Figure 24. In these ASDW orbitals, occupied and unoccupied RHF orbitals are mixed according to the transitions to cause the relevant triplet instability. For $\mathbf{e}$, $\mathbf{e}'$, and $\mathbf{e}'' = z$, the orbital mixings in up and down spin ASDW orbitals are made with different phases, so that they are localized toward two different atoms. We show in Figure 25 the structures of the ASDW orbitals. As

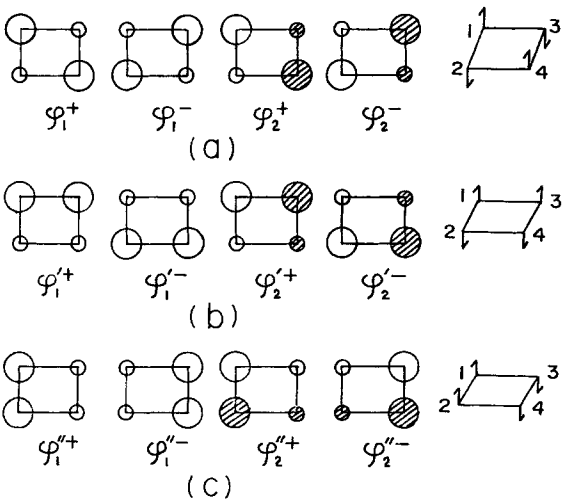

Figure 25. Structures of ASDW$_1$ (a), ASDW$_2$ (b), and ASDW$_3$ (c) orbitals in the H_4 system. The spin structures of the ASDW states are also shown.

seen in Figure 25, the three ASDW solutions have different orbital localizations. The parameter λ_2 in ASDW$_i$ becomes $\pm\frac{1}{2}\pi$ on the $D_{2d}^{(i)}$ and $D_{4h}^{(i)}$ conformations, so that the orbitals $\varphi_2^{\pm}$, etc., with different spins, become completely localized on two different atoms. Because of the spin polarized localizations of the ASDW orbitals, the ASDW ground states have the axial spin structures as depicted in Figure 25. Thus, the three ASDW solutions are characterized by different axial spin structures.

We show in Figures 26(a), 26(b), and 26(c) the adiabatic potentials of the RHF and ASDW solutions on a path traversing a $D_{4h}^{(1)}$ conformation, on $D_{4h}^{(1)}$ conformations, and on a path traversing a $D_{2d}^{(3)}$ conformation, respectively. We see in Figures 26(a) and 26(c) that the potential of ASDW$_1$ connects smoothly with those of RHF$_1$ and RHF$_2$. Similarly, ASDW$_2$ connects RHF$_1$ and RHF$_3$ and ASDW$_3$ RHF$_2$ and RHF$_3$. On the other hand, ASDW$_1$ and ASDW$_2$ cross on $D_{2d}^{(3)}$ conformations as seen in Figure 26(c). Similarly, ASDW$_2$ and ASDW$_3$ cross on

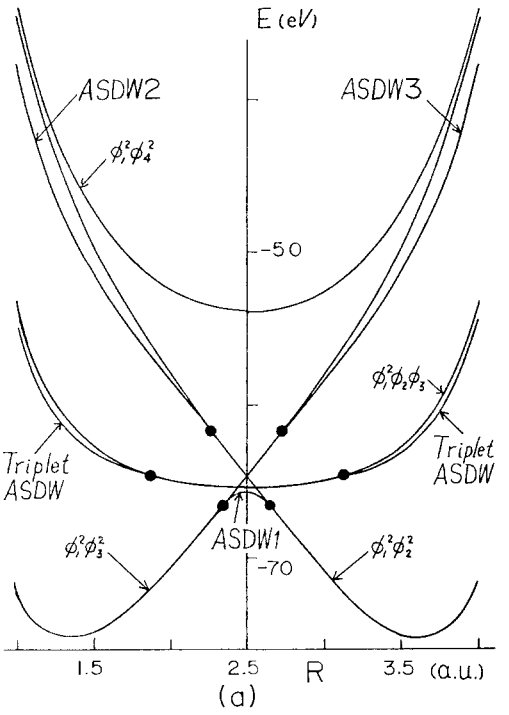

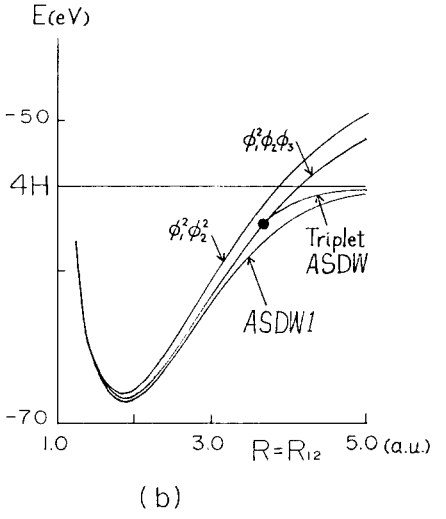

Figure 26. HF potentials in the H_4 system on the $D_{2h}^{(1)}$ path with $R_{12}+R_{13}=5.0$ a.u. (a), on square ($D_{4h}^{(1)}$) conformations (b), and on the path with $R=2.0$ a.u. and $R_{12}=2.5$ a.u. (c).

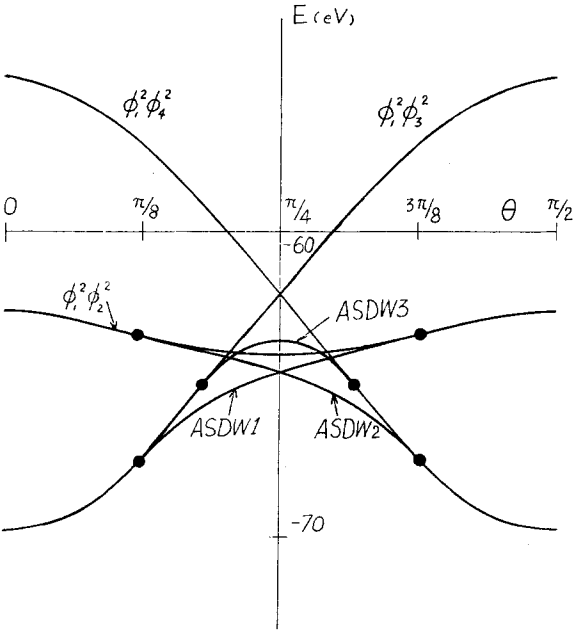

Figure 26. (*Continued from previous page.*)

$D_{2d}^{(1)}$ conformations and ASDW$_3$ and ASDW$_1$ on $D_{2d}^{(2)}$. The ASDW ground states become A_M unstable in regions near the D_{2d} conformations and TSDW solutions smoothly connecting them appear in the regions as we shall show below.

We note that at the $D_{4h}^{(1)}$ conformation the singlet RHF ground state RHF$_1$ is higher in energy than the triplet HF ground state, while the singlet UHF ground state ASDW$_1$ is lower than it as seen in Figures 26(a) and 26(b). The stabilization of ASDW$_1$ to reverse the ordering of the singlet and triplet HF ground states is due to the contribution from the deeper transition $1 \rightarrow 4$ which interferes with the main transition $2 \rightarrow 3$. If the contribution from transition $1 \rightarrow 4$ is neglected, ASDW$_1$ remains a little higher than the triplet HF ground state though it is stabilized compared to RHF$_1$. The ordering of the UHF ground states is in agreement with the result of *ab initio* calculations by Wilson Jr. and Goddard III (1969) and Rubinstein and Shavitt (1969). A similar situation also occurs in the internal rotation of ethylene as we have mentioned in Section 3.A.iii. In this case, the stabilization of the singlet ground state compared to the triplet is brought about by the deeper σ–σ^* transitions. Thus, the UHF theory is able to automatically incorporate the effect of deep transition that may affect the ordering of the singlet and triplet ground states.

(*c*). *TSDW and TSW ground states*: There are three TSDW solutions, each of which smoothly connects two of the ASDW solutions. The presence of the TSDW ground states is indicated by the presence of the three doubly degenerate triplet instability thresholds A, B, and C in Figure 24 as we have discussed in Section

2.C.ii (Fig. 6). A TSDW solution has a wedgelike existence domain with the vertex at a degenerate instability threshold and smoothly connects the two ASDW solutions appearing from the two triplet instability boundaries which cross at the degenerate instability threshold as we have indicated in Figure 8. We show in Figure 27 the existence domains of the three TSDW ground states.

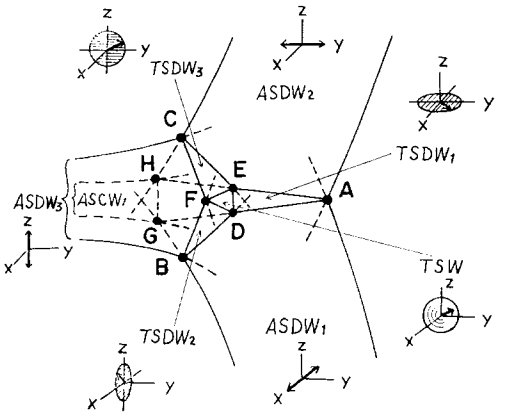

Figure 27. Domains of the TSDW and TSW ground state in the H_4 system. Black dots represent degenerate instability thresholds. The mode of spin modulation in each UHF phase is also shown. Dashed lines represent some instability boundaries leading to high energy UHF solutions.

The occurrence of the degenerate triplet instabilities on the D_{2d} conformations A, B, and C is due to the crossing of unoccupied orbitals on D_{2d} conformations as shown in the orbital correlation diagram of Figure 23(b). The T_1 and T_2 instabilities of RHF_1 involve the two transitions $2\rightarrow3$, $1\rightarrow4$ and $2\rightarrow4$, $1\rightarrow3$, respectively, as shown in Table VII. Consequently, $ASDW_1$ and $ASDW_2$ appearing from the T_1 and T_2 instabilities incorporate only the contributions of those two transitions. In the D_2 conformations not close to $D_{2d}^{(3)}$, the lowest transition $2\rightarrow3$ or $2\rightarrow4$ is the most important, so that $ASDW_1$ or $ASDW_2$ can correctly approximate the ground state. The two unoccupied orbitals ϕ_3 and ϕ_4 cross on $D_{2d}^{(3)}$ conformations, so that both transitions $2\rightarrow3$ and $2\rightarrow4$ become equally important in the D_2 conformations close to $D_{2d}^{(3)}$. The energy gaps of ϕ_3 and ϕ_4 to the HOMO ϕ_2 become small in the conformations close to $D_{2d}^{(3)}$ and T_d, so that the ground state begins to have the configuration mixings due to the transitions $2\rightarrow3$ and $2\rightarrow4$ with equally large weights. The ASDW wave function with only the configuration mixing due to either one of the two transitions, therefore, becomes unable to correctly approximate the ground state. The TSDW ground state, on the other hand, involves the contributions from both the two transitions and is able to correctly approximate the ground state. This example shows that a crossing of unoccupied orbitals may contribute to a change of the nature of the correlated ground state if the orbital energy gap at the crossing point is small.

The three orbitals ϕ_2, ϕ_3, and ϕ_4 become nearly degenerate in the conformations close to T_d. This brings about a further complication in the correlation of the ground state near T_d. As a reflection of this situation, a TSW state appears in a region near T_d depicted in Figure 27 which connects smoothly the three TSDW solutions.

The TSW solution has the orbitals in the form

$$\varphi_A^{\pm} = (\phi_1 b_{1A} + \sigma_3\phi_2 b_{2A} + \sigma_2\phi_3 b_{3A} + \sigma_1\phi_4 b_{4A})\eta_{\pm}, \qquad \sum_{i=1}^{4} b_{iA}^{*} b_{iB} = \delta_{AB}, \qquad A, B = 1, 2, \tag{208}$$

where the coefficients b_{iA} are complex. The TSW solution reduces to the three TSDW solutions when b_{iA}'s satisfy the conditions

$$\begin{aligned} &\text{TSDW}_1: \quad b_{2A} = \text{imaginary}; \quad b_{1A}, b_{3A}, b_{4A} = \text{real}, \\ &\text{TSDW}_2: \quad b_{3A} = \text{imaginary}; \quad b_{1A}, b_{2A}, b_{4A} = \text{real}, \\ &\text{TSDW}_3: \quad b_{4A} = \text{imaginary}; \quad b_{1A}, b_{2A}, b_{3A} = \text{real}. \end{aligned} \tag{209}$$

TSDW_1, TSDW_2, and TSDW_3 are M_z, M_y, and M_x invariant, respectively. TSDW_1 reduces to ASDW_1 with $\mathbf{e} = x$ and ASDW_2 with $\mathbf{e} = y$ in the limits

$$\text{TSDW}_1 \begin{cases} \text{ASDW}_1: & b_{21}, b_{31}, b_{12}, b_{42} = 0, \\ \text{ASDW}_2: & b_{21}, b_{41}, b_{12}, b_{32} = 0. \end{cases} \tag{210}$$

Similarly, TSDW_2 can reduce to ASDW_1 and ASDW_3 and TSDW_3 to ASDW_2 and ASDW_3.

The TSDW_1 orbitals on the $D_{2d}^{(3)}$ conformations become

$$\begin{aligned} \varphi_1^{\pm} &= \left(\phi_1 \cos\frac{\lambda_1}{2} + \frac{1}{\sqrt{2}}(\sigma_2\phi_3 + \sigma_1\phi_4)\sin\frac{\lambda_1}{2}\right)\eta_{\pm}, \\ -i\sigma_3\varphi_2^{\pm} &= \left(\phi_2 \cos\frac{\lambda_2}{2} + \frac{1}{\sqrt{2}}(\sigma_1\phi_3 + \sigma_2\phi_4)\sin\frac{\lambda_2}{2}\right)\eta_{\pm}. \end{aligned} \tag{211}$$

The orbitals (211) are quite analogous to the form of the helical SDW of Overhauser (1960, 1962). The TSW orbitals at the T_d conformation become

$$\begin{aligned} \varphi_1^{\pm} &= \left(\phi_1 \cos\frac{\lambda}{2} + \frac{1}{\sqrt{3}}(\sigma_3\phi_2 + \sigma_2\phi_3 + \sigma_1\phi_4)\sin\frac{\lambda}{2}\right)\eta_{\pm}, \\ \varphi_2^{\pm} &= \frac{1}{\sqrt{3}}(\sigma_3\phi_2 + \omega^2\sigma_2\phi_3 + \omega\sigma_1\phi_4), \qquad \omega = e^{\pm 2\pi i/3}. \end{aligned} \tag{212}$$

The structures of the TSDW and TSW solutions given above were determined by the group theory for the structure of UHF wave functions described in Section 2.B.iv. Their invariance groups are such that they give the ordered spin structures the most symmetrical under the relevant spatial symmetry group.

The spin structures of the TSDW and TSW ground states can be calculated from their spin density matrices. We show in Figure 28 their spin structures on a path traversing a $D_{2d}^{(3)}$ conformation [Fig. 28(a)] and on the path of $D_{2d}^{(3)}$ conformations [Fig. 28(b)]. The HF ground state passes through the three UHF phases ASDW_1–TSDW_1–ASDW_2 and TSDW_1–TSW–ASDW_3 on the former and latter paths, respectively. We also show in Figure 28 how the spin structure of the UHF ground state is transformed between those three UHF phases.

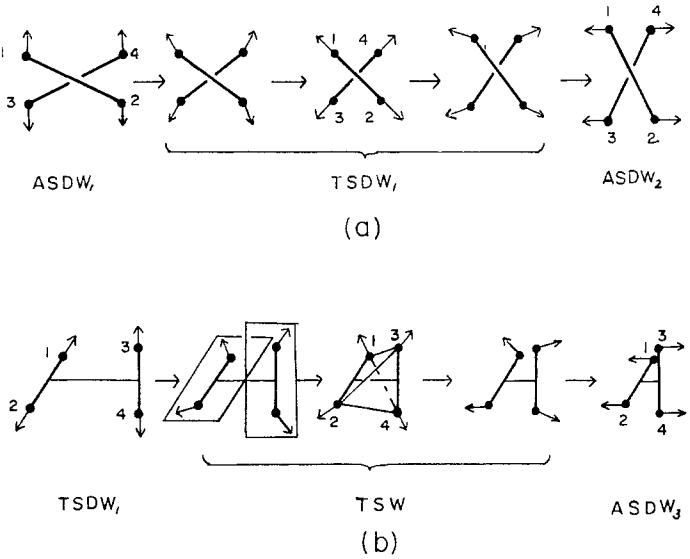

Figure 28. Spin structures of the TSDW_1 and TSW states in the H_4 system. (a) Illustrates how TSDW_1 interconnects ASDW_1 and ASDW_2 on a path with constant R. (b) Illustrates how TSW interconnects TSDW_1 and ASDW_3 on $D_{2d}^{(3)}$ conformations.

Thus, the singlet HF ground state of the H_4 system consists of ten phases; three RHF, three ASDW, three TSDW, and a TSW. The surprisingly complicated structure of the HF ground state is due to the presence of plentiful orbital crossings in the system. Though the HF ground state of the system is so much complicated, the HF phase map shown in Figures 24 and 27 and the spin structures of the UHF phases and the ways of their interconversion between the UHF phases shown in Figures 25 and 28 clearly visualize the physical natures of the UHF phases and the physical events underlying the transformations of the UHF phases.

The UHF pictures of diradicals discussed in the preceding paragraph are in agreement with the intuitive chemical pictures of diradicals. The present example shows that there are chemical reaction systems whose ground states enter into states of a multiradical nature with more complicated electronic structures than simple diradicals. It also shows that a reaction system may enter successively

into multiradical states of different natures which form a hierarchy of radical states with more and more complicated electronic structures.

The ASDW states of the H_4 system have the character of diradical in the vicinity of the triplet instability boundaries. However, they tend to have the character of tetraradicals in the vicinity of the D_{4h} and D_{2d} conformations. The splitting of the second ASDW corresponding orbital pair $\varphi_2^{\pm}$, etc., becomes complete on the conformations. The splitting of the first pair $\varphi_1^{\pm}$, etc., also becomes appreciable there. When all the interatomic distances are large, it has a large splitting. In the limit of infinite interatomic distances, the ASDW states converge to the tetraradical of four isolated hydrogen atoms as seen in the potential of Figure 26(b). The TSDW and TSW states represent tetraradicals of the other kinds. A two electron system cannot have TSDW and TSW states. For realization of them in a singlet state, at least four electrons are necessary. The ASDW, TSDW, and TSW tetraradicals are characterized by more and more complicated electronic correlations which produce spin structures with different modes in spin density vector modulation. An A_-M or M_- instability of an ASDW or TSDW ground state signals the growth of a correlation effect, which is not incorporated into the state, up to a critical point to alter the nature of spin structure. The resultant TSDW or TSW ground state incorporates the correlation effect into its wave function.

(*d*). *Configuration analysis of the ASDW and TSW wave functions*: A configuration analysis for the singlet projected ASDW and TSW wave functions at the D_{4h} and T_d conformations, respectively, was carried out by Yoshioka et al. (preprint). They showed that the singlet projected ASDW_1, $^1\text{PASDW}_1$, at the $D_{4h}^{(1)}$ conformation has the wave function

$$
\begin{aligned}
{}^1\text{PASDW}_1 &= \frac{1}{\sqrt{2}}\cos^2\frac{\lambda}{2}\Phi_G + \frac{\sqrt{3}}{6}\sin\lambda\,\Phi_{SP} - \frac{1}{\sqrt{2}}\sin^2\frac{\lambda}{2}\Phi_{DE},\\
\Phi_G &= \frac{1}{\sqrt{2}}(\|1\bar{1}2\bar{2}\| - \|1\bar{1}3\bar{3}\|),\\
\Phi_{SP} &= \frac{1}{2\sqrt{3}}(\|1\bar{2}3\bar{4}\| + \|\bar{1}2\bar{3}4\| + \|12\bar{3}\bar{4}\| + \|\bar{1}\bar{2}34\| - 2\|1\bar{2}\bar{3}4\| - 2\|\bar{1}23\bar{4}\|),\\
\Phi_{DE} &= \frac{1}{\sqrt{2}}(\|2\bar{2}4\bar{4}\| - \|3\bar{3}4\bar{4}\|).
\end{aligned}
\tag{213}
$$

where 1, $\bar{1}$, etc., in Slater determinants represent ϕ_1, $\bar{\phi}_1$, etc., and $\lambda = \lambda_1$ ($\lambda_2 = \pm\pi/2$ at the $D_{4h}^{(3)}$ conformation). The $^1\text{PASDW}_1$ wave function contains all the configurations contained in the full CI wave function. It becomes identical with the full CI one if a numerical factor is multiplied to the spin polarization configuration Φ_{SP} and is a good approximation to the full CI ground state.

The singlet projected TSW, ^{1}PTSW, at the T_d conformation has the wave function

$$
\begin{aligned}
&{}^1\text{PTSW} = -\frac{1}{\sqrt{3}}\cos^2\frac{\lambda}{2}\Phi_G + \frac{\mathrm{i}}{3\sqrt{2}}\sigma\sin\lambda\,\Phi_2 - \frac{1}{3\sqrt{3}}(2\sigma+1)\sin^2\frac{\lambda}{2}\Phi_{DE},\\
&\Phi_G = \frac{1}{\sqrt{3}}(\|1\bar{1}2\bar{2}\| + \omega\|1\bar{1}3\bar{3}\| + \omega^2\|1\bar{1}4\bar{4}\|),\\
&\Phi_2 = \frac{1}{\sqrt{6}}\{\|12\bar{3}\bar{4}\| + \|\bar{1}\bar{2}34\| + \omega(\|1\bar{2}3\bar{4}\| + \|\bar{1}2\bar{3}4\|) + \omega^2(\|1\bar{2}\bar{3}4\| + \|\bar{1}23\bar{4}\|)\},\\
&\Phi_{DE} = \frac{1}{\sqrt{3}}(\|3\bar{3}4\bar{4}\| + \omega\|2\bar{2}4\bar{4}\| + \omega^2\|2\bar{2}3\bar{3}\|),
\end{aligned}
\tag{214}
$$

where $\sigma = 1$ and $\omega = \exp(\pm\frac{2}{3}\pi i)$. The ^{1}PTSW wave function contains all the configurations contained in the full CI wave function. It becomes identical with the full CI one if the parameter σ is not constrained to 1 and is a good approximation to the full CI ground state. The two ^{1}PTSW wave functions with $\omega = \exp(\frac{2}{3}\pi i)$ and $\omega = \exp(-\frac{2}{3}\pi i)$ are orthogonal and belong to the irreducible E representation of the T_d group.

The full CI ground state, which has the E symmetry at the T_d conformation, has a Jahn–Teller (1937) cusp at T_d. On the other hand, the TSW ground state does not have it at T_d but has a continuous potential there. The failure of the TSW solution to give the Jahn–Teller cusp is explained as follows. The singlet component ^{1}PTSW of the TSW solution has the correct E symmetry but it is an equal weighted superposition of the real and imaginary components which have different symmetries with respect to the D_{2d} symmetry group. These two components show the Jahn–Teller behavior at T_d. Because of the equal weighted superposition of them, the Jahn–Teller cusp is smoothed out in the TSW solution. Therefore, the projection to a spin eigenstate is not sufficient to have the correct Jahn–Teller behavior, but the further projection to time reversal eigenstates recovers it.

(*e*). *Remarks on alternant hydrocarbon diradicals*: Alternant hydrocarbon diradicals have the HF ground state of ASDW type similar to the ASDW ground states of the H_4 system. Hashimoto and Fukutome (unpublished) studied the UHF ground states of the following alternant hydrocarbon diradicals:

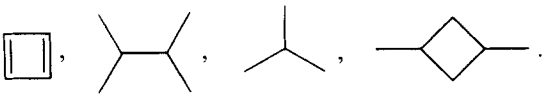

They found that the UHF ground states of these systems are the ASDW's with the alternant spin structures shown in Figure 29. If the numbers of up and down spin vectors in the alternant spin structure are the same, then the ASDW ground state is singlet; but if they are not equal, then the ASDW ground state is triplet.

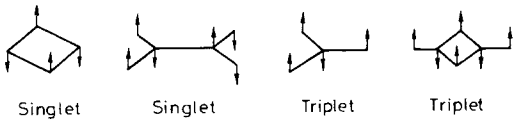

Figure 29. Ground state spin structures of alternant hydrocarbon diradicals.

This very simple rule for the spin multiplicity of the ground state of an alternant hydrocarbon diradical is in agreement with experiments and the result of an *ab initio* CI calculation by Borden and Davidson (1977).

ii. Dimerization of Carbenes. The second example we consider is the dimerization reactions of the carbenes CXY, X, $Y = H$ or F, in the planar least motion path depicted in Figure 30(a). The system was studied by Takabe and Fukutome (1976). The essential features of the system are similar to the H_4 system discussed in the preceding section since the four nonbonding electrons and the four nonbonding AO's depicted in Figure 30(a) are essential in the dimerization. The RHF orbitals concerned with the four electrons are

$$\begin{aligned} \sigma &= (1/\sqrt{2})(sp_1 + sp_2), & \pi &= (1/\sqrt{2})(p_1 + p_2), \\ \sigma^* &= (1/\sqrt{2})(sp_1 - sp_2), & \pi^* &= (1/\sqrt{2})(p_1 - p_2). \end{aligned} \tag{215}$$

Upon the correspondence $\sigma \to \phi_1$, $\sigma^* \to \phi_2$, $\pi^* \to \phi_3$, and $\pi \to \phi_4$, there is a straightforward formal analogy between the two systems.

The orbital correlation diagram for the dimerization process is shown in Figure 30(b). A crossing of the occupied and unoccupied orbitals π and σ^* is present. Note the presence of a crossing between the unoccupied orbitals σ^* and π^*. This crossing leads to a TSDW ground state as we shall see below. Because of the crossing of the orbitals π and σ^*, the RHF ground states at the final state of olefin and at the initial state of two isolated carbenes are different. They are $\text{RHF}_1 = (\sigma)^2(\pi)^2$ and $\text{RHF}_2 = (\sigma)^2(\sigma^*)^2$, respectively. The RHF_1 and RHF_2 in the present system correspond to the RHF_3 and RHF_1 in the H_4 system, respectively.

RHF_1 and RHF_2 become triplet unstable owing to the crossing of π and σ^*. Both RHF_1 and RHF_2 have two groups of transitions with different spatial sym-

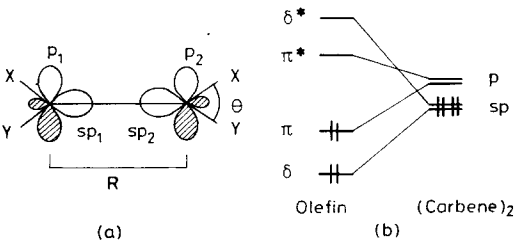

Figure 30. Conformation (a) and orbital correlation diagram (b) of the dimerization of carbenes in the least motion path. Essential AO's are also shown in (a).

metries:

$$\begin{aligned}
&\text{RHF}_1\text{:} \quad T_1, \quad \pi \to \pi^*, \quad \sigma \to \sigma^* \to \text{ASDW}_1, \\
&\qquad\quad T_2, \quad \pi \to \sigma^*, \quad \sigma \to \pi^* \to \text{ASDW}_2; \\
&\text{RHF}_2\text{:} \quad T_2', \quad \sigma \to \pi^*, \quad \sigma^* \to \pi \to \text{ASDW}_2, \\
&\qquad\quad T_3, \quad \sigma \to \pi, \quad \sigma^* \to \pi^* \to \text{ASDW}_3.
\end{aligned} \tag{216}$$

The triplet instabilities caused by transitions with different spatial symmetries lead to different ASDW ground states. We define in Eq. (216) the names of ASDW solutions appearing from the triplet instabilities of different symmetries. The T_2 and T_2' instabilities have the same symmetry leading to the same ASDW ground state. We show in Figures 31(a), 31(b), and 31(c) the triplet instability domains for RHF_1 and RHF_2 in the three systems $(CH_2)_2$, $(CHF)_2$, and $(CF_2)_2$, respectively.

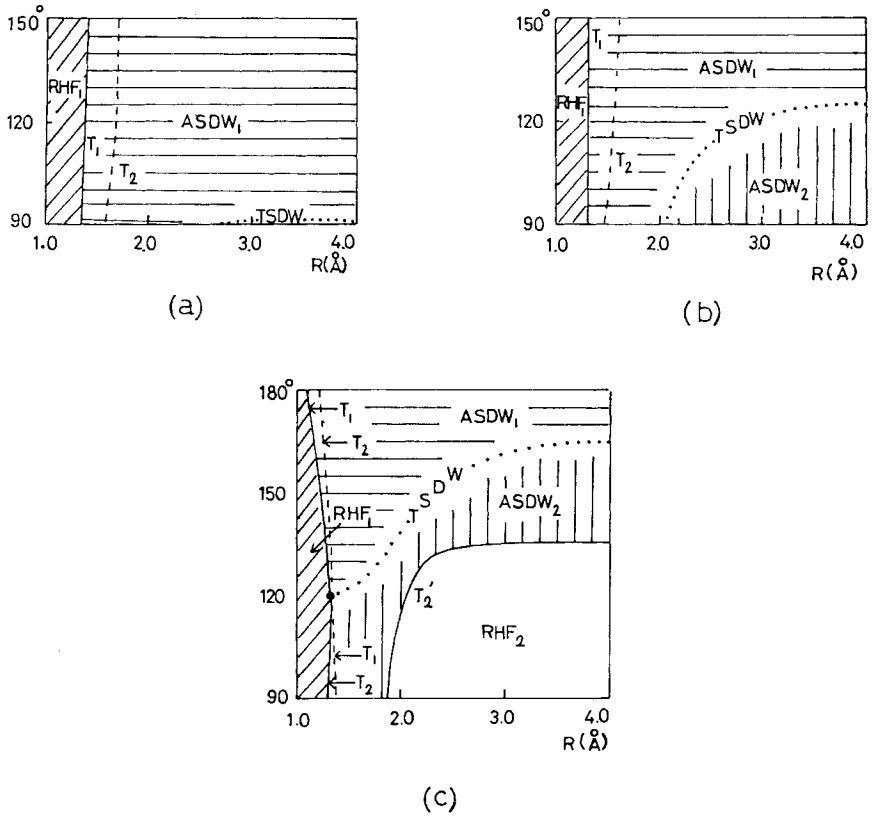

Figure 31. HF phase maps of the dimerizations of CH_2 (a), CHF (b), and CF_2 (c). Instability boundaries leading to high energy UHF solutions are shown by dashed lines. ASDW_1 and ASDW_2 cross on the dotted line. The TSDW ground state exists in a zone surrounding the crossing line. The dot in (c) is a degenerate triplet instability threshold.

As we have shown in Section 3.A.iii, the RHF ground state in CH_2 and CHF is always triplet unstable, so that the RHF_2 in $(CH_2)_2$ and $(CHF)_2$ is always triplet unstable. On the other hand, the RHF ground state of CF_2 has a wide stable domain, so that the RHF_2 of $(CF_2)_2$ has a stable domain as shown in Figure 31(c). RHF_1 always has a stable domain in all the three systems.

The T_1 instability occurs always first in the RHF_1 of $(CH_2)_2$ and $(CHF)_2$ in the whole range of bending angle θ shown in Figure 31. In $(CF_2)_2$, a crossing of the T_1 and T_2 instability boundaries, namely, a degenerate triplet instability, occurs at $\theta = 120°$ which is close to the equilibrium bending angle of the olefin. The instability to occur firstly in the RHF_2 of $(CF_2)_2$ is T_2'. No crossing of the T_2' and T_3 instability boundaries occurs, and we do not show the latter boundary in Figure 31. In $(CH_2)_2$ and $(CHF)_2$ also, the T_2' instability matrix has always a lower negative eigenvalue than T_3.

The three ASDW solutions have the orbitals

$$\begin{aligned} \text{ASDW}_1: \quad & \varphi_1^{\pm} = [\sigma \cos \lambda_1/2 + (\mathbf{e} \cdot \boldsymbol{\sigma})\sigma^* \sin \lambda_1/2]\eta_{\pm}, \\ & \varphi_2^{\pm} = [\pi \cos \lambda_2/2 + (\mathbf{e} \cdot \boldsymbol{\sigma})\pi^* \sin \lambda_2/2]\eta_{\pm}; \end{aligned} \tag{217}$$

$$\begin{aligned} \text{ASDW}_2: \quad & \varphi_{1'}^{\pm} = [\sigma \cos \lambda_1/2 + (\mathbf{e}' \cdot \boldsymbol{\sigma})\pi^* \sin \lambda_1/2]\eta_{\pm}, \\ & \varphi_{2'}^{\pm} = [\pi \cos \lambda_2/2 + (\mathbf{e}' \cdot \boldsymbol{\sigma})\sigma^* \sin \lambda_2/2]\eta_{\pm}; \end{aligned} \tag{218}$$

$$\begin{aligned} \text{ASDW}_3: \quad & \varphi_{1''}^{\pm} = [\sigma \cos \lambda_1/2 + (\mathbf{e}'' \cdot \boldsymbol{\sigma})\pi \sin \lambda_1/2]\eta_{\pm}, \\ & \varphi_{2''}^{\pm} = [\sigma^* \cos \lambda_2/2 + (\mathbf{e}'' \cdot \boldsymbol{\sigma})\pi^* \sin \lambda_2/2]\eta_{\pm}. \end{aligned} \tag{219}$$

We show in Figure 32 the structures of the ASDW orbitals and the spin structures of the ASDW solutions. We see from Figures 32 and 17 that $ASDW_1$ represents the state composed of two triplet carbenes whose spins are coupled antiparallelly and $ASDW_2$ and $ASDW_3$ represent the states with two singlet diradical carbenes whose spins are coupled antiparallelly and parallelly, respectively. Thus, the ASDW states represent

$$\begin{aligned} \text{ASDW}_1 &= {}^1({}^3CXY + {}^3CXY), && \text{antiparallel spin coupling;} \\ \text{ASDW}_2 &= {}^1({}^1CXY + {}^1CXY), && \text{antiparallel spin coupling;} \\ \text{ASDW}_3 &= {}^1({}^1CXY + {}^1CXY), && \text{parallel spin coupling.} \end{aligned} \tag{220}$$

We show in Figure 33 the potentials against R of the RHF and ASDW states. $ASDW_3$ is always higher in energy than $ASDW_2$ and cannot be a UHF ground state. $ASDW_2$ in $(CF_2)_2$ smoothly connects RHF_1 and RHF_2. The potentials of $ASDW_1$ and $ASDW_2$ cross. The dotted line in Figure 31 shows where $ASDW_1$ and $ASDW_2$ cross. $ASDW_1$ and $ASDW_2$ are the ASDW ground state in the regions above and below the crossing line, respectively.

A TSDW ground state exists in the vicinity of the crossing line of $ASDW_1$ and $ASDW_2$ which smoothly connects them. The existence of the TSDW ground state is confirmed by the presence of a doubly degenerate triplet instability threshold in Figure 31(c). Unfortunately, we could not calculate its existence domain since

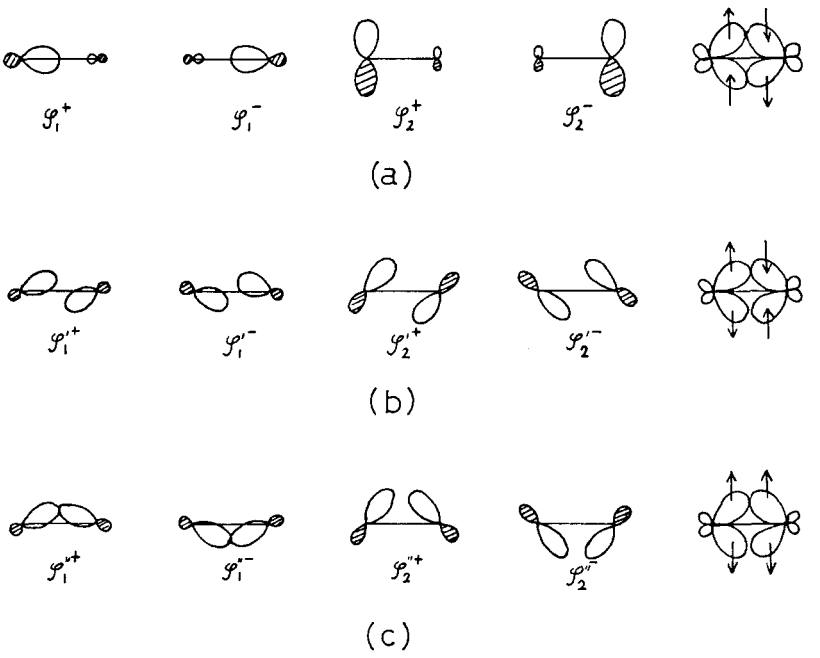

Figure 32. Structures of ASDW$_1$ (a), ASDW$_2$ (b), and ASDW$_3$ (c) orbitals in the dimerizations of carbenes. Their spin structures are also shown.

we used the MINDO/2 approximation. The TSDW state is stabilized by the interatomic exchange interaction (the same situation hold also for the TSDW states in the H_4 system) so that its existence domain cannot be obtained by the MINDO/2 approximation to neglect it. However, it is certain from the bifurcation theory given Section 2.C.iii that the TSDW state exists in a stripe region surrounding the crossing line of ASDW$_1$ and ASDW$_2$ and with a vertex at the degenerate triplet instability threshold.

The TSDW state has the orbitals

$$\varphi_A^{\pm} = (\sigma C_{1A} + \sigma_1 \pi C_{2A} + i\sigma_2 \pi^* C_{3A} + \sigma_3 \sigma^* C_{4A})\eta_{\pm}, \qquad \sum_{i=1}^{4} C_{iA} C_{iB} = \delta_{AB}, \quad A, B = 1, 2, \tag{221}$$

where the coefficients C_{iA} are real. The M_y invariant TSDW orbitals [Eq. (221)] reduce to those of ASDW$_1$ with $\mathbf{e} = z$ and ASDW$_2$ with $\mathbf{e}' = x$ in the limits

$$\text{TSDW} \rightarrow \begin{cases} \text{ASDW}_1: & C_{21}, C_{31}, C_{12}, C_{42} = 0, \\ \text{ASDW}_2: & C_{21}, C_{41}, C_{12}, C_{32} = 0. \end{cases} \tag{222}$$

We show in Figure 34 the spin structure of the TSDW state and how it interconnects ASDW$_1$ and ASDW$_2$. The triplet carbene moieties in ASDW$_1$ is converted to the

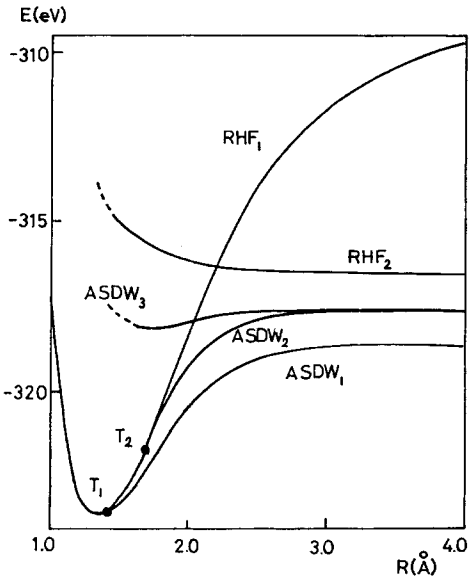

(a)

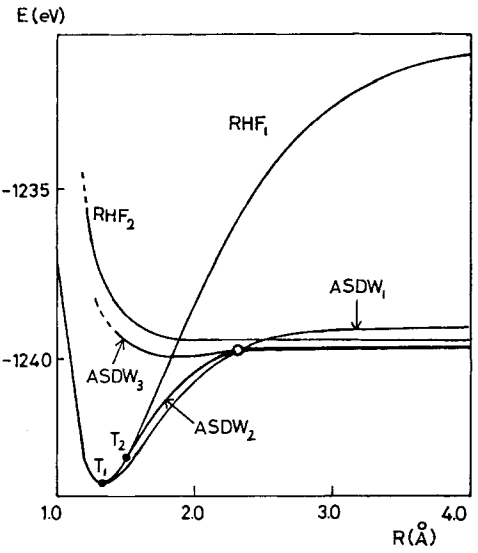

(b)

Figure 33. HF potentials in the dimerizations of CH_2 (a), CHF (b), and CF_2 (c). Triplet instability thresholds and crossing points of ASDW solutions are indicated by black and white circles, respectively.

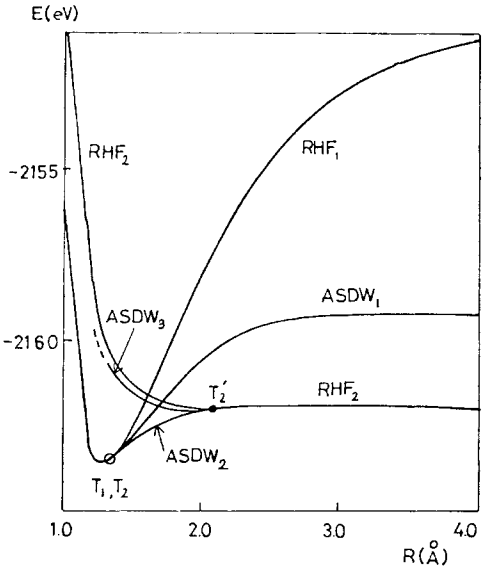

(c)

Figure 33 (*cont.*)

singlet diradical carbene moieties of ASDW$_2$ via the TSDW state with a rotation of the spin density vectors as seen in Figure 34.

As shown in Figure 18, the ground state of isolated CH_2 is triplet. The HF phase map of Figure 31(a) shows that the singlet ground state dimerization reaction $^3CH_2 + {}^3CH_2 \rightarrow (CH_2)_2$ proceeds via a path with the two HF phases ASDW$_1$–RHF$_1$. The ground state of CHF can be either triplet or singlet. The HF phase map of Figure 31(b) shows that the reaction $^3CHF + {}^3CHF \rightarrow (CHF)_2$ proceeds via the two HF phases ASDW$_1 \rightarrow$ RHF$_1$, while the reaction $^1CHF + {}^1CHF \rightarrow (CHF)_2$ proceeds via a path with the four HF phases traversing the TSDW region, ASDW$_2 \rightarrow$ TSDW $\rightarrow$ ASDW$_1 \rightarrow$ RHF$_1$. The ground state of CF_2 is singlet and Figure 31(c) shows that the equilibrium geometry of the final state olefin is near the degenerate triplet instability threshold and the reaction $^1CF_2 + {}^1CF_2 \rightarrow (CF_2)_2$ traverses the TSDW region or passes nearby the region, namely, it proceeds as RHF$_2 \rightarrow$ ASDW$_2 \rightarrow$ (TSDW $\rightarrow$ ASDW$_1$) $\rightarrow$ RHF$_1$. Thus, the above analyses indicate the

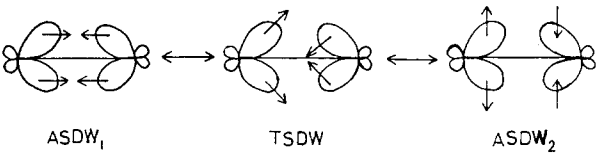

Figure 34. Spin structure of the TSDW ground state in the dimerization of carbenes and the way of interconnection of ASDW$_1$, ASDW$_2$ via TSDW.

possibility of real chemical reactions to proceed via a TSDW state. These reaction systems have complicated CI wave functions with heavy mixings of excited configurations as shown by MC SCF and CI studies by Basch (1971) and Kikuchi (1972). The UHF theory clearly visualizes the electronic processes involved in the complicated CI wave functions.

iii. H_3 System. As a typical model system for insertion and addition reactions of free radicals, the H_3 system with the isosceles triangular conformations as depicted in Figure 35(a) was studied by Yamaguchi and Fukutome (1975). The system has the three RHF orbitals

$$\begin{aligned}\phi_a &= (1/\sqrt{2})\cos(\theta/2)(\chi_1+\chi_2)+\sin(\theta/2)\chi_3,\\ \phi'_a &= -(1/\sqrt{2})\sin(\theta/2)(\chi_1+\chi_2)+\cos(\theta/2)\chi_3,\\ \phi_b &= (1/\sqrt{2})(\chi_1-\chi_2),\end{aligned} \tag{223}$$

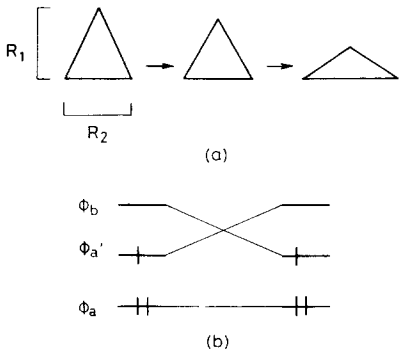

Figure 35. Conformation (a) and orbital correlation diagram (b) of the H_3 system with C_{2v} symmetry.

where χ_i's are the orthogonalized $1s$ AO's. The RHF orbitals ϕ_a and ϕ'_a cross at the equilateral triangular conformation as depicted in the orbital correlation diagram of Figure 35(b). Hence, there are the two doublet RHF ground configurations $\text{RHF}_1 = (\phi_a)^2(\phi'_a)$ and $\text{RHF}_2 = (\phi_a)^2(\phi_b)$, which are the lowest energy ones in the regions of acute and flat triangles, respectively, and cross at the equilateral triangular conformation.

A RHF configuration consisting of an open shell electron and closed shells is not in general a HF state to optimize the HF energy functional as proved by Paldus–Čižek (1970b), Fukutome (1974b), and Yamaguchi–Fueno (1976). It is a HF state only under the special circumstance that the open shell orbital ϕ_0 satisfies, for all closed shell occupied and unoccupied orbitals ϕ_c and ϕ'_c, the condition

$$\langle\phi_c\phi_0\,|\,\phi_0\phi'_c\rangle+\langle\phi_0\phi_c\,|\,\phi'_c\phi_0\rangle=0, \tag{224}$$

owing to the symmetry of ϕ_0. RHF_1 satisfies the condition (224) and is a HF state but RHF_2 is not. There is an ASDW solution $ASDW_2$ below RHF_2 that is the HF solution obtained by the SCF procedure starting from RHF_2. $ASDW_2$ has the orbitals

$$\begin{aligned} \varphi^{\pm} &= [(1/\sqrt{2})\cos(\omega^{\pm}/2)(\chi_1+\chi_2)+\sin(\omega^{\pm}/2)\chi_3]\eta_{\pm}, \\ \varphi^{0} &= \phi_b\eta_{+}, \qquad \omega^{+}=\omega^{-}. \end{aligned} \tag{225}$$

The pair $\varphi^{\pm}$ is spin polarized but has A_1 symmetry for the C_{2v} group, namely, $ASDW_2$ is spatial symmetry adapted though it is of broken spin symmetry.

RHF_1 and $ASDW_2$ are stable in the regions of acute and flat triangles not close to equilateral ones and the HF ground states in these regions, respectively. Owing to the crossing of the RHF orbitals ϕ'_a and ϕ_b, they become A_-M unstable in a region near equilateral triangles for the antisymmetric spin flipping transitions

$$\begin{aligned} RHF_1: &\quad \phi'_a\eta_{+}\rightarrow\phi_b\eta_{-}, \qquad \phi_a\eta_{-}\rightarrow\phi_b\eta_{+}, \\ ASDW_2: &\quad \varphi^{0}\rightarrow\bar{\varphi}^{-}, \qquad \varphi^{-}\rightarrow\bar{\varphi}^{+}, \end{aligned} \tag{226}$$

where $\bar{\varphi}^{\pm}$ are the unoccupied orbitals of $ASDW_2$ forming a corresponding orbital pair. The A_-M instabilities of RHF_1 and $ASDW_2$ have the same spatial symmetry and lead to the TSDW ground state smoothly connecting RHF_1 and $ASDW_2$. RHF_1 also becomes A_+M_+ unstable a little later than the A_-M instability and an ASDW solution $ASDW_1$ appears. However, $ASDW_1$ is not the HF ground state. We show in Figure 36 the HF phase map of the H_3 system. We show in Figures 37(a) and 37(b) the potentials of the HF solutions along a path traversing an equilateral triangle and on equilateral triangular conformations, respectively. In Figure 37(b), the potentials of the doublet projected TSDW state and the full CI ground state are also shown.

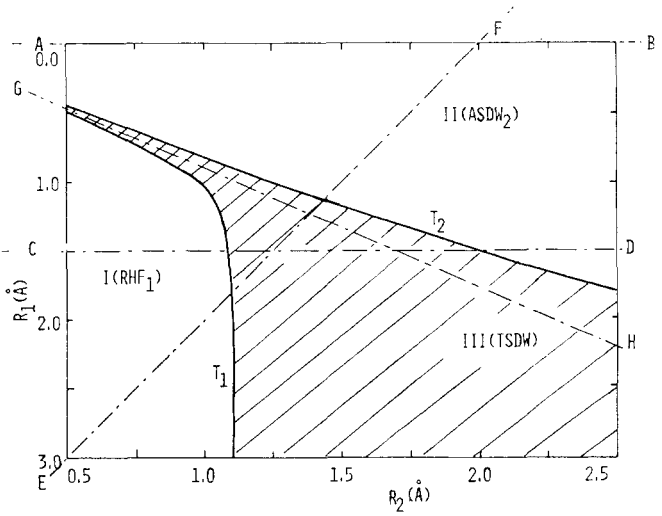

Figure 36. HF phase map of the H_3 system. The conformations on the line G–H has D_{3h} symmetry.

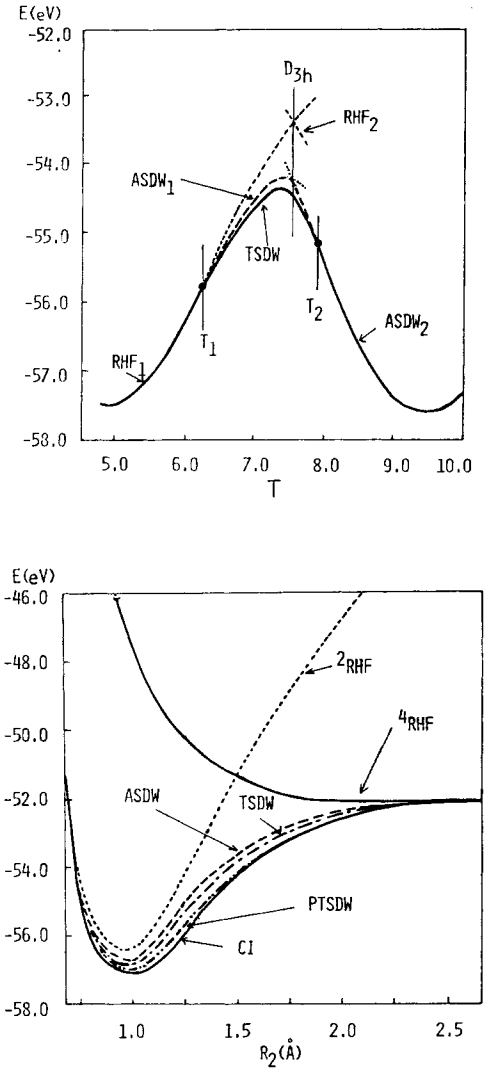

Figure 37. HF potentials of the H_3 system on the lines E–F (a) and G–H (D_{3h}) (b) in Figure 36. ^{2}PTSDW and full CI potentials are also shown in (b).

The TSDW state has the orbitals

$$\varphi^{\pm} = [(1/\sqrt{2})C_1^{\pm}(\chi_1+\chi_2)+C_2^{\pm}\chi_3]\eta_{\pm}+(1/\sqrt{2})C_3^{\pm}(\chi_1-\chi_2)\eta_{\mp},$$
$$\varphi^{0} = [(1/\sqrt{2})C_1^{0}(\chi_1+\chi_2)+C_2^{0}\chi_3]\eta_{+}+(1/\sqrt{2})C_3^{0}(\chi_1-\chi_2)\eta_{-}, \qquad (227)$$
$$\sum_{i=1}^{3} C_i^A C_i^B = \delta_{AB}, \qquad A, B = 0, \pm,$$

where the coefficients C_i^A are real. The TSDW orbitals at equilateral triangles become

$$\varphi^{\pm} = \left(\phi_a \cos\frac{\mu}{2} + \frac{1}{\sqrt{2}}(\sigma_3\phi'_a + \sigma_1\phi_b)\sin\frac{\mu}{2}\right)\eta_{\pm},$$
$$\varphi^0 = (1/\sqrt{2})(\phi'_a\eta_+ - \phi_b\eta_-), \tag{228}$$

where $\cos(\theta/2) = (\frac{2}{3})^{1/2}$ in the RHF orbitals ϕ_a and ϕ'_a. We show in Figure 38 the spin structures of RHF_1, TSDW, and $ASDW_2$ and how TSDW interconnects RHF_1 and $ASDW_2$.

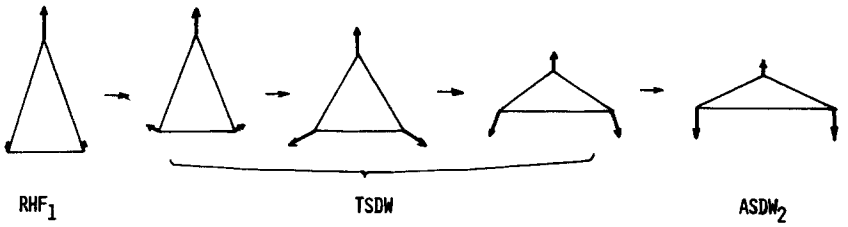

Figure 38. Spin structure of the TSDW ground state in the H_3 system and the way of interconnection of RHF_1 and $ASDW_2$ via TSDW.

We compare the doublet projected TSDW wave function ^{2}PTSDW with the full CI one at equilateral triangles. To do this, it is convenient to use the complex RHF orbitals

$$\phi_a = (1/\sqrt{3})(\chi_1 + \chi_2 + \chi_3),$$
$$\phi_e = (1/\sqrt{3})(\chi_3 + \omega\chi_1 + \omega^2\chi_2), \qquad \phi_{-e} = \phi_e^*, \tag{229}$$

where $\omega = \exp(\frac{2}{3}\pi i)$. M_y invariant TSDW orbitals [Eq. (228)] can be transformed to M_z invariant ones by a spin rotation

$$\varphi^{\pm} = \phi_a \cos(\mu/2)\eta_{\pm} + \phi_{\pm e}\sin(\mu/2)\eta_{\mp},$$
$$\varphi^0 = (1/\sqrt{2})(\phi_e\eta_+ + \phi_{-e}\eta_-). \tag{230}$$

Using Eq. (230), we obtain

$$^2\text{PTSDW} = (1+\cos\mu)\|\phi_a\bar{\phi}_a\phi_e\| + \sin\mu\|\phi_{-e}\bar{\phi}_{-e}\phi_a\| + (1-\cos\mu)\|\phi_e\bar{\phi}_e\phi_{-e}\|. \tag{231}$$

^{2}PTSDW contains all the configurations contained in the full CI ground state wave function and becomes identical with it if a numerical factor is multiplied to the second configuration. ^{2}PTSDW is a good approximation to the full CI wave function both in energy and CI coefficients.

^{2}PTSDW and its complex conjugate are orthogonal and span the irreducible E' representation of the D_{3h} group. It is an equal weighted superposition of real and imaginary components with A_1 and B_2 symmetries with respect to the C_{2v}

group

$$^2\Psi_{\text{TSDW}} = (1/\sqrt{2})(^2\Phi_{A1} + i\,^2\Phi_{B2}). \tag{232}$$

Owing to this property, the TSDW potential shows no Jahn–Teller cusp as shown in Figure 37(a) similarly to the TSW potential in the H_4 system. However, the Jahn–Teller cusp can be recovered by the projection to time reversal eigenstates.

As we have seen above, in a doublet system, a crossing of half occupied orbitals may lead to a TSDW ground state. A doublet TSDW state represents a tri- or higher order radical because at least three electrons are necessary to construct a doublet TSDW. The TSDW state in the H_3 system tends to the complete triradical consisting of three hydrogen atoms in the limit of infinite interatomic distances as seen in the potential of Figure 37(b). A doublet ASDW state consists of an open shell electron and spin polarized pairs, so that it has more or less triradical character. A doublet RHF state is in general not an HF state as we have noted above, so that a doublet system of pure monoradical character is a rather exceptional event. The present example shows that triradical states of different natures may arise in a doublet reaction system.

We finally add remarks about the electronic structures of odd cycle hydrocarbon radicals

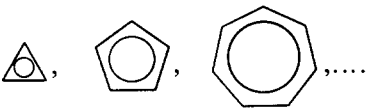

The HF ground state of the odd cyclic radicals at the D_{2n+1h} conformation must be a TSDW. The group theory described in Section 2.B.iv eliminates the possibility of ASDW ground state. The π electrons in cyclopropenyl radical $(CH)_3$ must have the triangular spin arrangement same as the TSDW state in the H_3 system. Hashimoto (unpublished) showed that the HF ground state of cyclopentadienyl radical $(CH)_5$ has the spin structure shown in the second diagram of Figure 4. He pointed out that among the possible spin structures the one with nearest neighbor spins having the largest extent of antiparallelness is realized as the ground state. The ground state of odd cyclic radicals are doubly degenerate and have a Jahn–Teller cusp at the D_{2n+1h} conformation, so that their stable geometries are somewhat deformed. If the Jahn–Teller distortions are small, their ground state may remain to be a TSDW. They are known to have unusually large hyperfine coupling constants and g values in their ESR spectra, Cirelli et al. (1974), Silverstone et al. (1965), Liebling and McConnel (1965), Krusic and Kochi (1968), Segal et al. (1965), and Carter and Vincow (1967). The anomaly in their ESR spectra might be due to the TSDW nature of the ground state.

C. HF Ground State of Homopolar Diatomic and Triatomic Molecules

We consider here the HF ground state of the nitrogen molecule, oxygen molecule, and ozone with varying interatomic distance or bending angle. The

ground states of these molecules have complicated structures when they are expressed in the CI form. The HF pictures for them make clear the electronic processes underlying the complicated CI wave functions. The UHF theory is able to describe correctly the dissociations of the single bond of H_2 and the double bond of olefin as we have discussed in Sections 3.A.iii and 3.B.ii. The theory also describes correctly the dissociations of the triple bond of N_2 and the triplet double bond of O_2.

i. Nitrogen Molecule. The HF ground state of N_2 was studied by Igawa and Fukutome (1980). The ground state dissociation of N_2 is the process

$$N_2(^1\Sigma_g^+) \rightarrow N(^4S) + N(^4S). \tag{233}$$

Among the ten valence electrons, the six electrons occupying the highest σ bonding orbital σ and the two π bonding orbitals π_x and π_y dominantly contribute to the triple bond of N_2. So, in the following, we do not explicitly write the σ electrons with mainly $2s$ character. The RHF ground state is $(\sigma)^2(\pi_x)^2(\pi_y)^2$. It is stable at the equilibrium interatomic distance but becomes triplet unstable at a little longer distance.

The triplet transitions to cause the instability have the Σ_u^+ symmetry. They contain the $\pi - \pi^*$ transition in the combination $(\pi_x \rightarrow \pi_x^*) + (\pi_y \rightarrow \pi_y^*)$ and the $\sigma - \sigma^*$ transition. We show in Figure 39 the potentials of the RHF solution and the ASDW solution $ASDW_1$ appearing from the triplet instability. The $ASDW_1$ potential converges to the correct dissociation limit as seen in Figure 39. $ASDW_1$ has the orbitals

$$\begin{aligned} \phi_i^{\pm} &= \pi_i \cos(\lambda/2) \pm \pi_i^* \sin(\lambda/2), \qquad i = x, y, \\ \phi_\sigma^{\pm} &= \sigma \cos \lambda'/2 \pm \sigma^* \sin(\lambda'/2). \end{aligned} \tag{234}$$

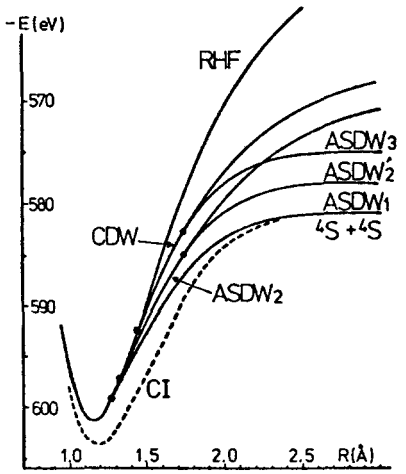

Figure 39. HF and full CI potentials in the dissociation of N_2.

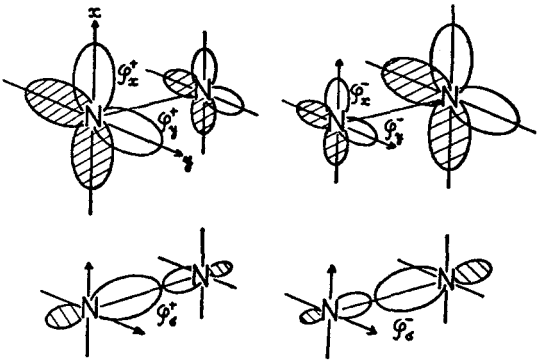

Figure 40. Structures of the ASDW orbitals in N_2.

Owing to the Σ_u^+ symmetry of the transitions which imposes the equal weight and phase for the transitions π_x–π_x^* and π_y–π_y^*, the mixing parameters in $\phi_x^{\pm}$ and $\phi_y^{\pm}$ have the same value λ. The parameter λ' has the same sign as λ. We show in Figure 40 the structures of the ASDW_1 orbitals. The three up spin electrons localize simultaneously toward an atom, and the three down spin ones toward another atom. The simultaneous localizations of the three electrons of the same spin toward the same atom are due to the Σ_u^+ symmetry of the instability to produce ASDW_1. In the dissociation limit, the localizations become complete. The three up spin electrons localize on an atom and the down spin ones on another atom producing two isolated nitrogen atoms in the ^4S state. Thus, the wave function of ASDW_1 converges to the correct atomic state, though it contains components with incorrect total spins.

The singlet projected ASDW_1 wave function $^1\text{PASDW}_1$ has the correct spatial symmetry Σ_g^+. It contains ten configurations, the ground one, five closed shells with pairwise excitations, and four configurations with two triplet excitations coupled to the singlet state. Among the nine excited configurations, there are four double excitation configurations, four quadruple ones and a hexaple one. All the ten configurations have nonvanishing contributions at $R = \infty$. $^1\text{PASDW}_1$ becomes identical with the full CI wave function at $R = \infty$. The full CI ground state wave function considering only the excitations of the six bonding electrons consists of 18 configurations. However, all the eight configurations not contained in $^1\text{PASDW}_1$ do not involve the atomic ^4S state and vanish at $R = \infty$. They appear only transiently with small weights. Their total weight in the full CI wave function amounts only 6.8%, 2.0%, and 0.0% at $R = 1.6$, 2.0, and 3.0 Å, respectively. $^1\text{PASDW}_1$ is a good approximation to the full CI wave function in the region $R > 2$ Å. It is not so good in the region $R < 2$ Å, but the tendencies of the ten CI coefficients are in agreement with those of the full CI wave function. This result shows that a CI to limit the number of excitations fails to describe correctly the dissociation process. The ASDW_1 ground state incorporates all the essential configurations including those with multiple excitations. We also note the importance of the configurations with two triplet excitations. The total weight of those

configurations amounts to 50% at $R = \infty$. The complexity of the ground state of N_2 at large R is due to its hexaradical nature.

ii. Oxygen Molecule. The triplet and singlet HF ground states of O_2 were studied by Takahashi and Fukutome (1978). We mention here only the triplet ground state. The triplet RHF ground state ^{3}RHF of O_2 is $(\sigma)^2(\pi_+)^2(\pi_-)^2(\pi_+^*\pi_-^*)$, where $\pi_\pm$ and $\pi_\pm^*$ have the orbital angular momentum ± 1 around the molecular axis and we do not write the σ electrons of $2s$ character. ^{3}RHF is not an HF state similar to the doublet RHF case but the triplet HF ground state at the equilibrium geometry is an ASDW, ^{3}ASDW$_0$, with a small spin polarization in the σ orbitals

$$^3\text{ASDW}_0 = (\sigma^+\bar{\sigma}^-)^2(\pi_+)^2(\pi_-)^2(\pi_+^*\pi_-^*). \tag{235}$$

As shown in the HF potential of Figure 41, instability occurs twice in the triplet HF ground state of O_2 in the dissociation process. ^{3}ASDW$_0$ becomes A_+M_- unstable and an ASW ground state ^{3}ASW$_1$ appears. ^{3}ASW$_1$ also becomes A_- unstable and a TSW ground state ^{3}TSW appears. ^{3}TSW converges to the correct

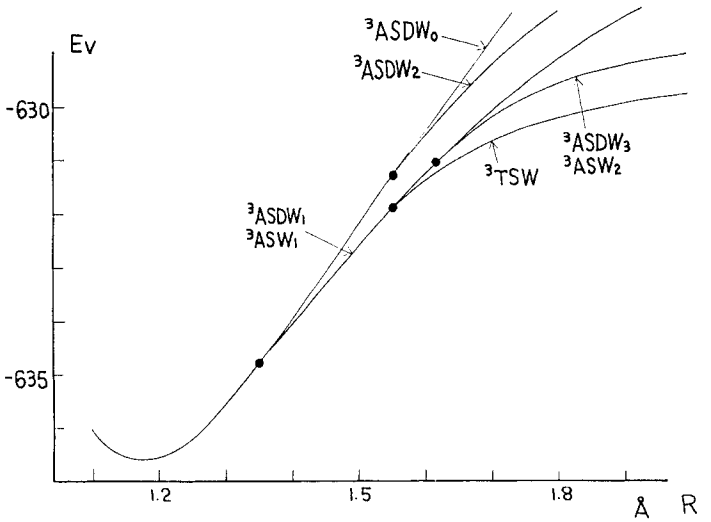

Figure 41. Triplet HF potentials in the dissociation of O_2.

dissociation limit $O(^3P) + O(^3P)$. Thus, the triplet HF ground state of O_2 consists of the three HF phases ^{3}ASDW$_0$–^{2}ASW$_1$–^{3}TSW.

The A_+M_- instability of ^{3}ASDW$_0$ is caused by the spin unflipping π–π^* transition with the Σ_u^- symmetry in down spin π orbitals which consists of the $\pi_\pm \rightarrow \pi_\pm^*$ transitions in the combination $(\pi_- \rightarrow \pi_-^*) - (\pi_+ \rightarrow \pi_+^*)$. No σ–σ^* transition of Σ_u^- symmetry is possible and σ orbitals are not involved in the instability. In ^{3}ASW$_1$, only the orbitals π_- and π_+ with down spins are altered to the following

orbitals but the other orbitals remain unchanged:

$$
\begin{aligned}
&{}^3\mathrm{ASW}_1 = (\sigma^+\bar{\sigma}^-)(\pi_+\bar{\pi}_{2+})(\pi_-\bar{\pi}_{1-})(\pi_+^*\pi_-^*),\\
&\pi_{1-} = \pi_- \cos\lambda/2 + \pi_-^* \sin\lambda/2,\\
&\pi_{2+} = \pi_+ \cos\lambda/2 - \pi_+^* \sin\lambda/2.
\end{aligned}
\tag{236}
$$

Owing to the Σ_u^- symmetry of the instability which contains the $\pi_- \rightarrow \pi_-^*$ and $\pi_+ \rightarrow \pi_+^*$ transitions with equal weight but with opposite sign, the mixing parameters in the orbitals π_{1-} and π_{2+} are of equal magnitude but of opposite sign. Equation (236) shows that the electron in the orbital π_{1-} with the orbital angular momentum -1 localizes toward an atom while the electron in the orbital π_{2+} with the orbital angular momentum $+1$ localizes toward another atom. Thus, in the ${}^3\mathrm{ASW}_1$ state, a polarization of the orbital angular momentum density occurs within the electrons with down spins as depicted in Figure 42(a). The states of

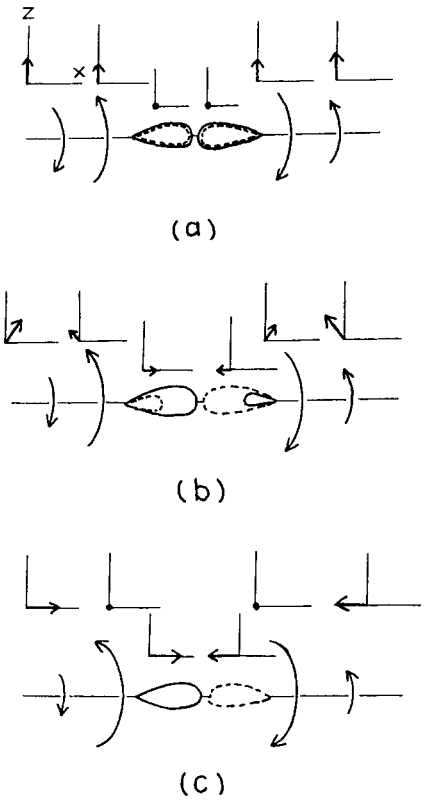

Figure 42. Structures of the ${}^3\mathrm{ASW}_1$ (a) and ${}^3\mathrm{TWS}$ (b) (at finite R), (c) (at $R = \infty$) wave functions of ${}^3O_2$. Spin density vectors are indicated on each AO component. The σ lobes drawn by real and dashed lines represent σ orbital components with opposite directions of spin. The radii of circular arrows represent magnitudes of orbital angular momentum density of $\pi_\pm$ electrons.

up spin π electrons and σ electrons remain unchanged from ^{3}ASDW$_0$. At a nearly same position as the A_+M_- instability, an A_+M_+ instability occurs in ^{3}ASDW$_0$ and a new ASDW solution, ^{3}ASDW$_1$, appears which is almost degenerate to ^{3}ASW$_1$. However, ^{3}ASDW$_1$ does not lead to the correct dissociation behavior and is regarded as an unphysical solution.

By introducing the orbitals

$$\begin{aligned} \pi_{2-} &= \pi_-^* \cos\lambda/2 - \pi_- \sin\lambda/2, \\ \pi_{1+} &= \pi_+^* \cos\lambda/2 + \pi_+ \sin\lambda/2, \end{aligned} \tag{237}$$

which are orthogonal to π_{1-} and π_{2+}, respectively, ^{3}ASW$_1$ can be written

$$^3\text{ASW}_1 = (\sigma^+\bar{\sigma}^-)(\pi_{2+})^2(\pi_{1-})^2(\pi_{1+}\pi_{2-}). \tag{238}$$

The A_- instability of ^{3}ASW$_1$ leading to the ^{3}TSW ground state is caused by the spin flipping transitions with the Σ_u symmetry (^{3}ASW retains the C_∞ and inversion symmetries but breaks the C_2 symmetries) which contain the σ–σ^* transitions $\sigma^\pm \to \sigma^{*\pm}$ and the π transitions $\pi_{1+} \to \bar{\pi}_{1+}$ and $\pi_{2-} \to \bar{\pi}_{2-}$ in the combination $(\pi_{1+} \to \bar{\pi}_{1+}) - (\pi_{2-} \to \bar{\pi}_{2-})$. Consequently, ^{3}TSW has the orbitals in the GSO forms

$$\begin{aligned} ^3\text{TSW} &= (\varphi_\sigma^+\varphi_\sigma^-)(\pi_{1-})^2(\pi_{2+})^2(\varphi_{1+}\varphi_{2-}), \\ \varphi_\sigma^\pm &= \sigma^\pm \cos(\mu^\pm/2)\eta_\pm + \sigma^{*\mp} \sin(\mu^\pm/2)\eta_\mp, \\ \varphi_{1+} &= \pi_{1+}[\cos(\nu/2)\eta_+ + \sin(\nu/2)\eta_-], \\ \varphi_{2-} &= \pi_{2-}[\cos(\nu/2)\eta_+ - \sin(\nu/2)\eta_-]. \end{aligned} \tag{239}$$

Because the differences between the σ orbitals σ^+ and σ^-, σ^{*+} and σ^{*-} and the parameters μ^+ and μ^- are small, we may put $\sigma^+ = \sigma^- = \sigma$, $\sigma^{*+} = \sigma^{*-} = \sigma^*$, and $\mu^+ = \mu^- = \mu$. Then, $\varphi_\sigma^\pm$ can be written

$$\begin{aligned} \varphi^\pm = (1/\sqrt{2})(\sigma \cos\mu/2 + \sigma^* \sin\mu/2)(1/\sqrt{2})(\eta_+ + \eta_-) \pm (1/\sqrt{2}) \\ \times (\sigma \cos\mu/2 - \sigma^* \sin\mu/2)(1/\sqrt{2})(\eta_+ - \eta_-). \end{aligned} \tag{240}$$

Since $(\eta_+ \pm \eta_-)/\sqrt{2}$ are the eigenstates of the x component of spin, Eq. (240) shows that a localization of the σ electrons occurs accompanying a spin polarization in the $\pm x$ directions. Equation (239) shows that the spins of the electrons in the orbitals π_{1+} and π_{2-} begin to rotate toward opposite directions. We show in Figures 42(b) and 42(c) the structure of the ^{3}TSW wave function. The polarization of the orbital angular momentum density, the spin polarized localization of the σ electrons and the rotation of the spins of the π electrons become complete at $R = \infty$ as depicted in Figure 42(c). All the spins are in the $\pm x$ directions at $R = \infty$.

The triplet HF ground state ^{3}ASDW$_0$–^{3}ASW$_1$–^{3}TSW makes clear the electronic processes involved in the dissociation process $O_2(^3\Sigma_g^-) \to O(^3P) + O(^3P)$. The ^{3}ASDW$_0$ ground state at the equilibrium geometry has no orbital angular momentum density because of the $^3\Sigma_g^-$ symmetry of the system. In the ^{3}ASW$_1$ phase, the π bond begins to break accompanying growing orbital angular momentum densities with opposite rotations on the two atoms. In the ^{3}TSW phase, the σ

bond begins to break accompanying growing spin polarization. At the same time, the spins of the open shell electrons begin to rotate toward the directions to align to the spins of localizing σ electrons. In the dissociation limit, both the π and σ bonds break completely. The polarizations of the orbital angular momentum and spin of the bonding π and σ electrons , respectively, and the alignment of the spins of the open shell π electrons and the σ electrons become complete at $R = \infty$ attaining the atomic ^3P state.

The triplet projected ^{3}ASDW$_0$, ^{3}ASW$_1$, and ^{3}TSW have the Σ_g^- symmetry. ^{3}PASDW$_0$ and ^{3}PASW$_1$ contain only one and two RHF configurations

$$\begin{aligned} ^3\text{PASDW}_0\text{:} \quad & \text{(I)} = (\sigma)^2(\pi_+)^2(\pi_-)^2(\pi_+^*\pi_-^*), \\ ^3\text{PASW}_1\text{:} \quad & \text{(I) and (II)} = (\sigma)^2(\pi_+^*)^2(\pi_-^*)^2(\pi_+\pi_-). \end{aligned} \tag{241}$$

^{3}PTSW contains five configurations including (I) and (II):

^{3}PTSW: (I), (II), and

$$\begin{aligned} \text{(III)} &= (\sigma^*)^2(\pi_+)^2(\pi_-)^2(\pi_+^*\pi_-^*), \\ \text{(IV)} &= (\sigma^*)^2(\pi_+^*)^2(\pi_-^*)^2(\pi_+\pi_-), \\ \text{(V)} &= \tfrac{1}{2}\|\Phi_1(\alpha\beta - \beta\alpha)\alpha\alpha\|, \\ \Phi_1 &= \{(\pi_-)^2(\pi_+^*)^2(\pi_+\pi_-^*) - (\pi_+)^2(\pi_-^*)^2(\pi_-\pi_+^*)\}(\sigma\sigma^*). \end{aligned} \tag{242}$$

The full CI $^3\Sigma_g^-$ wave function neglecting the transitions from the σ orbitals with $2s$ character contains nine RHF configurations. All the five configurations in ^{3}PTSW have nonvanishing weights at $R = \infty$ and essential in obtaining the correct dissociation limit. On the other hand, the four configurations not contained in ^{3}PTSW do not involve the atomic ^3P state, so that they appear only transiently with small weights and disappear at $R = \infty$. This result is in agreement with an *ab initio* CI calculation by Schaefer (1971). The most important configurations are the five contained in ^{3}PTSW, if one restricts configurations to those constructed from the minimal basis set. We note that ^{3}PTSW has a four electron excitation configuration (IV), confirming again the ability of UHF wave function incorporating essential multiple excitations.

The ^{3}ASDW$_0$ state is a triplet diradical because the spin polarized splitting of the σ orbitals is small. Equation (238) shows that the ^{3}ASW state is still a diradical. However, orbital angular momentum polarized localizations of the two bonding π electrons take place in this stage and those two π electrons become strongly correlated. The ^{3}TSW state is a triplet tetraradical because of the presence of the spin polarized splitting of the σ orbitals. However, the ^{3}TSW tetraradical is composed of six strongly correlated electrons since it involves also the angular momentum polarized localizations of the bonding π electrons. This system is an example of the multiradicals with strongly correlated electrons more than the number of the radical electrons.

iii. Ozone. The singlet HF ground state of O_3 in the conformations with C_{2v} symmetry was studied by Kitayama et al. (unpublished). We show in Figure 43

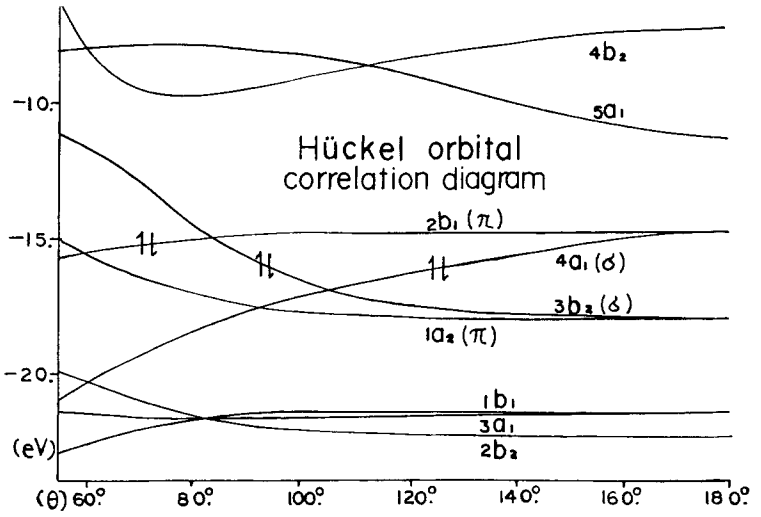

Figure 43. Orbital correlation diagram of O_3 against the bending angle.

the orbital correlation diagram against the bending angle θ and in Figure 44 the potentials of the HF states which will be discussed below. Owing to the presence of a HOMO–LUMO crossing, there are two RHF ground states

$$\begin{aligned} \mathrm{RHF}_1 &= \cdots (1a_2)^2(4a_1)^2(3b_2)^2, \\ \mathrm{RHF}_2 &= \cdots (1a_2)^2(4a_1)^2(2b_1)^2, \end{aligned} \tag{243}$$

which cross at a bending angle near 90°. RHF_1 is always triplet unstable for the

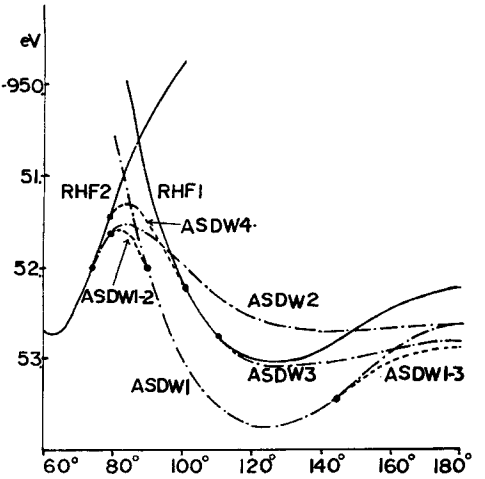

Figure 44. HF bending potentials of O_3.

transitions $1a_2 \rightarrow 2b_1, \ldots$, with B_2 symmetry. An ASDW solution, $ASDW_1$, exists below RHF_1. RHF_2 is stable in a region close to the equilateral triangular conformation. For larger bending angles, it becomes triplet unstable for the transitions $4a_1 \rightarrow 3b_2, \ldots$, with B_2 symmetry and an ASDW solution, $ASDW_2$, appears from the instability.

The dominant transitions to cause the triplet instabilities of RHF_1 and RHF_2 are not the HOMO–LUMO transition but π–π and σ–σ transitions from deeper π and σ orbitals, respectively. The HOMO–LUMO transition is of the σ–π or π–σ type, so that the Coulombic attraction of the particle–hole pair and the exchange interaction of the excited electron are not large. This is the reason why the instability due to the HOMO–LUMO transition is less easy to occur in spite of the smallest orbital energy gap. Owing to the π–π and σ–σ characters of the dominant transitions to cause the relevant instabilities, $ASDW_1$ and $ASDW_2$ have the character of π and σ diradicals, respectively, with the radical centers at the terminal two atoms. Only one corresponding orbital pair of π and σ types, respectively, is largely splitting in them. $ASDW_1$ is stable in a region surrounding the equilibrium flat triangular geometry. The π diradical character of O_3 at the equilibrium geometry was reported by Hay et al. (1975).

$ASDW_1$ and $ASDW_2$ cross at a bending angle near 90° as seen in Figure 44 owing to the difference of the main transitions in the instabilities to produce them. Both $ASDW_1$ and $ASDW_2$ become A_+M_+ unstable in a region near the crossing point and an ASDW solution, $ASDW_{12}$, appears which connects them smoothly. The dominant spin unflipping transitions to cause the A_+M_+ instabilities are the transitions from one of little splitted occupied orbital pair to the largely splitted unoccupied orbital pair which are of σ–π or π–σ type. Owing to the σ–π character of the instabilities to produce $ASDW_{12}$, its orbitals, not only the corresponding ones but also the ASDW NO's, are mixtures of σ and π RHF orbitals. Only one corresponding orbital pair is largely splitting indicating that $ASDW_{12}$ is also a diradical state. $ASDW_{12}$ represents a diradical with a π–σ mixed character that is nothing but the diradical under the conversion from the π diradical $ASDW_1$ to the σ diradical $ASDW_2$.

Three transitions $1a_2 \rightarrow 2b_1$, $4a_1 \rightarrow 2b_1$, and $3b_2 \rightarrow 2b_1$ of RHF_1 or $4a_1 \rightarrow 3b_2$, $1a_2 \rightarrow 3b_2$, and $2b_1 \rightarrow 3b_2$ of RHF_2 are contributing to the $ASDW_{12}$ wave function with equally large weights, so that the $ASDW_{12}$ wave function has a complicated structure with heavy mixings of a lot of excited configurations due to the three transitions when it is expanded into the CI form with RHF configurations. The configuration mixing changes rapidly in the narrow existence domain of $ASDW_{12}$. The importance of a π–π transition at the equilibrium geometry and the presence of a complicated configuration mixing in a region near $\theta = 90°$ were reported in an *ab initio* CI calculation by Shih et al. (1974). Our UHF calculation shows that the conversion of π diradical O_3 to σ diradical O_3 occurs in the region and the process leads to a complicated CI wave function. In spite of the complicated CI wave function in the RHF basis, $ASDW_{12}$ is a diradical. This indicates the necessity of a modification of the CI characterization of diradicals by Hayes and Siu (1971) and Salem and Rowland (1972) in terms of RHF configuration mixings.

ASDW$_1$ becomes A_+M_+ unstable also in a region near the linear conformation and an ASDW solution, ASDW$_{13}$, appears from the instability as shown in Figure 44. The main transition to cause the instability is of the σ–π type, so that ASDW$_{13}$ has the orbitals with σ–π mixing. ASDW$_{13}$ also is a diradical. Thus, the singlet HF ground state of O_3 consists of the five HF phases, RHF$_2$–ASDW$_2$–ASDW$_{12}$–ASDW$_1$–ASDW$_{13}$. The surprising complexity of the HF ground state of O_3 is due to the fact that the four RHF orbitals $4a_1$, $1a_2$, $2b_1$, and $3b_2$ are lying close enough to cause instabilities and the six electrons residing in the four orbitals are strongly correlated to each other in the ASDW$_{12}$ and ASDW$_{13}$ states. Thus, ASDW$_{12}$ and ASDW$_{13}$ are diradical states with six strongly correlated electrons.

D. Conclusions

The examples discussed in this section demonstrate the great ability of the UHF theory in describing electronic structures of molecules and electronic mechanisms of chemical reactions with strong correlations of electrons. We summarize here the main conclusions obtained from the preceding results.

(i) The UHF theory demonstrates that a ground state reaction system with strong electronic correlation may enter into a number of different multiradical states as represented by different UHF phases.

(a) Such multiradical states are distinguished by different ordered spin structures when the same AO's are involved in them as in the cases of H_4, H_3, and carbene dimer systems or by differences of AO's concerned with radical electrons as in the case of O_3. The spin structure of a multiradical state visualizes the overall correlation structure of radical electrons. We shall discuss further in Section 4 on the physical significance of UHF spin structures.

(b) A reaction system may enter into a state with not only a spin structure but also a correlation structure in orbital angular momentum, namely, in electron current as shown by the ^{3}ASW$_1$ state in $^3O_2$. The possibility of the occurrence of a charge density correlation structure in the ground state has not yet been demonstrated but it may be present in excited states of ionic character as seen in the CDW state in the internal rotation of C_2H_4.

(c) Different UHF phases in a reaction system reflect the presence of a hierarchy in the underlying essential correlation effects with increasing complexities. The number n_r of radical electrons and the type of spin density vector modulation are a measure for the complexity of the correlation in a multiradical state. UHF phases of ASDW, TSDW, and TSW types with one, two, and three dimensionally modulated spin structures, respectively, have correlations with increasing complexities. We show in Table VIII the multiplicity n_r of radical states realizable in the three UHF classes. We have yet had no example of doublet TSW state and the lower bound for the n_r in it is still unknown.

The number n_c of strongly correlated electrons in a multiradical state is always larger than n_r, $n_c \geq n_r$, except for doublet ASDW monoradicals and triplet ASDW diradicals with only weak spin polarization effects in which no strongly correlated electron exists. Multiradical states can be classified into two types:

TABLE VIII. Multiplicity of radical states realizable in the three UHF classes.

	Singlet	Doublet	Triplet
ASDW	2, 4, . . .	1, 3, . . .	2, 4, . . .
TSDW	4, 6, . . .	3, 5, . . .	4, 6, . . .
TSW	4, 6, . . .	?	4, 6, . . .

without and with a pool of strongly correlated electrons, according to $n_c = n_r$ and $n_c > n_r$, respectively. Among multiradical states with the same n_r and in the same UHF class, those with a pool of strongly correlated electrons have more complex correlations than the ones without it. For instance, the $ASDW_{12}$ and $ASDW_{13}$ diradical states in O_3 have a pool with $n_c = 6$, so that they have much more complicated correlations than the $ASDW_1$ and $ASDW_2$ diradical states without pool.

(d) In connection with the above comments, we note that the electronic correlations underlying in the most basic processes of chemical reactions, breaking of a chemical bond, are very different for bonds of different types. The breaking of the single bond of H_2 proceeds via an ASDW diradical state without pool. The breaking of the double bond of olefin proceeds via an ASDW tetraradical state or two ASDW and a TSDW tetraradical states depending on the bond angle and substituents. All the radical states have no pool. The breaking of the triple bond of N_2 proceeds via an ASDW hexaradical state without pool. The breaking of the triplet double bond of O_2 proceeds via an ASW diradical and a TSW tetraradical states with pools. We shall show in Section 4 that the breaking of the double bond of CO involves a complicated correlation which cannot be approximated by a UHF wave function.

(ii) An instability of the HF ground state signals critical importance of a correlation effect and entrance into a multiradical state or conversion of a multiradical state to another one.

(a) $^3ST_-$ instabilities in an RHF ground state represent conversion of a nonradical state to an ASDW radical state. A_+M_+ instabilities in an ASDW ground state represent conversion of an ASDW radical to another ASDW one accompanying an increase in the size of strongly correlated electron pool. A_-M instabilities represent conversion of an ASDW radical to a TSDW one. A_+M_- instabilities represent conversion of an ASDW radical to an ASW one accompanying introduction of an electron current correlation structure. M_- instabilities of a TSDW ground state and A_- instabilities in an ASW ground state represent conversions of TSDW and ASW radicals to a TSW radical, respectively. The five HF classes, RHF(TICS), ASDW, ASW, TSDW, and TSW, and the nondegenerate instabilities to connect them, were shown to occur in chemical reactions.

(b) Occurrence of a degenerate instability represents a complicated situation where correlations of two different kinds become simultaneously of critical

importance. A one step entrance into a much complicated radical state, say from RHF to TSDW, occurs at a degenerate instability threshold.

(c) Instability boundaries provide an HF phase map indicating where different HF phases arise. The radical character of a UHF phase becmes maximal at the innermost place of the domain of the phase or at the boundary where the phase connects with another HF phase with more complicated radical character. The HF phase map and the spin and electron current structures of each phase visualize how the electronic structure due to the essential correlation changes with nuclear conformation.

(iii) UHF wave functions incorporate the essential correlations signaled by instabilities.

(a) The transitions to contribute to an instability of the HF ground state have the significance that the excited configurations derived from them are the most stabilizing the ground state when they are superposed to the original HF ground configuration. The UHF wave function arising from the instability automatically selects out the transitions involved in the instability and incorporates the excited configurations derived from them. This is the reason why UHF wave functions are able to incorporate the most important configurations in the ground state. As we have shown, the projected UHF ground state in many systems is a good approximation to the full CI ground state. It contains all the important configurations with large CI weights or in some cases even all configurations in the full CI wave function. It is usually a very good approximation in the strong correlation regime where the orbital energy gap is zero or very small but is not quantitatively so good approximation in the region near an instability threshold.

The ability of UHF wave functions to be a good approximation to the ground state was demonstrated also by DODS NO CI calculations by Yamaguchi et al. (1977, 1978a, 1978b, 1980). They showed that the DODS natural orbitals of the ASDW ground state in diradical molecules bring about an excellent convergence in the CI expansion when they are used as the CI basis.

The theory described in Section 2.E.iii provides a deeper theoretical basis for the validity of the UHF approximation. However, we should note that there are systems whose ground state cannot be approximated by a UHF wave function as we shall discuss in Section 4.

(b) The correlation incorporated into a UHF wave function has a collective and coherent character. The transitions involved in an instability have the same symmetry and exhaust all the transitions with the symmetry. Owing to the coherence in the symmetry of the transitions, all the electrons in the resultant UHF state concerned with the transitions become to have an ordered correlation structure in spins and electron current which is determined by the symmetry of the transitions. Owing to the collective nature of the correlation, not only the dominant low energy transitions but also the minor high energy transitions with the same symmetry as the dominant ones are incorporated into the UHF wave function. Those high energy transitions most effectively interfere to the dominant ones because of the same symmetry. The properties determined by an interference of low and high energy transitions, such as the ordering of the singlet and

triplet ground states, can therefore be correctly described by the UHF approximation.

(iv) The UHF theory clarifies in a unified manner the important factors to affect electronic mechanisms of chemical reactions.

(a) Gap control: In systems with small HOMO–LUMO energy gap, reaction paths forbidden by the Woodward–Hoffman selection rule become realizable. Small gap is the necessary condition for a diradical reaction to occur.

(b) Heteropolarity effects: Introduction of heteropolarity into a reaction system either enlarges or decreases the HOMO–LUMO gap. In the former situation, conversion of a diradical mechanism to a zwitter ionic one may be brought about. In the latter situation, a charge transfer reaction, i.e., ionic radical mechanism, may become realizable.

(c) Unoccupied MO control: Events in low lying unoccupied MO's affect the correlated ground state. Strong LUMO–LUMO interaction between reactant and reagent leading to a wide delocalization of the LUMO of the total system may suppress the triplet instability of the ground state leading to a conversion of diradical mechanism to ionic one. Crossing of low lying unoccupied MO's brings about a complication of the correlation in the ground state leading to a change in the multiradical character of the ground state.

(v) The UHF theory has defects due to broken symmetries of its wave functions. In a system where one center exchange interaction has an important role, the UHF potential may have a large error. It also is unable to correctly describe Jahn–Teller effects. However, these defects can be eliminated by the projection to the spin and time reversal eigenstates. The most important defect of the UHF theory is the inability of describing both the ground and excited states in a straightforward unified manner. However, on the other hand, the UHF theory sheds a new light about the natures of electronic correlation in excited states. We shall discuss this problem in Section 4.

4. Further Outlooks

We consider here some basic problems concerning the nature of electronic correlations in exact eigenstates of molecules. Although the UHF theory is a powerful approximation and correlations of many kinds can be reasonably approximated by it, there are also correlations which are undescribable by the UHF theory. Because of the special position of the UHF approximation in fermion many-body systems as we have discussed in Section 2.E, analysis of exact correlations starting from the UHF approximation seems to be a fruitful approach in elucidating their natures. We shall discuss in the following some aspects of exact correlations which are shed new light by analyses from UHF theoretical view.

A. Relation of UHF Spin Structures to Exact Spin Correlation Structures

As we have shown in Section 2.B.ii, a UHF wave function except for the TICS and CCW classes has a nonvanishing spin density matrix and its real and imaginary parts give the spin and spin current densities, respectively. We call the structure

of the spin density the UHF spin structure. We have given in Section 3 examples of UHF spin structures in molecules and chemical reactions and have shown that the UHF spin structures reasonably represent behaviors of correlated electrons. The spin density of a UHF wave function, however, does not represent a real spin density. A singlet state has no first order spin density but the UHF wave function to approximate the state has it. UHF spin structures, however, are not mere mathematical artifacts due to broken spin symmetries of UHF wave functions but represent the spin correlation structures in the states they are approximating. This was first demonstrated by Misurkin and Ovchinnikov (1974). They showed that the alternating spin structure of the ASDW ground state of infinite polyene is approximating the spin correlation function in the singlet projected ASDW wave function. Yamaguchi and Fueno (1977) pointed out that the spin structure of the ASDW state in the two electron system is approximating the spin correlation in the ground state.

The spin correlation function in a state $|f\rangle$ is defined by

$$S(x, y) = \tfrac{1}{4} \sum_{rsuv} \langle f|a^{\dagger}(x, r)\boldsymbol{\sigma}_{rs}a(x, s) \cdot a^{\dagger}(y, u)\boldsymbol{\sigma}_{uv}a(y, v)|f\rangle. \tag{244}$$

The first order density matrix of the state is

$$D(xr, ys) = \langle f|a^{\dagger}(x, r)a(y, s)|f\rangle. \tag{245}$$

We define the linked spin correlation function by subtracting the unlinked contribution

$$S'(x, y) = S(x, y) - \tfrac{1}{4} \sum_{rsuv} \boldsymbol{\sigma}_{rs} \cdot \boldsymbol{\sigma}_{uv}\{D(xr, xs)D(yu, yv) - D(xr, yv)D(yu, xs)\}. \tag{246}$$

The spin correlation function can be expanded by the orthogonalized AO bases as

$$S(x, y) = \sum_{ijkl} S(ij, kl)\chi_i(x)\chi_j(x)\chi_k(y)\chi_l(y). \tag{247}$$

The two site spin correlation function

$$S(i, j) = S(ii, jj) \tag{248}$$

is the most important component in the spin correlation function.

The relation of a UHF spin structure to the exact spin correlation function can be most easily examined for the two electron–two orbital model discussed in Section 3.A.ii. The spin correlation function of the exact singlet ground state [Eq. (196)] is calculated to be

$$S(x, y) = -\tfrac{3}{2}C_1^2\phi_1^2(x)\phi_1^2(y) - \tfrac{3}{2}C_2^2\phi_2^2(x)\phi_2^2(y) + 3C_1C_2\phi_1(x)\phi_2(x)\phi_1(y)\phi_2(y). \tag{249}$$

The first order density matrix of the state is

$$\begin{aligned} D(xr, ys) &= \delta_{rs} D(x, y), \\ D(x, y) &= C_1^2 \phi_1(x)\phi_1(y) + C_2^2 \phi_2(x)\phi_2(y). \end{aligned} \tag{250}$$

Hence, the linked spin correlation function is given by

$$S'(x, y) = S(x, y) + \tfrac{3}{2} D^2(x, y). \tag{251}$$

By using Eqs. (181), (251), and

$$\begin{aligned} &D(x, y) = \sum_{ij} D(i, j)\chi_i(x)\chi_j(y), \\ &D(1, 1) = D(2, 2) = \tfrac{1}{2}, \qquad D(1, 2) = \tfrac{1}{2}(C_1^2 - C_2^2), \end{aligned} \tag{252}$$

the two site spin correlation function are obtained as

$$\begin{aligned} &S(1, 1) = S(2, 2) = -\tfrac{3}{8} + \tfrac{3}{4} C_1 C_2, \\ &S(1, 2) = -\tfrac{3}{8} - \tfrac{3}{4} C_1 C_2, \qquad C_1 C_2 = 1/2(1 + 4q^2)^{1/2}; \end{aligned} \tag{253}$$

$$\begin{aligned} &S'(1, 1) = S'(2, 2) = \tfrac{3}{4} C_1 C_2, \\ &S'(1, 2) = -\frac{3}{8}\left(\frac{1}{(1 + 4q^2)^{1/2}} + \frac{1}{1 + 4q^2}\right). \end{aligned} \tag{254}$$

On the other hand, the ASDW solution (189) has the spin density

$$\begin{aligned} &\mathbf{S}(x) = \mathbf{e} \sin \lambda \phi_1(x)\phi_2(x) = \mathbf{e}[S(1)\chi_1^2(x) + S(2)\chi_2^2(x)], \\ &S(1) = -S(2) = \tfrac{1}{2} \sin \lambda. \end{aligned} \tag{255}$$

The correlation function of the ASDW spin density (255) is

$$\begin{aligned} \mathbf{S}^2(1) &= \mathbf{S}^2(2) = \tfrac{1}{4} \sin^2 \lambda, \\ \mathbf{S}(1) \cdot \mathbf{S}(2) &= -\tfrac{1}{4} \sin^2 \lambda, \qquad \sin^2 \lambda = 1 - [q/(1 + r)]^2, \end{aligned} \tag{256}$$

where $\mathbf{S}(i) = \mathbf{e}S(i)$. Since the ASDW spin density vanishes at the RHF limit, its correlation function must be compared with $S'(i, j)$ to have the same property. Furthermore, the spin density $\mathbf{S}(i)$ is a classical vector, while the spin vector in $S'(i, j)$ is quantum mechanical, so that $\mathbf{S}(i) \cdot \mathbf{S}(j)$ and $S'(i, j)$ must be normalized by the squared lengths $\frac{1}{4}$ and $\frac{3}{4}$ of the classical and quantum mechanical spin vectors, respectively. We show in Figure 45(a) the q dependences of the ASDW spin density correlation and the exact linked spin correlation function thus normalized. We see in Figure 45(a) that the ASDW spin density correlation for different sites is a reasonable approximation to the exact spin correlation function but that for the same site gives about twice larger value compared to the exact one. The ASDW spin density at a site is mainly due to an electron, so that the ASDW spin density correlation at the same site includes the spin density of an electron overestimating the spin correlation, while the ASDW spin densities at

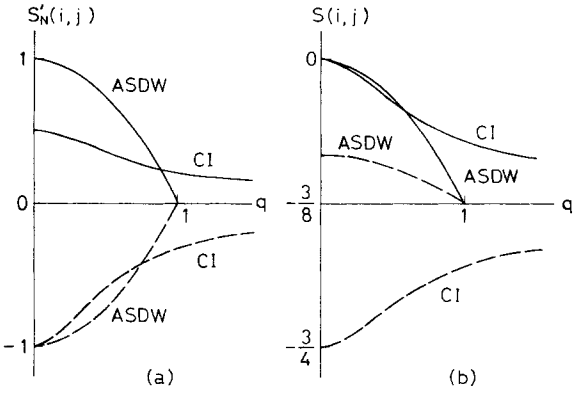

Figure 45. UHF and exact spin correlation functions in the two electron–two orbital model. (a) Normalized ASDW spin density and exact linked spin correlation functions, and (b) ASDW and exact spin correlation functions. The different site and same site correlation functions are represented by real and dashed lines, respectively. $r = 0$ in these graphs.

different sites are mainly due to different electrons so that it gives a reasonable approximation for the spin correlation between different sites.

Although the ASDW spin density fails to correctly approximate the spin correlation at the same site, the ASDW wave function can do it. The spin correlation function of a UHF state is given in terms of its density matrix as

$$S_{\mathrm{UHF}}(x, y) = \tfrac{1}{4} \sum_{rsuv} \boldsymbol{\sigma}_{rs} \cdot \boldsymbol{\sigma}_{uv}[Q(xs, xr)Q(yv, yu) - Q(xs, yu)Q(yv, xr)]$$
$$= \mathbf{S}(x, x) \cdot \mathbf{S}(y, y) - \tfrac{3}{2}N(x, y)N(y, x) + \tfrac{1}{2}\mathbf{S}(x, y) \cdot \mathbf{S}(y, x), \qquad (258)$$

$$Q(xs, yr) = \sum_{\alpha} \varphi_{\alpha}(x, s)\varphi^{*}_{\alpha}(y, r).$$

The spin correlation function of the ASDW state (197) is calculated to be

$$S_{\mathrm{ASDW}}(1, 1) = -\tfrac{3}{8} + \tfrac{3}{8}\sin^2 \lambda,$$
$$S_{\mathrm{ASDW}}(1, 2) = -\tfrac{3}{8} + \tfrac{1}{8}\sin^2 \lambda. \qquad (259)$$

We compare in Figure 45(b) the ASDW and exact spin correlation functions. We see in Figure 45(b) that the ASDW spin correlation function at the same site is a reasonable approximation to the exact one while that for different sites gives only about three times smaller correlation than the exact one. This is due to the contamination of the triplet component. Two electrons of parallel spins cannot enter into an AO because of the Pauli principle, so that the contribution from the contaminating triplet state is eliminated in the correlation function at the same site. The triplet state contributes to the different site correlation decreasing the antiparallel spin correlation. Thus, the approximation of the spin correlation

structure by the ASDW state is not wholly self-consistent. The ASDW spin density structure approximates the spin correlation between different sites and the ASDW spin correlation function the one at the same site. We conjecture that such a situation holds in general but we have not yet succeeded to prove it.

Hashimoto (unpublished) studied the spin and change correlation structures of the full CI eigenstates of cyclobutadiene, cyclopentadienyl radical, and benzene in the *P–P–P* approximation. His result is schematically illustrated in Figure 46. He found that a number of full CI eigenstates in these systems has a spin or charge correlation structure which fits with a UHF spin or change structure. The spin and charge correlation structures of those states are illustrated in Figure 46. The states with UHF type spin correlation structures are of covalent character and those with UHF type charge correlation structures are ionic.

He also found that there are states with different spin and spatial symmetries but sharing a common spin correlation structure. Those states are shown in Figure 46. He showed that the wave functions of the states sharing a common spin correlation structure can be well approximated by the different spin components of a UHF wave function having the corresponding spin structure. For

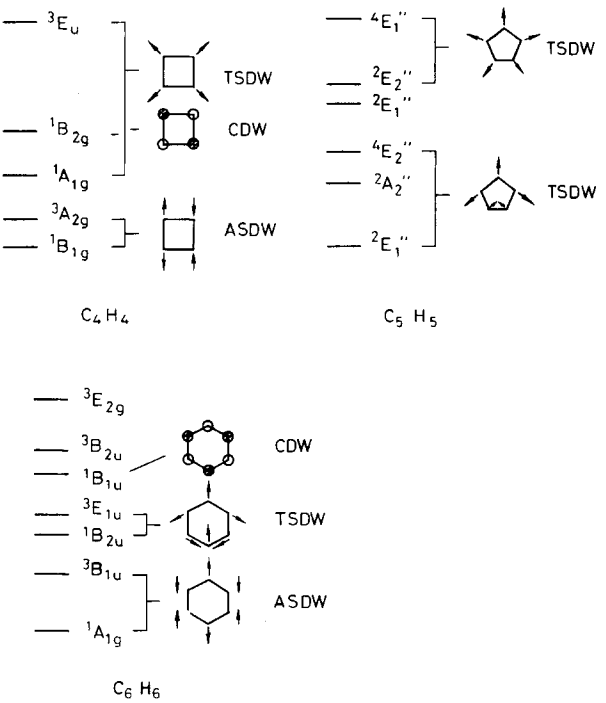

Figure 46. Spin and charge correlation structures of full CI eigenstates of $(CH)_4$, $(CH)_5$, and $(CH)_6$ in the *P–P–P* approximation. UHF spin and charge correlation structures possessed by these systems and the states having those correlation structures are shown. The energy ordering is also shown for low lying eigenstates.

instance, the lowest $^1B_{1g}$ and $^3A_{2g}$ states of cyclobutadiene can be well approximated by the singlet and triplet components of an ASDW wave function with the alternating spin structure, respectively. Similarly, the lowest $^1A_{1g}$ and ^3E_u states can be well approximated by the singlet and triplet components of a TSDW wave function having the helical spin structure shown in Figure 46. This indicates that the $^3A_{2g}$ and ^3E_u states are the Peierls–Yoccoz type excited states produced from the $^1B_{1g}$ and $^1A_{1g}$ states, respectively, by coherent rotation of spins. Thus, his result confirms the presence of excited states due to coherent rotation of spins as predicted in Section 2.E.ii. The possibility that a projected UHF wave function can be a good approximation to an excited state was pointed out by the author (Fukutome, 1972) for the CDW solution in the two electron model and by Dancz and Jordan (1974) for the ASDW solution in the π electron model of acetylene.

Another important result obtained by Hashimoto is the presence of excited states whose spin correlation structures cannot be represented by a UHF type spin structure. He showed that the wave functions of those states cannot be reasonably approximated by spin projected UHF wave functions. This indicates that there are excited states with complicated electronic correlations beyond the scope of the UHF approximation.

B. Electronic Correlations in Excited States

As we have shown in Section 3, a chemical reaction system with strong electronic correlation may have plentiful instabilities of the HF ground state. Instabilities of the HF ground state pose a serious problem in the many-body theoretical description of excited states. A standard many-body theoretical approach to excited states is the random phase approximation (RPA). The lowest excitation energy given by the RPA, however, becomes zero just at instability thresholds of the HF ground state. The equivalence of HF and RPA instabilities were first shown by Thouless (1961). The TDHF formulation of the RPA (see, for instance, McLachlan and Ball, 1964) shows that the RPA excitation modes arise from small amplitude harmonic oscillations of orbitals around the HF stationary point in the variation space of the HF energy functional. However, the second order curvature of the HF energy functional in a direction of the variation space becomes zero at a HF instability threshold as shown in Figure 7(a), so that the harmonic RPA oscillation mode in the direction becomes to have zero frequency. This explanation for the equivalence of the HF and RPA instabilities also indicates invalidity of the RPA in a system with unstable RHF ground state. The HF energy functional in such a system has an anharmonic structure as depicted in Figure 10. The anharmonicity of the HF energy functional surface becomes of essential importance in the description of excited states in the region near an HF instability. This so called anharmonicity problem was firstly recognized by Belyaev and Zelevinsky (1962) in nuclear many-body theory. The essential importance of the anharmonicity means that nonlinear couplings between RPA excitation modes have dominant roles in determining the excited states in the region. Hence, it

is also called the problem of mode–mode coupling. The anharmonicity problem is the basic problem in nulei in the transition regions from spherical to deformed and in spin wave excitations of magnetic solids near phase transitions. It is a very difficult problem how to treat the strong anharmonicity, and no universal solution has yet been obtained. Therefore, excited states of a molecule or chemical reaction with plentiful HF instabilities are considered to be of very different natures from those describable by the RPA.

Fortunately, molecules and chemical reaction systems usually have only small number of strongly correlated electrons except for large conjugated molecules, so that approaches not starting from the RPA are possible. Large scale CI is of course able to treat such molecular systems. However, it is very difficult to understand the essential physical contents of correlations from a table of configurations in a large scale CI calculation. It has been customary to use only the energies, the first order electron density, and the other physical quantities such as the dipole moment, etc., in the analysis of large scale CI calculations. Hashimoto's work showed that the spin and charge correlation functions are very important and useful quantities in understanding the physical natures of correlations involved in complicated CI wave functions.

Hashimoto's work indicates that there are at least three groups of full CI eigenstates with different characters in the spin and charge correlation structures.

(i) States with UHF type spin correlation structures: States in this group have spin correlation structures which can be represented by UHF spin structures but have little charge correlation structure. They are further subdivided into groups with different UHF type spin correlation structures. Both axial and torsional spin structures are possible. The wave function of a state in this group can be approximated by a projected UHF wave function. States with a common spin structure can be approximated by different spin components of a UHF wave function, forming a series of Peierls–Yoccoz type excitations due to coherent rotation of spins.

(ii) States with CDW type charge correlation structures: States in this group have charge correlation structures which are similar to CDW charge structures but have little spin correlation structure.

(iii) States with spin correlation structures unrepresentable by UHF spin structures: States in this group have spin correlation structures which cannot be represented by any UHF spin structure. The wave function of a state in this group cannot be reasonably approximated by a projected UHF wave function.

This classification of full CI eigenstates shows that the essential correlations may be different from state to state. The three groups have correlations of different characters. States in the group (i), but with different spin structures, have different essential correlations. It is almost certain that a limited CI calculation is unable to describe correctly the essential correlations in a number of states simultaneously. The classification also shows that the natural orbitals may be largely dependent on state. States in the group (i) with a common spin structure are considered to have nearly the same NO's, but states with different spin structures may have different NO's. States in the group (iii) are considered to

have NO's which have no resemblance to any NO's derived from UHF wave functions. This consideration shows that unless one is satisfied in fool proofed full CI calculation there is a big unsolved problem how to describe excited states with essential correlations of different characters in a unified manner. The fact that some states can be approximated by projected UHF wave functions might provide a breakthrough for this problem.

We note finally that not only the spin and charge correlation functions but also the spin and charge current correlation functions are considered to be useful in analyzing correlation structures, since there are states having current correlation structures as the ground state of O_2. The systems considered by Hashimoto are homopolar and highly symmetrical. In systems with asymmetry or heteropolarity, there may be states with transient character having both spin and charge correlation structures.

C. System Whose Ground State Cannot be Approximated by a UHF Wave Function

As we have discussed in the preceding paragraphs, there are excited states whose wave functions cannot be approximated by projected UHF wave functions. Such a situation can happen also in the ground state. Igawa and Fukutome (unpublished) found that the ground state of carbon mono-oxide cannot be approximated by a projected UHF wave function.

We show in Figure 47 the HF ground state potential of CO. The HF ground state of CO consists of the two phases, RHF and an ASDW called $ASDW_1$. The potential of $ASDW_1$ converges correctly to the dissociation limit of $C(^3P)+O(^3P)$. However, there are two UHF states, ASW and $ASDW_2$, with lower energies than $ASDW_1$. Their potentials also converge to the correct dissociation limit. They, however, connect with neither $ASDW_1$ nor RHF but cross with RHF.

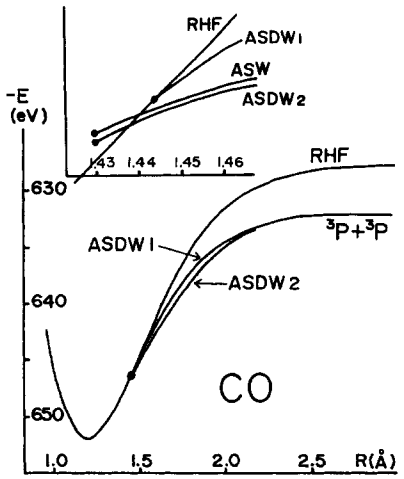

Figure 47. HF potentials in the dissociation of CO.

We made configuration analysis for the three UHF states $ASDW_1$, ASW, and $ASDW_2$ projected to $^1\Sigma^+$ symmetry and compared the three projected UHF wave functions with the full CI ground state wave function. We found that $PASDW_1$ has only about half the RHF configurations with large weights in the full CI wave function. PASW and $PASDW_2$ have nearly the same configuration contents. The configurations in them are also about half of the important configurations in the full CI wave function but are complementary to those contained in $PASDW_1$. All the $PASDW_1$, PASW, and $PASDW_2$ wave functions do not correctly approximate the full CI wave function but they contain only atomic ^3P states in the dissociation limit, so that they give the potentials with the correct dissociation behavior.

The failure of the UHF states to correctly approximate the full CI ground state was demonstrated also by the structures of the natural orbitals. The NO's of the UHF states are delocalized at the dissociation limit but those of the full CI ground state are localized.

The configuration contents of $PASDW_1$ and $PASDW_2$ (or PASW) are complementary but exhaust all the important configurations in the full CI wave function, so that the full CI wave function can be well approximated by a superposition of $PASDW_1$ and $PASDW_2$,

$$\Psi_0 \simeq C_1 \text{ PASDW}_1 + C_2 \text{ PASDW}_2. \tag{260}$$

Approximation (260) was shown to be very nice.

The reason why the ground state of CO has the structure like Eq. (260) can be explained by the structure of the HF energy functional surface. The HF energy functional of CO do not have a single valley structure as shown in Figure 10, but has a double valley one. We show in Figure 48 the profile of the HF energy functional surface in a direction passing near the $ASDW_1$ and $ASDW_2$ stationary points which was calculated by the method described in Section 2.D. According to the theory described in Section 2.E.iii, the wave function of quantized TDHF motion, which is the exact wave function, must have probabilities on the two

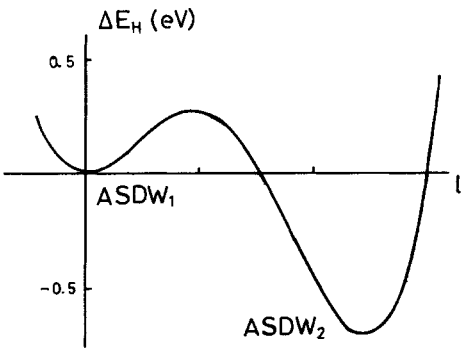

Figure 48. Profile of the HF energy functional in a direction passing near the $ASDW_1$ and $ASDW_2$ stationary points. The profile is for CO with $R = 1.8$ Å.

minima when the HF energy functional has a double valley structure depicted in Figure 48. Therefore, the ground state wave function cannot be approximated by a UHF wave function under such a situation, but can be approximated by a superposition of two UHF wave functions.

This example, as well as Hashimoto's, forces us to change the starting point for the many-body theory of molecules. The many-body theory of molecules as well as those of nuclei and solids has been constructed on the assumption that the ground state can be reasonably approximated by the HF (or HB) wave function with independent (or independent quasiparticle) character. This assumption means that the ground state has either truly independent particle character, when the RHF ground state is a good approximation, or the character of Bose condensation of particle–hole (or particle–particle) pairs. The ground state of CO, which can be approximated by a superposition of two UHF wave functions, has the character of two resonating Bose condensates. It is the ground state of hitherto unknown type. Therefore, in order to describe both the ground and excited states including states of such complicated characters in a unified manner, a new novel many-body theory is required.

Acknowledgments

The author would like to thank Dr. K. Yamaguchi, Dr. M. Ozaki, Dr. A. Igawa, Dr. M. Takahashi, Dr. T. Takabe, H. P. Kitayama, K. Hashimoto, and M. Fukazawa for their fruitful collaborations in the works reviewed in this paper. He is particularly indebted to Dr. K. Yamaguchi for many interesting and enlightening discussions about chemical facts. He would also like to thank Professor M. Yamamura and Professor S. Nishiyama for stimulating discussions about problems common in the many-body theories of molecules and nuclei. The following tables and figures are reproduced from *Progress of Theoretical Physics* with permission of Riron Butsurigaku Kankōkai: Table I (Fukutome, 1974a); Tables V and VI (Fukutome, 1974b); and Table VII (Fukutome, 1975). Figures 3 and 4 (Ozaki and Fukutome, 1978); Figures 5 and 6 (Fukutome, 1974b); Figures 7 and 8 (Fukutome, 1975); Figure 9 (Igawa and Fukutome, 1975); Figure 14 (Fukutome, 1972); Figure 16 (Fukutome, 1973b); Figure 18 (Takabe et al., 1976); Figures 22–28 (Fukutome et al., 1975); Figures 31–34 (Takabe and Fukutome, 1976); Figures 36–38 (Yamaguchi and Fukutome, 1975); Figures 39 and 40 (Igawa and Fukutome, 1980); and Figures 40 and 41 (Takahashi and Fukutome, 1978).

Bibliography

Amos, A. T. and Hall, G. G. (1961), Proc. R. Soc. (London), Ser. A **263**, 483.
Andre, J. M. and Leroy, J. (1971), Int. J. Quantum Chem. **5**, 557.
Bardeen, J., Cooper, L. N., and Schrieffer, J. R. (1957), Phys. Rev. **108**, 1175.
Basch, H. (1971), J. Chem. Phys. **55**, 1700.
Belyaev, S. T. (1959), K. Dan. Vidensk. Selsk. Mat. Fys. Medd. **31**, No. 11.
Belyaev, S. T. and Zelevinski, V. G. (1962), Nucl. Phys. **39**, 582.
Bénard, M. and Paldus, J. (1980), J. Chem. Phys. **72**, 6546.

Bogoliubov, N. N. (1958), Dokl. Akad. Nauk USSR **119**, 244 (Sov. Phys. Dokl. **3**, 292).
Bonacić, V. and Koutecký, J. (1972), J. Chem. Phys. **56**, 4563.
Borden, W. T. and Davidson, E. R. (1977), J. Am. Chem. Soc. **99**, 4587.
Bradley, C. J. and Cracknell, A. P. (1972), *The Mathematical Theory of Symmetry in Solids* (Clarendon, Oxford).
Carter, M. K. and Vincow, G. (1967), J. Chem. Phys. **47**, 292.
Cazes, D., Salem, L., and Tric, C. (1970), J. Polym. Sci., Part C **29**, 109.
Cirelli, G., Graf, F., and Gunthard, H. H. (1974), Chem. Phys. Lett. **28**, 494.
Čižek, J. and Paldus, J. (1967), J. Chem. Phys. **47**, 3976.
Čižek, J. and Paldus, J. (1970), J. Chem. Phys. **53**, 821.
Čižek, J. and Paldus, J. (1971), Phys. Rev. A **3**, 525.
Coulson, C. A. and Fisher, I. (1949), Philos. Mag. **40**, 386.
Dancz, J. and Jordan, K. D. (1974), J. Chem. Phys. **61**, 2977.
Falicov, L. M. and Harris, R. A. (1969), J. Chem. Phys. **51**, 3153.
Fletcher, R. (1970), Mol. Phys. **19**, 55.
Fletcher, R. and Reeves, C. M. (1964), Comput. J. **7**, 149.
Fukutome, H. (1968), Prog. Theor. Phys. **40**, 998, 1227.
Fukutome, H. (1971), Prog. Theor. Phys. **45**, 1382.
Fukutome, H. (1972), Prog. Theor. Phys. **47**, 1156.
Fukutome, H. (1973a), Prog. Theor. Phys. **49**, 22.
Fukutome, H. (1973b), Prog. Theor. Phys. **50**, 1433.
Fukutome, H. (1974a), Prog. Theor. Phys. **52**, 115.
Fukutome, H. (1974b), Prog. Theor. Phys. **52**, 1766.
Fukutome, H. (1975), Prog. Theor. Phys. **53**, 1320.
Fukutome, H. (1977), Prog. Theor. Phys. **58**, 1692.
Fukutome, H. (1978), Prog. Theor. Phys. **60**, 1624.
Fukutome, H., Takahashi, M., and Takabe, T. (1975), Prog. Theor Phys. **52**, 1580.
Fukutome, H., Yamamura, M., and Nishiyama, S. (1977), Prog. Theor. Phys. **57**, 1554.
Glauber, R. J. (1963), Phys. Rev. **130**, 2529; **131**, 2766.
Goddard III, W. A. (1972), J. Am. Chem. Soc. **94**, 793.
Halperin, B. I. and Rice, T. M. (1968), Solid State Phys. **21**, 116.
Harriman, J. E. (1964), J. Chem. Phys. **40**, 2827.
Harris, R. A. and Falicov, L. M. (1969), J. Chem. Phys. **51**, 5034.
Harrison, J. F. (1971), J. Am. Chem. Soc. **93**, 4112.
Hashimoto, K. (unpublished).
Hashimoto, K. and Fukutome, H. (unpublished).
Hay, P. J., Dunning, Jr., T. H., and Goddard III, W. A. (1975), J. Chem. Phys. **62**, 3912.
Hayes, E. F. and Siu, A. K. O. (1971), J. Am. Chem. Soc. **93**, 2090.
Herring, C. (1966), *Magnetism* (Academic, New York), Vol. IV.
Hill, D. L. and Wheeler, J. A. (1953), Phys. Rev. **89**, 1106.
Hinze, J. and Roothaan, C. C. J. (1967), Prog. Theor. Phys. Suppl. **40**, 37.
Igawa, A. and Fukutome, H. (1975), Prog. Theor. Phys. **54**, 1266.
Igawa, A. and Fukutome, H. (1980), Prog. Theor. Phys. **64**, 491.
Igawa, A. and Fukutome, A. (unpublished).
Itoh, T. and Yoshizumi, H. (1955), J. Phys. Soc. Jpn. **10**, 201.
Jahn, H. A. and Teller, E. (1937), Proc. R. Soc. (London), Ser. A **161**, 220.
Jancovici, B. and Schiff, D. H. (1964), Nucl. Phys. **58**, 678.
Jordan, D. and Silbey, R. (1973), Chem. Phys. Lett. **18**, 27.
Kikuchi, O. (1972), Chem. Lett. 1121.
Kitayama, H. P., Fukazawa, M., and Fukutome, H. (unpublished).
Krusic, P. J. and Kochi, J. K. (1968), J. Am. Chem. Soc. **90**, 7155.
Kotani, M. (1951), Proceedings of the Shelter Island Conference on Quantum Mechanical Methods in Valence Theory, p. 139.
Laforgue, A., Čižek, J., and Paldus, J. (1973), J. Chem. Phys. **59**, 2560.

Laidlaw, W. G. (1973), Int. J. Quantum Chem. **7**, 87.
Liebling, G. R. and McConnel, H. M. (1965), J. Chem. Phys. **42**, 3931.
Linderberg, J. and Öhrn, Y. (1977), Int. J. Quantum Chem. **12**, 161.
Longuet-Higgins, H. C. and Abrahamson, E. W. (1965), J. Am. Chem. Soc. **87**, 2045.
Longuet-Higgins, H. C. and Salem, L. (1959), Proc. R. Soc., Ser. A **251**, 172.
Löwdin, P.-O. (1954), *Proceeding of the Nikko Symposium on Molecular Physics, 1953* (Maruzen, Tokyo), p. 13.
Löwdin, P.-O. (1955), Phys. Rev. **97**, 1509.
Löwdin, P.-O. (1963), Rev. Mod. Phys. **35**, 496.
Malshalek, E. R. and Holzwarth, G. (1972), Nucl. Phys. A **191**, 438.
Matsen, F. A. and Nelin, C. J. (1979), Int. J. Quantum Chem. **15**, 751.
Matsubara, T. and Yokota, T. (1954), Proceedings of the International Conference on Theoretical Physics, Kyoto–Tokyo, 1953, p. 693.
McLachlan, A. D. and Ball, M. A. (1964), Rev. Mod. Phys. **36**, 844.
McWeeny, R. (1956), Proc. R. Soc., Ser. A **235**, 496.
Misurkin, I. A. and Ovchinnikov, A. A. (1967), Zh. Eksp. Teor. Fiz. **3**, 431.
Misurkin, I. A. and Ovchinnikov, A. A. (1974), Mol. Phys. **27**, 237.
Misurkin, I. A. and Ovchinnikov, A. A. (1977), Russ. Chem. Rev. **40**, 967.
Moshinsky, M. (1968), *Group Theory and the Many-Body Problem* (Gordon and Breach, New York).
Mott, N. F. (1949), Proc. Phys. Soc. (London) **62**, 416.
Ostlund, N. S. (1972), J. Chem. Phys. **57**, 2994.
Ovchinnikov, A. A., Ukrainskii, I. I., and Kventsel, G. V. (1973), Sov. Phys. Usp. **15**, 575.
Overhauser, A. W. (1960), Phys. Rev. Lett. **4**, 462.
Overhauser, A. W. (1962), Phys. Rev. **128**, 1437.
Ozaki, M. (1979), Prog. Theor. Phys. **62**, 1183.
Ozaki, M. (1980), Prog. Theor. Phys. **63**, 84.
Ozaki, M. and Fukutome, H. (1978), Prog. Theor. Phys. **60**, 1322.
Paldus, J. (1976), in *Theoretical Chemistry, Advances and Perspectives*, H. Eyring and D. Henderson, s. (Academic, New York), Vol. 2, p. 131.
Paldus, J. and Čižek, J. (1969), Chem. Phys. Lett. **3**, 1.
Paldus, J. and Čižek, J. (1970a), J. Polym. Sci., Part. C **29**, 199.
Paldus, J. and Čižek, J. (1970b), J. Chem. Phys. **52**, 2919.
Paldus, J. and Čižek, J. (1970c), Phys. Rev. A **2**, 2268.
Paldus, J. and Čižek, J. (1971), J. Chem. Phys. **54**, 2293.
Paldus, J. and Veillard, A. (1978), Mol. Phys. **35**, 445.
Pauncz, R. (1967), *Alternant Molecular Orbital Method* (Saunders, Philadelphia and London).
Peierls, R. E. and Yoccoz, J. (1957), Proc. Phys. Soc. (London), Sect. A **70**, 381.
Perlemov, A. M. (1972), Commun. Math. Phys. **26**, 222.
Perlemov, A. M. (1977), Sov. Phys. Usp. **20**, 703.
Pople, J. A. (1971), Int. J. Quantum Chem. **5**, 175.
Rubinstein, M. and Shavitt, I. (1969), J. Chem. Phys. **51**, 2014.
Salem, L. and Rowland, C. (1972), Angew. Chem. Int. Ed. **11**, 92.
Salotto, A. W. and Burnelle, L. (1970), J. Chem. Phys. **52**, 2936.
Schaefer III, H. F. (1971), J. Chem. Phys. **54**, 2207.
Segal, B., Kaplan, M., and Frankel, G. K. (1965), J. Chem. Phys. **43**, 4191.
Shih, S., Buenker, R. J., and Peyerimhoff, S. D. (1974), Chem. Phys. Lett. **28**, 463.
Silverstone, H. J., Ward, D. E., and McConnell, H. M. (1965), J. Chem. Phys. **42**, 3931.
Slater, J. C. (1951), Phys. Rev. **82**, 538.
Takabe, T. and Fukutome, H. (1976), Prog. Theor. Phys. **56**, 689.
Takabe, T., Takahashi, M., and Fukutome, H. (1976), Prog. Theor. Phys. **56**, 349.
Takabe, T. and Yamaguchi, K. (1976), Chem. Phys. Lett. **40**, 347.
Takahashi, M. and Fukutome, H. (1978), Prog. Theor. Phys. **59**, 1787.
Takahashi, M. and Fukutome, H. (unpublished).
Thouless, D. J. (1960), Nucl. Phys. **21**, 225.

Thouless, D. J. (1961), Nucl. Phys. **22**, 78.
Tric, C. (1970), J. Polym. Sci., Part *C* **29**, 119.
Wigner, E. P. (1959), *Group Theory* (Academic, New York).
Wilson, Jr., C. W. and Goddard III, W. A. (1969), J. Chem. Phys. **51**, 716.
Woodward, R. B. and Hoffmann, R. (1969), Angew. Chem. Int. Ed. **8**, 781.
Yamaguchi, K. (1975a), Chem. Phys. Lett. **33**, 330.
Yamaguchi, K. (1975b), Chem. Phys. Lett. **35**, 230.
Yamaguchi, K. (1978), Chem. Phys. **29**, 117.
Yamaguchi, K. and Fueno, T. (1973), Chem. Phys. Lett. **22**, 471.
Yamaguchi, K. and Fueno, T. (1976), Chem. Phys. Lett. **38**, 47.
Yamaguchi, K. and Fueno, T. (1977), Chem. Phys. **19**, 35.
Yamaguchi, K., Fueno, T., and Fukutome, H. (1973a), Chem. Phys. Lett. **22**, 461.
Yamaguchi, K., Fueno, T., and Fukutane, H. (1973b), Chem. Phys. Lett. **22**, 466.
Yamaguchi, K. and Fukutome, H. (1975), Prog. Theor. Phys. **54**, 1599.
Yamaguchi, K., Yabushita, S., and Fueno, T. (1977), Chem. Phys. Lett. **49**, 555.
Yamaguchi, K., Yabushita, S., and Fueno, T. (1978a), J. Chem. Phys. **68**, 4323.
Yamaguchi, K., Yabushita, S., Fueno, T., Kato, S., Morokuma, K., and Iwata, S. (1980), Chem. Phys. Lett. **71**, 563.
Yamaguchi, K., Yabushita, S., Minokawa, O., and Fueno, T. (1978b), Chem. Phys. Lett. **59**, 303.
Yamamura, M. and Nishiyama, S. (1976), Prog. Theor. Phys. **56**, 124.
Yoshioka, Y., Fueno, T., and Yamaguchi, K. (preprint).
Yoshizumi, H. and Itoh, T. (1955), J. Chem. Phys. **23**, 412.

Received October 6, 1980
Accepted for publication January 21, 1981